uOttawa

L'Université canadienne
Canada's university

FACULTÉ DES ÉTUDES SUPÉRIEURES ET POSTOCTORALES

uOttawa

L'Université canadienne
Canada's university

FACULTY OF GRADUATE AND POSDOCTORAL STUDIES

Shane Greene

AUTEUR DE LA THÈSE / AUTHOR OF THESIS

M.Sc. (Earth Sciences)

GRADE / DEGREE

Department of Earth Sciences

FACULTÉ, ÉCOLE, DÉPARTEMENT / FACULTY, SCHOOL, DEPARTMENT

Noble Gases of the Canadian Shield from the Lupin and Con Mines, Canada, as indicators of deep groundwater flow dynamics and residence time

TITRE DE LA THÈSE / TITLE OF THESIS

I. Clark

DIRECTEUR (DIRECTRICE) DE LA THÈSE / THESIS SUPERVISOR

T. Kotzer

CO-DIRECTEUR (CO-DIRECTRICE) DE LA THÈSE / THESIS CO-SUPERVISOR

EXAMINATEURS (EXAMINATRICES) DE LA THÈSE / THESIS EXAMINERS

J. Blenkinsop

D. Bottomley

Gary W. Slater

LE DOYEN DE LA FACULTÉ DES ÉTUDES SUPÉRIEURES ET POSTDOCTORALES / DEAN OF THE FACULTY OF GRADUATE AND POSTDOCORAL STUDIES

Noble Gases of the Canadian Shield from the Lupin and Con Mines, Canada, as indicators of deep groundwater flow dynamics and residence time

by

Shane Greene

A thesis submitted to the Faculty of Graduate and Postdoctoral Studies in partial fulfillment of the requirements for the degree of MSc in Earth Sciences

Department of Earth Sciences
Faculty of Science
University of Ottawa

Your file Votre référence
ISBN: 0-494-11285-9
Our file Notre référence
ISBN: 0-494-11285-9

Abstract

Dissolved noble gas geochemistry provides insight on origin of saline groundwaters in two Canadian Shield mines, the Lupin and Con mines in Northern Canada. Within the Con major ion and isotope geochemistry indicate groundwaters from the deepest levels sampled remain relatively undisturbed by mining. Estimates of residence time for the Con mine brines, based on radiogenically produced helium and argon, indicate a Paleozoic age, consistent with recharge during the presence of Devonian seawater in this region. This is largely corroborated by krypton and xenon concentrations which reflect concentrated brine that has equilibrated with air before infiltration. Saline waters in the Lupin mine have an age of at least 130 Ma. At the Lupin mine, neon, krypton and xenon concentrations indicate degassing has occurred, likely caused by depressurization during mining along the V1 fault/fracture zone.

Résumé

La géochimie des gaz rares fournit un aperçu de l'origine des eaux souterraines salées se trouvant dans deux mines du Bouclier canadien, les mines Lupin et Con. L'analyse des concentrations des ions principaux et la géochimie des isotopes révèlent que le minage a peu d'effet sur les eaux souterraines des niveaux les plus creux de la mine Con. Le temps de résidence de ces eaux basé sur l'hélium et l'argon radiogénique indique un age paléozoïque pour la mine Con et au moins 130 Ma pour Lupin. En tenant compte des contraintes dues aux incertitudes, ce projet de recherche indique que les eaux souterraines de la mine Con sont de l'origine de la recharge d'eaux marines salées durant le Dévonien. Ceci est épaulé par les concentrations de krypton et de xénon qui reflètent des saumures en équilibre avec l'air avant infiltration. À la mine Lupin, les concentrations de néon, krypton et xénon indiquent qu'il y a eu perte de gaz probablement causée par une baisse de pression durant les activités minières le long de la faille et zone de fracture V1.

Acknowledgements

Ian Clark, my thesis supervisor at the University of Ottawa whose brains, brawn and boisterous enthusiasm provided the right elixir to rejuvenate my spirits and sharpen my pencil. His unconditional patience, guidance and willingness to listen brought me through this.

Raphaelle Cardyn, for her love and support which are irreplaceable, as well as her statistical/mathematical genius which are unrivalled.

Tom Kotzer, my co-supervisor whose upbeat attitude and wealth of knowledge and supplies for high-vacuum contraptions helped me avoid ultra-torr blunders.

Financial support provided by Dennis Bottomley and the Canadian Nuclear Safety Commision (CNSC) at the Con Mine, Mark Jensen and Ontario Power Generation (OPG) for the Lupin Mine and the National Science and Engineering Council of Canada (NSERC) for everyday life and study.

Monique Hobbs, Randy Stoller, Shaun Frape and Timo Ruskeeniemi for their assistance at depth in the Lupin mine.

My Parents, whose unending phone calls helped me through the rough times during the migration from Newfoundland and through many after.

Table of Contents

List of Figures

List of Tables

1 Introduction

Interest in subsurface burial of nuclear fuel waste within the plutonic rocks of the Canadian Shield has prompted scientific investigation aimed at understanding the current properties and dynamics of these rocks. The concept behind the deep geologic repository necessitates burying nuclear waste in resilient containers within an engineered vault at a depth of 500 to 1000 meters (Gierszewski et al., 2002). An understanding of the past and present thermal, hydrologic, and mechanical properties of the rock is essential to guarantee safe burial in the future on a geologic time scale.

The evolution and origin of saline and brine groundwaters found within the Canadian Shield at depths up to and exceeding 1000 m has relevance to the safe disposal of nuclear waste in a deep burial repository scenario. Intensive scientific investigation into the composition and origin of these fluids has been ongoing since the late 1900's (Frape and Fritz, 1981; Frape, et al., 1984; Gascoyne, et al., 1987; Bottomley et al., 1994; Bottomley et al., 2002;). One geochemical tool of interest is the concentration of noble gases in deep Shield brines, which can be of atmospheric or geogenic origin. Noble gas concentrations can provide information on the recharge history and age of these fluids.

1.1 Terms of Reference

Understanding the dynamics of the hydrologic systems of the Canadian Shield largely began with the creation of mines within it. The research program described herein focuses on deep groundwaters collected from two mines in northern Canada; the Con and Lupin mines (Figure 1.1).

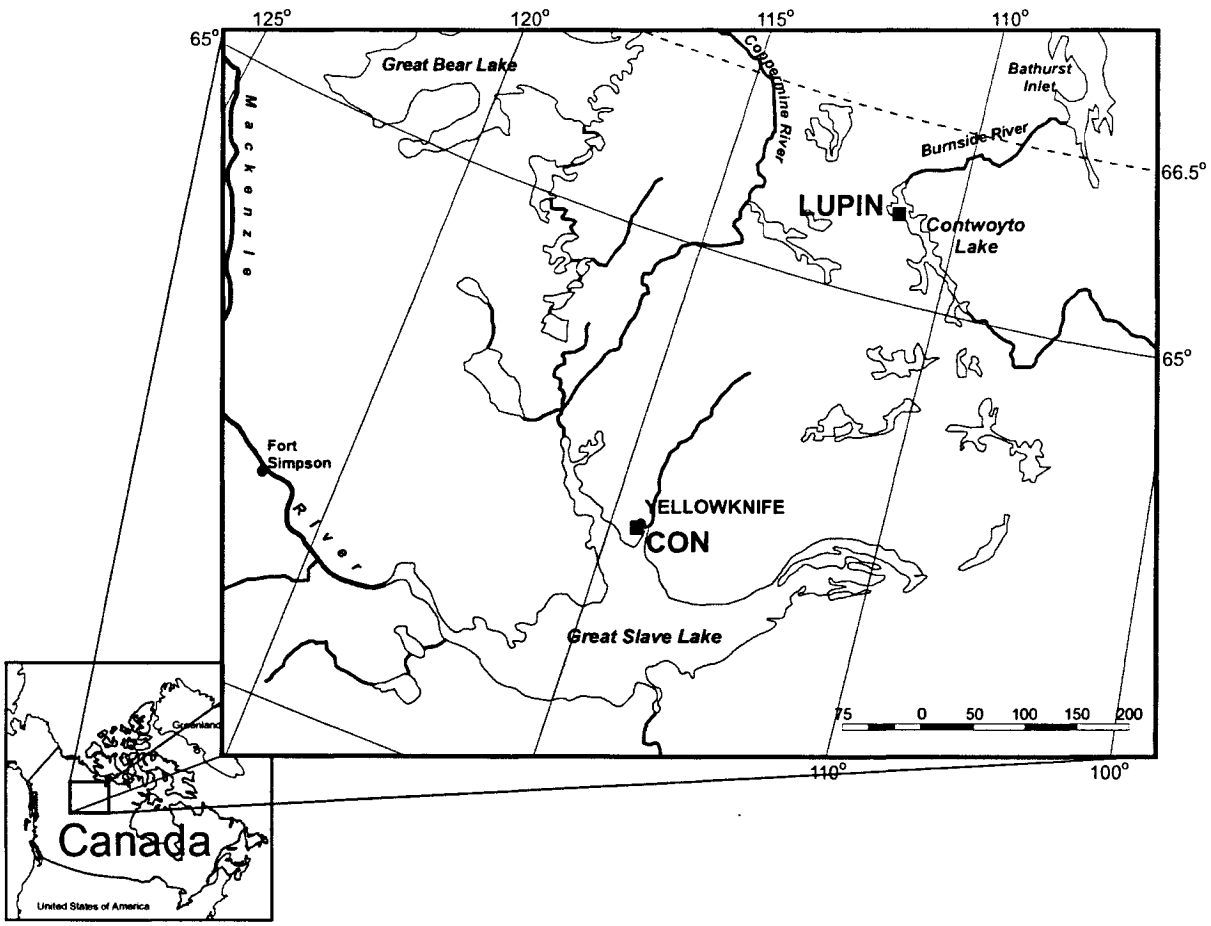

Figure 1.1 Site Location Maps for Lupin and Con Mines

The research program for the Con Mine was Phase II of a program funded by the Canadian Nuclear Safety Commission and developed from the Phase I program presented in Battye, 2002. Phase I involved the design and building of a noble gas extraction line with quadrupole mass spectrometer analyzer. Phase II involved improvements to the noble gas measurement methodology followed by its application to a final round of samples collected in May 2002 at the now closed Con Mine, Yellowknife. A final round of sampling and analysis for stable isotope and geochemical analysis was also included in this Phase II study.

A nuclear waster repository must perform safely over a geologic time scale during which glacial and peri-glacial conditions will alter the thermal, hydraulic and mechanical properties of the host rock. Among other things, these changes may potentially affect the groundwater flow system stability. To further advance the scientific understanding of how permafrost may affect a nuclear waster repository the international PERMAFROST project was initiated by the Geological Survey of Finland, Posiva, Nirex, Svensk Kärnbränslehantering (SKB), and Ontario Power Generation in May of 2001 in Helsinki, Finland.

Part of this initiative involved investigation of the potential impact permafrost may have on flow system evolution and fluid movement in crystalline rock at and around the Lupin Mine, Nunvaut. Phase I of the project consisted of reconnaissance level investigations to develop an understanding of the occurrence, geologic and hydrogeologic setting of permafrost within and around the Lupin mine, Nunvaut (Frape et al., 2004).

The research program for the Lupin Mine described herein was part of the PERMAFROST project Phase II operations and completed in conjunction with researchers from the University of Waterloo and the Geological Survey of Finland. It involved two rounds of water sampling (May 2003, 2004) designed to determine noble gas concentrations from deep groundwaters at the site. The overall objective of the PERMAFROST project is to study groundwater recharge through permafrost.

1.2 Background to Noble Gases in Groundwater Studies

Noble gases have been used extensively as conservative tracers in groundwater studies to provide estimates of paleotemperature of recharge (Andrews and Lee, 1979;

Youngman, 1989; Stute and Schlosser, 1992; Aeschbach-Hertig, 2002) as well as subsurface residence time (Andrews and Lee, 1979; Torgersen and Clark, 1985; Osenbrück et al., 1998 and Lippmann et al., 2003). Both of these variables are useful in helping to determine the flow system evolution and fluid movement of the deep groundwaters in the crystalline rock of the Canadian Shield. Essential to these studies is a thorough knowledge of individual noble gas abundance and solubility constraints.

Noble gases are cosmically abundant but rare terrestrially. As a result of their inert nature, the concentrations of these gases present in the atmosphere today are largely the same as concentrations throughout geologic time (Youngman, 1989). With the exception of helium and argon the atmospheric abundance of the noble gases (Table 1.1) can be ascribed to quantities of primeval gas captured by earth during its formation. Both helium and argon are produced geogenically, which accounts for their comparatively higher concentrations in groundwaters and the atmosphere today. Their production mechanisms will be discussed in more detail below.

The principal components affecting the solubility of the five noble gases of interest (helium,, neon, argon, krypton and xenon) are partial pressures of the atmospheric gases and water temperature (Andrews, 1992). Sensitivity of gas solubility to changes in temperature is different for each noble gas (Stute and Schollsser, 1992). That is, with an increasing mass there is an increase in sensitivity of gas solubility (Figure 1.2).

During recharge the noble gases contained within soil air are mainly dissolved in the unsaturated zone with final equilibration occurring at the water table which records the temperature at the soil air-water interface. Recharge rates vary according to the time of year and recharge system characteristics such as substrate porosity. Rain or surface water infiltrating through the subsurface may take several days to several years depending on these

characteristics. In addition, seasonal temperature variations a few meters below the surface are small and as such, the recharge temperature at the base of the unsaturated zone is essentially equal to the mean annual air temperature (Heaton and Vogel, 1981).

Table 1.1 Isotopic Composition of Atmospheric Noble Gases (from Andrews, 1992).

	Volume % in atmosphere	Mole % of isotope in gas
^{3}He	6.8E–10	0.00014
^{4}He	5.2E–04	100
Total helium	*5.2E–4 (partial pressure = 5.239E–6 atm*	
^{20}Ne	1.7E–03	91.05
^{21}Ne	4.7E–07	0.03
^{22}Ne	1.6E–04	8.94
Total neon	*1.8E–3 (partial pressure = 1.818E–5 atm)*	
^{36}Ar	3.2E–03	0.34
^{38}Ar	5.9E–04	0.06
^{40}Ar	9.3E–01	99.99
Total argon	*9.3E–1 (partial pressure = 9.34E–3 atm)*	
^{78}Kr	4.0E–07	0.35
^{80}Kr	2.6E–06	2.27
^{82}Kr	1.3E–05	11.56
^{83}Kr	1.3E–05	11.55
^{84}Kr	6.5E–05	56.9
^{86}Kr	2.0E–05	17.37
Total krypton	*1.1E–4 (partial pressure = 1.139E–6 atm)*	
^{128}Xe	1.7E–7	1.92
^{129}Xe	2.3E–6	26.44
^{130}Xe	3.5E–7	4.08
^{131}Xe	1.8E–6	21.18
^{132}Xe	2.5E–6	28.89
^{134}Xe	9.0E–7	10.44
^{136}Xe	7.6E–7	8.89
Total xenon	8.7E–6 (partial pressure = 8.60E–8 atm)	

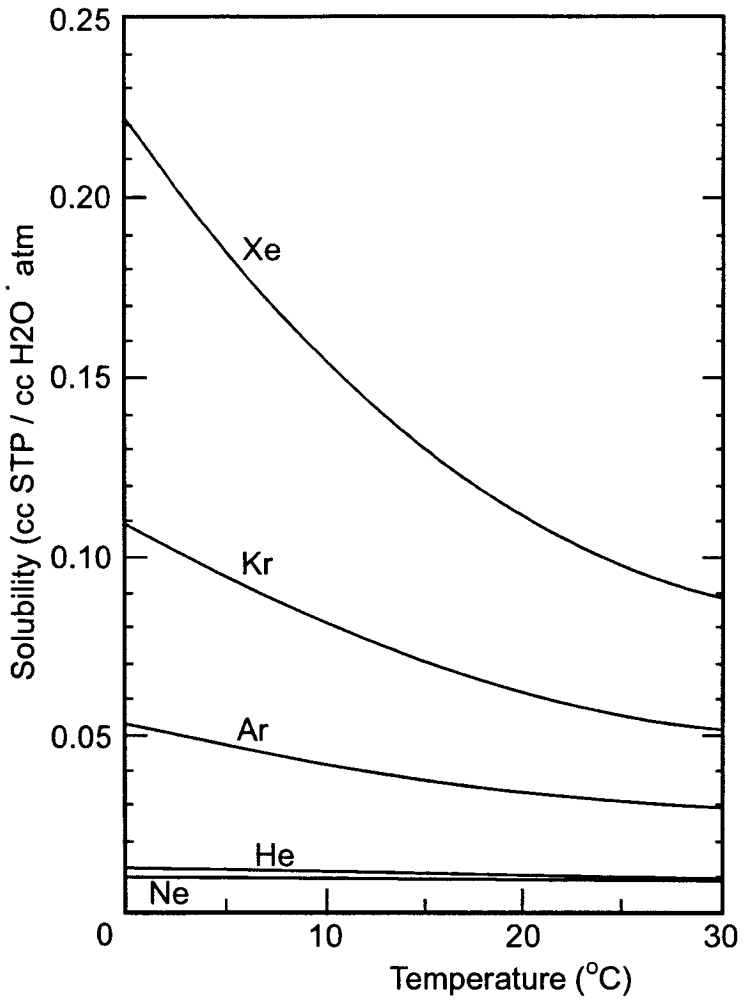

Figure 1.2 Variation of noble gas solubility with changes in temperature and mass (modified from Pinti and Van Drom, 1998).

Ideally all five of the noble gases examined should give a similar recharge temperature, however other factors affecting solubility must be accounted for. Elevation, gas loss, salinity, geogenic production and excess air can all a ffect the concentration of each noble gas in groundwater (Pinti and Van Drom, 1998).

1.2.1 Elevation, Gas Loss and Salinity

Differences in elevation of the recharge area affects atmospheric pressure which consequently affects the concentration of noble gases found within the atmosphere. At

higher elevations atmospheric pressure is lower and accordingly, noble gas concentrations are as well. This factor is easily corrected if the elevation of recharge is known.

Gas loss can occur when a groundwater becomes heated in high-enthalpy geothermal reservoirs or if decompression occurs during sampling or mining activities. In water containing large amounts of CO_2, H_2S, or CH_4 decompression can mean large volumes of these gases dissolve out of solution which can "strip" noble gases out with them. Ignoring degassing leads to an overestimation of temperature because it appears that there is less dissolved noble gases present (Pinti and Van Drom, 1998).

The presence of large volumes of dissolved electrolytes leads to a decrease in the noble gas solubility of the water (Smith and Kennedy, 1983). If salinity is present from the initial recharge, concentration will be greatly affected; however if salinity is obtained along the groundwater flow path noble gas concentration will be unaffected but may be more prone to degassing and an overestimation of temperature.

Geogenic production of noble gases in the subsurface can cause a large underestimation of temperature if uncorrected. The two most important gases produced in the subsurface are argon and helium. Radiogenic production of neon, krypton and xenon are small and largely restricted to isotopes that are not measured in this study.

1.2.2 Radiogenic Helium

Most of the helium present in the atmosphere today originates from radiogenic production in the crust and atmosphere (Youngman, 1989). Helium isotopes ^3He and ^4He, which are measured in this study, are produced and accumulate in the subsurface. Over

geologic time helium migrates into groundwater flowpaths and may become trapped in structures similar to those containing natural gas and petroleum.

Radioactive decay of uranium (U) and thorium (Th) are responsible for the production of ^4He according to the following simplified reactions:

1) $^{238}U \rightarrow {}^{206}Pb + 8\ {}^4He$
2) $^{235}U \rightarrow {}^{207}Pb + 7\ {}^4He$
3) $^{232}Th \rightarrow {}^{208}Pb + 6\ {}^4He$

Uranium and thorium produce ^4He at a rate of $1.19x10^{-7}[U] + 2.28x10^{-8}$ cm^3 [Th] (cm^3 STP/g_{rock} /yr), respectively (Youngman, 1989; Lippmann et al., 2003). A naturally high geochemical abundance of these two elements exists in rocks meaning ^4He production is wide-spread in the crust. Enrichments in dissolved concentrations of up to 5 to 6 orders of magnitude above atmospheric equilibrium concentrations have been observed by Bottomley et al. (1984), Andrews et al. (1989), Poole et al. (1997), and Battye (2002).

The creation of the lighter helium isotope, ^3He, in the subsurface is largely controlled by neutron and alpha particle flux. Neutrons are produced in the subsurface by cosmic muons (down to a few hundred meters), reactions of the type (α, n), and spontaneous and neutron induced fission of U and Th (Florkowski et al, 1988). Alpha particles are created mainly from the decay of naturally occurring uranium and thorium. Production of ^3He in the sub-surface occurs largely via the following reaction:

$^6Li + n \rightarrow \alpha + {}^3H$
$^3H \rightarrow {}^3He + \beta$

Total helium concentrations in groundwaters generally increase with depth in porous media aquifers (Andrews and Lee, 1979; Bath et al., 1979; Heaton and Vogel, 1981). The age and radioelement content of continental basement rocks is such that they will contain 10

to 100 times the helium of most sediments. This means that diffusion of deep crustal helium into overlying sediments, when present, is likely (Youngman, 1989).

A consequence of the geogenic production of both helium isotopes of interest is that a correction for their individual production to determine their excess air component is impossible within the scope of this project and helium is therefore excluded from recharge temperature calculations.

1.2.3 Radiogenic Argon

The radioactive decay of potassium is principally responsible for the large quantity of argon present in the atmosphere today and is described by the following equation:

(1) $^{40}K \rightarrow {}^{40}Ar + \beta^-$

Subsurface production of ^{40}Ar and subsequent release into groundwater flowpaths has the same general consequences as those explained for helium. That is, an overpressuring of dissolved argon should be present in old groundwaters. Argon is produced in the subsurface by K at a rate of 3.887×10^{-14}[K as 5] $cm^3STP/g_{rock}/yr$ (Lippmann et al., 2003).

Unlike helium only one of the argon isotopes of interest is produced in measurable quantities in the subsurface and as a result it is possible to use the atmospheric ratio of $^{36}Ar/^{40}Ar$ to correct for subsurface production. Consequently, it is possible to use this corrected value in paleotemperature recharge calculations.

1.2.4 Excess Air

During recharge the water table may fluctuate, causing air bubbles trapped within pore spaces to become totally dissolved under the increased hydrostatic pressure of an elevated water table (Heaton and Vogel, 1981). This entrainment process can cause relatively large amounts of noble gases to enter solution (Table 1.2) and in turn affect the derived recharged temperature, making recharge appear colder than what is truly the case. Simply put, excess air correction involves an iterative calculation that subtracts successive aliquots of air until agreement between individual noble gas recharge temperatures is maximized.

Table 1.2 The effect of air contamination on inert gas contents of air saturated.

	He	Ne	Ar	Kr	Xe
A. Volume of gas in 1cm^3 fresh water equilibrated with air at cm^3 STP (0^{o}C)	4.99E-08	2.29E-07	5.00E-04	1.27E-07	1.94E-08
B. Volume of gas in 0.01cm^3 air (cm^3 STP)	5.24E-08	1.82E-07	9.34E-05	1.14E-08	8.60E-10
C. Volume of gas in 0.001cm^3 air (cm^3 STP)	5.24E-09	1.82E-08	9.34E-06	1.14E-09	8.60E-11
D. Volume of gas in a 1% volume air contamination i.e. a+b (cm^3 STP)	1.02E-07	4.11E-07	5.93E-04	1.38E-07	2.03E-08
E. Volume % contamination of each gas in D	51.2%	44.2%	15.7%	8.2%	4.2%
F. Volume of gas in a 0.1% volume air contamination i.e. a+c (cm^3 STP)	5.52E-08	2.48E-07	5.09E-04	1.28E-07	1.95E-08
G. Volume % contamination of each gas in F	9.5%	7.3%	1.8%	0.9%	0.4%

1.3 Canadian Shield Brine Origin

Early mining activities into the crystalline rock of the Canadian Shield quickly led to the discovery of the deep shield highly saline water or brines of a calcium-sodium type with TDS concentrations as high as 325 g /L (Lane, 1914; Frape et al., 1984; Bottomley et al,

1994). These brines are generally found within major faults and shear zones at depths below 650 m but have been noted to occur at shallower depths (Frape et al., 1984; Gascoyne et al., 1987). Brines across the entire Canadian Shield have a strikingly similar chemical composition which may suggest a common geochemical history. Although it is widely accepted that these brines are on the order of thousands to millions of years old (Kelly et al., 1986; Haynes, 1988; Nordstrom et al., 1989; Bein and Arad, 1992) there are a number of theories describing their genesis and origin.

Frape et al. (1984), along with Kamineni (1987), Vovk (1987), and Nordstrom (1989) propose that various extensive low-temperature water-rock interactions provide possible mechanisms for the creation of the brines. These mechanisms all describe different processes requiring the removal of water from the system, such as hydration of silicates (Fritz and Frape, 1982) or radiolysis (Vovk, 1987). Kelly et al. (1986), Haynes (1988), and Spencer (1987) on the other hand, argue for an external saline source.

Bottomley et al. (1994) argue that the creation of brines that may be 35 times more concentrated than seawater is not supported by the minerals available within the rock of the Canadian Shield and therefore negates the water-rock interaction theories. Instead, they suggest an origin by concentration of Palaeozoic seawater that covered much of the Canadian Shield during the Lower Palaeozoic. After the evaporative concentration of these seawaters it is suggested that recharge to the deep subsurface would occur through existing fractures and fault zones. The elevated density of the brines would aid in their migration to the deep subsurface where they form isolated pockets. Further evidence of a marine origin was later revealed by Bottomley et al. (2002) using iodine isotope data highly characteristic of marine waters. Although these data give a minimum residence time of 80 Ma it is suggested that these brines are likely Devonian in age.

Herut et al. (1990) demonstrate that evaporation and freezing of seawater can produce brine with a composition similar to the Canadian Shield brines. It is suggested that concentration of the seawater would have occurred during glacial maxima when land-locked seawater bodies freeze. Freezing would remove a significant portion of water and concentrate the brines whose intrusion potential would be increased by the elevated hydraulic pressure created by the overlying ice, and their increased density (Bein and Arad, 1992).

Despite an increasing amount of evidence, these theories remain ambiguous as brine origin is heavily obscured by secondary reactions that have modified the chemical and isotopic geochemistry (Frape et al., 1984). Consequently additional evidence is necessary that is unconstrained by chemical exchange reactions. The deduction of recharge temperautre from noble gas concentrations can indicate the prevailing climatic conditions during recharge. In addition, back-calculation of radiogenically produced helium and argon may provide age estimates of groundwater residence time. Consequently, the combination of these data may distinguish between a Pleistocene (glaciogenic freezing) or Devonian (evaporitic enrichment) mechanism for the creation of the Canadian Shield brines from a marine source.

1.4 Study Objectives

The previous efforts of research by such organizations as the Canadian Nuclear Safety Commission (CNSC), the University of Ottawa, the University of Waterloo, Ontario Power Generation (OPG) and the Geological Survey of Finland at the two mines of interest, the Con and Lupin mines have provided detailed geochemical and hydrogeologic information. This

information has been used to construct a detailed picture of both the past and present processes present deep within the Canadian Shield. In addition, this information has provided the basis for the creation of theories regarding the origin and genesis of the Canadian Shield brines.

Along with increasing the scientific knowledge of the Canadian Shield, the end goal of this research has been to provide information on the ability of the Canadian Shield to support a long term nuclear waste repository. The four objectives of this study are likewise centered on this goal.

Monitoring of the geochemical nature of the deep groundwaters found within and around the Con mine has been ongoing since the early 1980's. Data from Frape et al. (1984), McDonald (1986), Intera Consultants et al. (1997) and Battye (2002) provide a historical record of changes occurring within the deep shield brine at the Con mine. A summary of the geochemical character at the Lupin mine is provided in Ruskeeniemi et al. (2002) as well as Frape et al. (2004). Although some references have been made to the concentration of noble gases from the Canadian Shield brines (Bottomley et al., 1984; Battye, 2002), the majority of the previous studies have concentrated on major ions and environmental isotopes such as ^{18}O and ^{2}H. Therefore, the first objective of this study is two-fold;

- **to provide a final geochemical data set and analysis of the deep groundwaters within the Con mine before its closure; as well as provide a data set of noble gas concentrations (helium, neon, argon, krypton, xenon) found within Canadian Shield brines at the Lupin and Con mines.**

Noble gas concentration data have been used in the past to provide paleotemperatures of recharge for various deep groundwaters (Andrews and Lee, 1979; Youngman, 1989; Stute

and Schlosser, 1992). Recharge temperature provides important information concerning the prevailing climatic conditions during groundwater infiltration. Along with age estimation from back-calculation of geogenic helium and argon production, a more precise indication of the origin and genesis of the Canadian Shield brines may be possible. In view of this, the second and third objectives of this study are;

- **to calculate the paleotemperature of recharge for deep groundwaters collected from the Lupin and Con mines, and**
- **to provide an estimation of the age of Canadian Shield brines collected from the Lupin and Con mines by describing geogenic production and solubility of helium and argon.**

The techniques used to sample the groundwaters at the Con and Lupin mines have, in the past, been mainly restricted to sampling either less saline brine or ground waters closer to surface (Andrews and Lee, 1979; Youngman, 1989; Stute and Schlosser, 1992; Sheldon, 2002). The extremely high salinities and formation pressures encountered at some locations during sampling have never been encountered before in this type of study. For that reason the fourth objective of this study is;

- **to assess the applicability of this type of noble gas study in deep mine settings.**

2 Study Sites

The project included two study sites both of which are gold mines within the Canadian Shield Yellowknife Supergroup, Slave Geological Province (Henderson and Brown, 1966; Henderson, 1970; McDonald et al., 1993; Legault and Charbonneau, 1993; Bullis et al., 1994;). Both mines are located within the Bear-Slave Upland physiographic region and have a sub-arctic climate. The Lupin mine and Con mine both provided an opportunity to travel to a depth of over 1 km and sample Canadian Shield deep groundwaters from diamond drill boreholes.

2.1 Lupin

The Lupin mine, run by Echo Bay Mines Limited, is located near the shore on the northeast portion of Lake Contwoyto in Nunavut Territory, Canada at an elevation of ~ 450 m above sea level (Figure 1.1). It is roughly 400 km northeast of Yellowknife, NWT, and 300 km south of the White Sea with coordinates 65.76°N, 111.25°W. The mine is located about 80 km south of the Artic Circle and within the continuous permafrost zone (Figure 2.1). Normally reached by air from the Echo Bay Mine hangar in Edmonton International Airport, the site is also accessible by winter road from early January to late March. The Lupin mine has been in operation since 1982.

The station ID for the Environment Canada weather observation station on Contwoyto Lake is 2300850 and displays a current mean annual air temperature of -11.8 °C with extreme values ranging from -53.9 °C to +27.2 °C (Environment Canada). Quick and dramatic changes are common for the area in that temperatures can fluctuate by more than 20°C within a few days. Arid conditions prevail with a mean precipitation of roughly 250

mm, with the majority of this amount received in the summer months between June and September

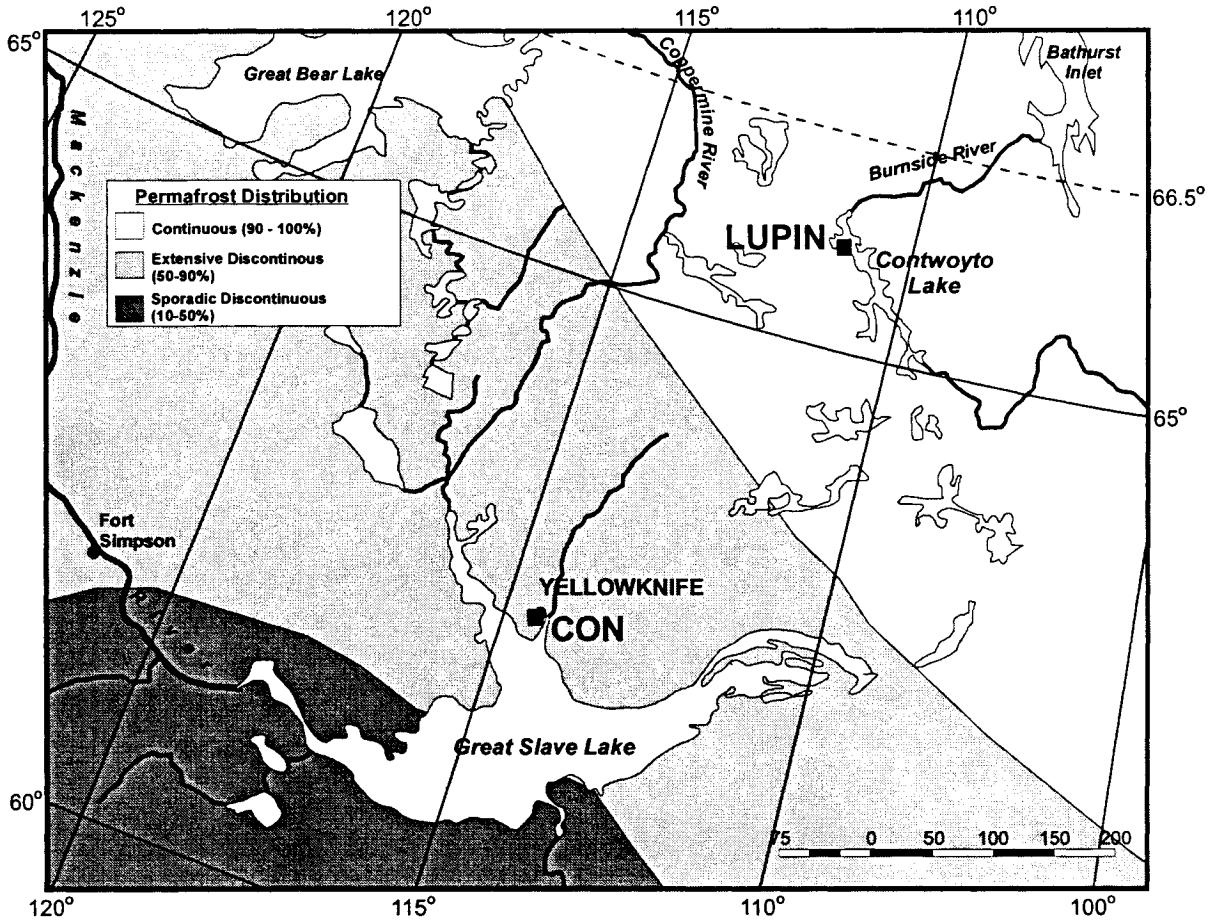

Figure 2.1 Permafrost distribution around the Lupin and Con mines (modified from Permafrost, 1995 Map).

Vegetation cover is predominately tundra characterized by treeless arctic and alpine vegetation with nearly continuous plant cover. Plant cover includes low shrubs and tussock cottongrass tundra with wetlands dominated by sedge-moss meadows (Vegetation Cover, 1993 map).

The landscape in the region of the Lupin mine is dominated by Lake Contwoyto, which is approximately 130 km long by 3 – 16 km wide and drains into Bathurst Inlet via the Burnside River. The lake is surrounded by low eskers, delta formations, flat boulder fields

and bedrock outcrop (Ruskeeniemi et al., 2002). Relief in the general vicinity of the mine ranges from 30 – 40 m with the highest locations (elevation > 479 masl) 3.5 - 5 km to the northwest, west and southwest of the mine. Soil cover around the mine is generally thin (1 - 5 m) with typical soil type being till.

2.1.1 Permafrost at Lupin

Permafrost is historically an important factor for groundwater movement in glacial and periglacial environments. Permafrost, by definition, is ground that remains at or below 0°C for at least two consecutive years (French, 1996). Presently the permafrost at the Lupin mine extends to between 400 – 500 m (Ruskeeniemi et al., 2002). A main objective of the PERMAFROST project has been to examine groundwater recharge through this permafrost and the potential impacts a permafrost layer may have on geochemical character of Canadian Shield groundwaters.

2.1.2 Regional and Mine Geology

The Lupin Mine is situated in an Archean metaturbidite sequence of the Contwoyto Formation which is part of the supracrustal metasedimentary and metavolcanic rocks of the Yellowknife Supergroup within the Slave geologic province (Tremblay, 1976; Legault and Charbonneau, 1993; Bullis et al., 1994). The sequence here has undergone both regional and contact metamorphism. The Contwoyto Formation is composed of interbedded metagreywacke, phyllite and mudstone with lenses and horizons of iron-formation (Legault and Charbonneau, 1993; Bullis et al., 1994). All ore-zones at Lupin are restricted to the sulphide-rich amphibolitic iron formation containing interbeds of phyllite and quartzite.

Deformation and fracturing at the mine due to various metamorphic events are important in determining the hydrogeological structure of the mine. The combined effect of three major deformation periods has created a complex fold structure (Bullis et al., 1994). The mined mineralization roughly trends from north to south with lithological units steeply dipping at 80-85°. The major fault movements have occurred along roughly north and northest trending structures that are parallel to the fold axial planes resulting in widespread slickenslide structures (Ruskeeniemi et al., 2002).

There are open fractures present in boreholes on the 250 m, 890 m, 1105 m and 1130m levels as surveyed by the PERMAFROST Project. Fracture distribution appears an many of the fractures produced gas bubbles indicating either degassing or unsaturated zones within the mine.

Major fault zones trend nearly west to east in the southern portion of the mine complex and to the north, in the north end. These two major fault zones concur with western and eastern extremities of the formation. The Western Fault Zone is a regional shear zone but there has only been weak water flow in boreholes intersecting this structure. Several younger, minor sub-vertical faults cut the western and central zones and may be important hydrogeologically as conduits for groundwater flow (Ruskeeniemi et al. 2002).

2.1.3 Hydrology

The majority of the information below has been modified from information found in Ruskeeniemi et al. (2002) and Frape et al. (2004), unless otherwise indicated. The main surface water feature near the mine is Lake Contwoyto which acts as a local basin for most of the drainage from the small system of lakes and ponds existing around the mine. Lake

Contwoyto's long and narrow form suggests its basin is within a local fault line. Although the mine is located only 1.3 km from the closest shoreline, it is believed that the permafrost layer present beneath the mine prevents surface water infiltration at the mine site.

Furthermore, the low permeability of the rocks and the tight fracture system at the mine itself make it very dry with an average inflow between 24,000 – 53,000 m^3/yr. This number includes surface water pumped into the mine via pipelines from Lake Contwoyto. Consequently there are few subsurface locations that have relatively large amounts of groundwater flow.

Boreholes producing the most water tend to be drilled eastwards. Faults and fracture zones releasing the largest water volumes also indicate that a prevailing water conducting zone is located to the east of the mine. This zone appears to trend N-S with the underground mine workings. In Phase 1 of the PERMAFROST Project this zone was identified using video survey data found on the 890 m and 1130 m levels and was termed the V1 fracture zone (Figure 2.2). The fracture zone seems to support strong groundwater flow with significant and continuous water flow indicating notable lateral extent since permafrost is believed to disconnect this zone from surface water recharge.

Despite the presence of this fracture zone and two other conformable structures, hydraulic conductivity within the first 350 m of the mine is low and fracture dominated. In addition the hydraulic field appears disconnected, to very poorly connected, as revealed by poor response between boreholes during borehole response tests reported in Ruskeeniemi et al., 2002.

Hydraulic head measurements at depth indicate that the water table is located at approximately 600 m below ground surface. As mentioned above, depth of permafrost has been estimated at 500 m indicating an unsaturated zone of approximately 100 m below the

permafrost. This unsaturated zone is likely a result of dewatering of the bedrock due to the presence of the mine.

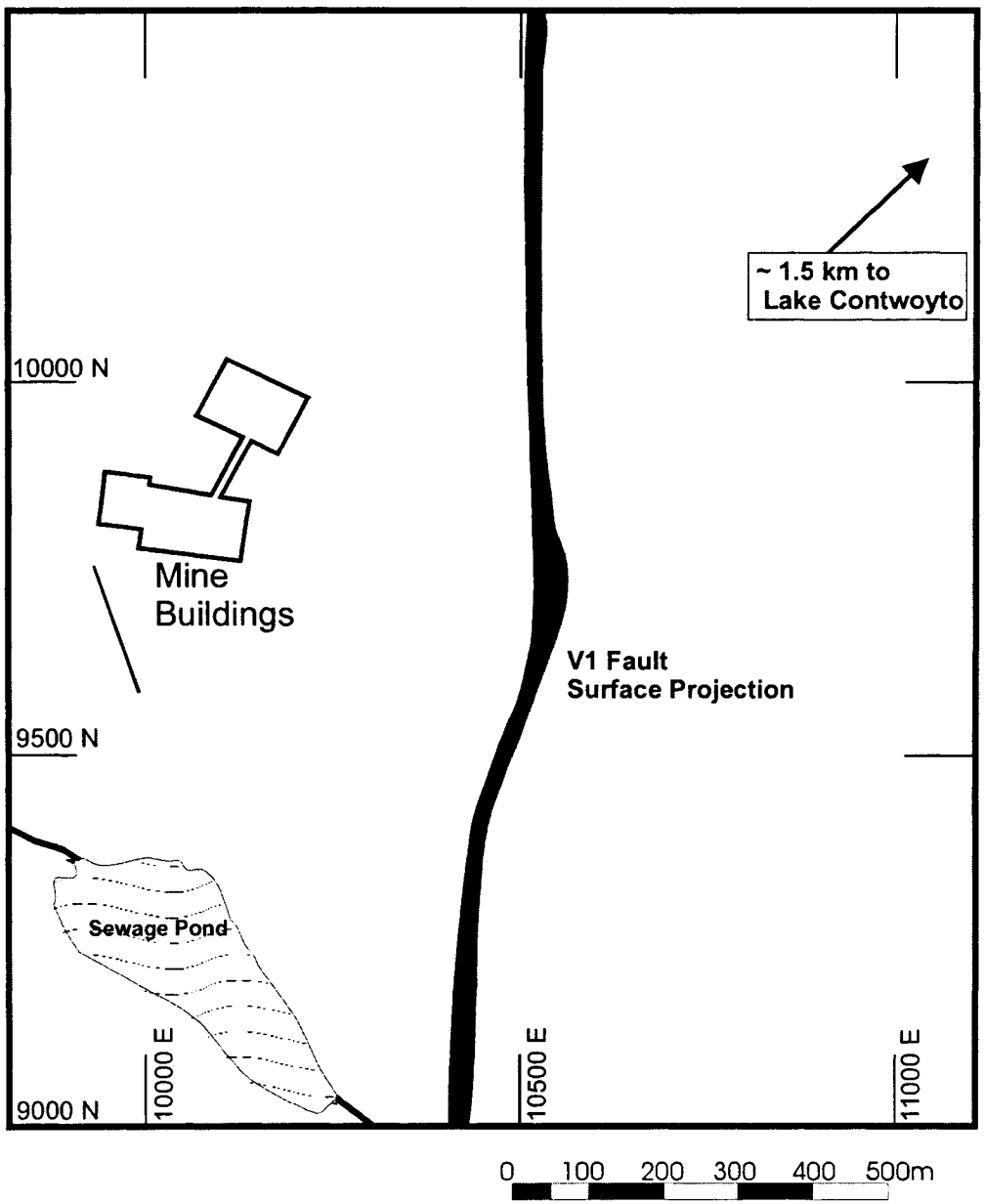

Figure 2.2 Surface features immediately surrounding the Lupin Mine site (modified from Ruskeeniemi et al., 2002). Mine eastings and northings are in meters.

2.1.4 Hydrogeochemistry

The following section briefly describes the hydrogeochemistry at the Lupin mine with a focus on the deepest levels. A more detailed description of hydrogeochemistry can be found in Ruskeeniemi et al. (2002) and Frape et al. (2004), from which the following was summarized.

Surface water sampled from Lake Contwoyto as well as precipitation are very dilute (TDS 0.006 - 0.022 g/L) and show no indications of a deep discharge component through talik. Stable isotope values from Lake Contwoyto fall between $\delta^{18}O$ values of -19.1 to -20.1 ‰ and $\delta^{2}H$ values of -158 to -160 ‰. Tritium measurements were high ranging from 15.8 to 20 TU.

In the upper parts of the mine, most boreholes and seepage surfaces intersect a common fault/joint structure, referred to as the ramp fault. A large spill of a Na-Cl brine created to prevent freezing during drilling in permafrost has reached this fault and in recent years, has spread throughout mine levels below. Ammonium nitrate, contained within the explosives used at the mine was also flushed with the spill and is the probable reason for the elevated nitrate levels observed. Finally, because waters used to create the drilling brine were from Lake Contwoyto there are elevated tritium levels (15 TU) found within them as well.

Groundwaters collected from within the permafrost above 540 m depth, the lower limit of permafrost, are of a Na-Cl or Na-Cl-SO_4 type. Salinity values vary between 7 and 40 g/L and exceptionally high NO_3 concentrations between 400 and 2600 mg/L are found. These waters are therefore likely present because of either their close proximity to the lower limit of permafrost or an increase in salinity caused by contamination from the Na-Cl spill.

The contamination from this spill has not yet reached the deep groundwaters found on the 890 m and 1130 m levels, as indicated by low tritium (<0.8) and nitrate values on these levels. The deep groundwaters are Na-Ca-Cl brines with TDS values ranging from 2 to 36 g/L. On the 1130 m level both high and low salinity water have been reported for boreholes within relative close proximity to one another (~100 m between the lowest and highest salinity boreholes). This supports the idea of a lack of connectedness of the hydrological framework deep within the Lupin mine.

On the other hand, comparison of trace elements and TDS suggests a common origin and mixture between highly saline and fresh, tritium free water at depth. The geochemical results given in Frape et al. (2004) reveal a lack of dissolved oxygen and tritium along with redox values between -10 and +24 mv. Such results indicate that the deep groundwater from the 890 m and 1130 m levels is most likely unmixed with mine water, and should be representative of natural conditions at this depth.

Due to elevated pressure on deep groundwaters they often contain more dissolved gases than waters of the same chemistry at surface. The main input source for the additional dissolved gases is geogenic production from deep bedrock (ie. methane, helium and argon). Within the deep groundwaters at the Lupin mine, methane usually accounts for 73 – 87 % of the dissolved gas, with ethane and propane as minor constituents.

2.2 Con Mine

The second mine included in this study, the Miramar Con Mine, is located in the town of Yellowknife, on the northwestern arm of Great Slave Lake, Northwest Territories, Canada

(Figure 1.1). It is located in the extensive discontinuous permafrost zone (Figure 2.1) with coordinates 62.27°N, 114.22°W and at an elevation of approximately 200 masl.

Present day climate includes a mean annual air temperature of - 4.6°C with extreme values between 32.5°C and - 51.2°C. The region is relatively dry receiving 280 mm of precipitation yearly. Vegetation cover is classified as transitional forest where tree cover is present but occupies less than 50% of the area. Low dense lichen mats, shrubs and mossy peatlands grow throughout the rolling topography and low relief.

The mine began operation in 1938 with the sinking of the C1 shaft followed by the Robertson shaft in 1974. Before decommissioning at the end of 2003 the mine had reached a depth of approximately 1902 m (6240 ft).

2.2.1 Regional and Mine Geology

The Con Mine is situated within the Yellowknife greenstone belt, southwestern portion of the Archean Slave Structural Province of the Precambrian Shield. Volcanic rocks of the Kam Group dating to 2.6-2.7 Ga compose the majority of the rock surrounding the mine. These rocks are dip sharply east to vertical and are mafic to intermediate tholeiitic volcanics that have been regionally metamorphosed by the Western Plutonic Complex (Helmstaedt and Padgham, 1986; McDonald et al., 1993). This complex is the eastern portion of a batholith extending along the western edge of the Slave Structural Province.

Gold mineralization is associated with the emplacement of the Western Plutonic Complex along northerly striking, westward dipping shear zones trending with the margins of the batholith in this region. The Con and Campbell shear zones are the main hosts for mineralization within the Con mine. Exploitation of the gold deposits has historically

concentrated around the Campbell Shear (Henderson and Brown, 1966; McDonald et al., 1993). The Con and Campbell shear zones are cut by post-diabase, Proterozoic fault structures which are important for groundwater movement within the mine. Four major faults systems have been identified within the underground mine workings: the West Bay, Pud, Negus and Angel fault systems (Henderson and Brown, 1966; Lindberg, 1987). The Pud, Negus and Angel Fault systems play an important role in the current research as they are present in the sections of the mine where sampling occurred.

The West Bay Fault, although a major regional feature for mine hydrology, is not directly intersected by mine openings and has only been observed in exploratory boreholes. The feature is oriented north-south with a westward dip direction. On the other hand, the Pud fault, which is also oriented approximately north-south, has hanging and footwall splays exposed in openings and drill holes at the southern end of the mine.

The Negus Fault is a northeast-southwest oriented system that dips to the southeast and is offset by the Pud Fault system by approximately 290 m with left lateral displacement. The Angel system consists of many east-west striking, near vertical faults observed at the southern end of the mine throughout its depth.

2.2.2 Hydrology

The hydrology of the Con mine is dependent on the fault and fracture systems listed above for groundwater flowpaths. Figure 2.3 shows the surface expression of these features and some nearby surface water bodies. Unlike at Lupin, there is no existing permafrost in the upper portions of the mine that prevents transport of surface water through these fault structures to depth. However, the local climate is such that surface water is frozen from

October to June and therefore groundwater recharge may only occur in significant quantities for roughly 3 months of the year.

Groundwater flow within the mine is primarily controlled by the fault systems listed and the related regional stress directions in relation to these faults. Accordingly, the Pud Fault, which is located normal to the principal direction of stress, has the lowest hydraulic conductivity and borehole flow rates (Intera Consulting Ltd et al., 1997). On the other hand, the Negus and Angel faults are oriented subparallel to the principal stress and have the highest hydraulic conductivities with inflows of up to 90 L/s (Intera Consulting Ltd et al., 1997, Clark et al. 2000).

The Negus and Angel faults have been flowing for over 45 years (Intera Consulting Ltd., 1997) indicating significant groundwater flow into the mine throughout its lifetime. These faults have changed the hydrogeochemistry of waters found at various levels in the mine. Significant depressurization and dewatering of the faults have introduced a steep hydraulic gradient around the mine causing an influx of surface water to replace water pumped from the mine. Surface water infiltration is a concern for the current research as it is important that brines are unaffected by recent recharge for the most accurate results. To overcome the dilemma of the surface water content present within mine groundwaters Clark et al. (2000) describe a mixing relationship using molar chloride concentration and oxygen isotopes.

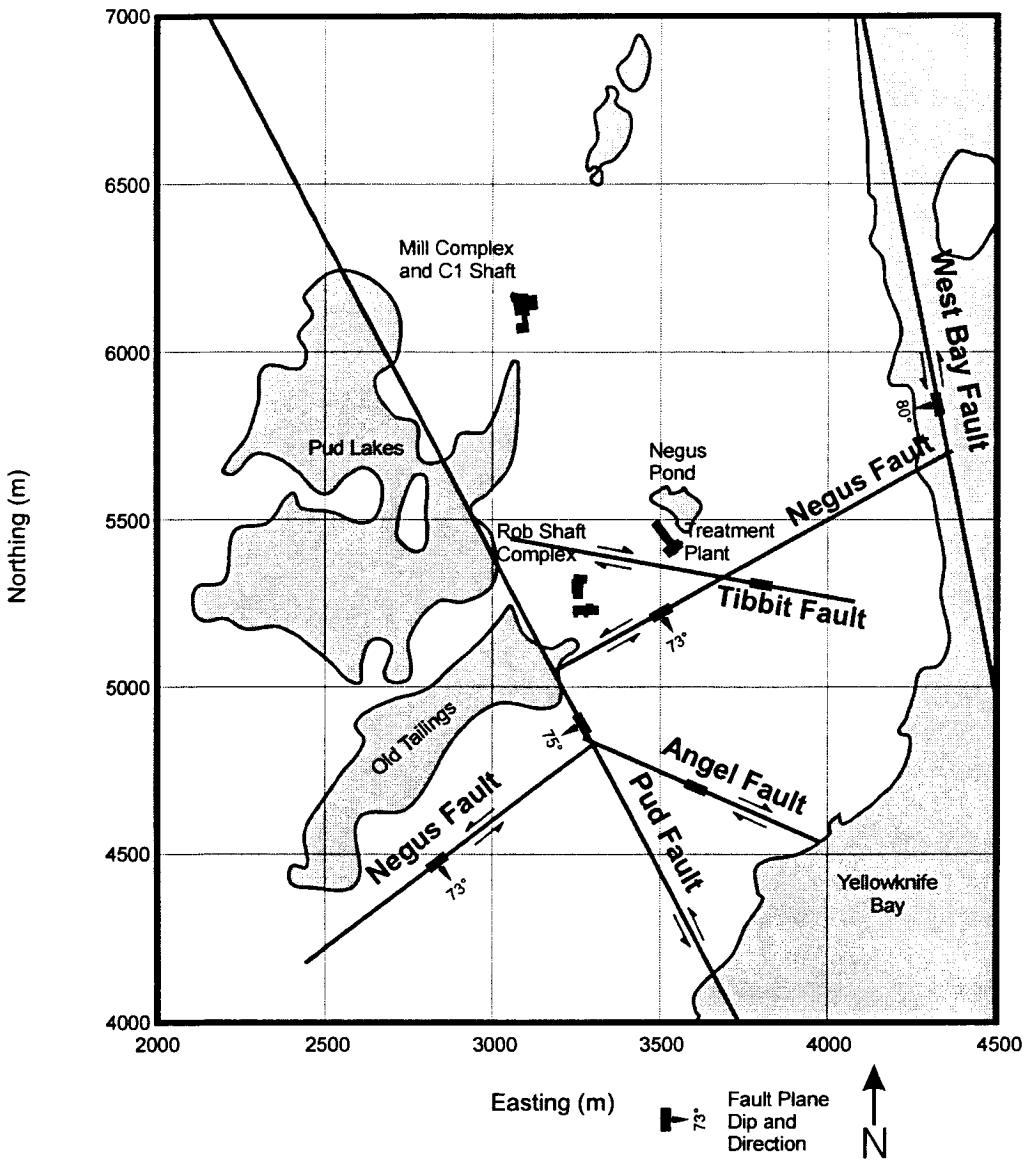

Figure 2.3 The Con Mine site and surrounding significant features (modified from Intera Consulting Ltd., 1997).

This mixing relationship includes three end members; Canadian Shield brine, recent meteoric surface water and glacial meltwater from the Wisconsin Glaciation. The calculation of the percent abundance for each component is described in detail in Intera Consulting Ltd., 1997. It is proposed that glacial meltwater was able to infiltrate up to

approximately 200 m below ground surface. However, movement and mixing of water induced by mine operation has pulled glacial meltwaters as deep as the 5300 ft level.

Under this mechanism the percentage of the three components present in mine water varies with depth. Shallow mine levels generally contain the most surface water while brine concentration increases with depth. The glacial component tends to vary as pockets of the meltwater are encountered from the 700 m (2300 ft) level all the way down to the deepest level sampled at 1615 m (5300 ft) (Intera Consulting Ltd., 1997).

2.2.3 Hydrogeochemistry

The hydrogeochemistry at various levels within the Con mine is generally governed by the fractions of the three identified end-members present within an individual groundwater. As outlined in Clark et al. (2000), the brine fraction is a high TDS, Ca-Na-Cl type groundwater with a $\delta^{18}O$ value near -10 ‰. The modern fraction, composed of surface water, is very dilute with relatively enriched sulphate concentrations compared to the other fractions. The modern fraction has a $\delta^{18}O$ value of -18.9 ‰. Finally, the glacial fraction has relatively high concentration of bicarbonate, relatively low TDS values and a $\delta^{18}O$ value near -28 ‰. Hydrogeochemistry of the Con mine will be discussed in further detail in Chapter 4.

3 Methods

The following chapter describes the techniques used to both sample and analyze the deep groundwaters from the Con and Lupin mines.

3.1 Major Ion Geochemistry and Stable Isotopes

Water samples were collected from several deep boreholes at the Lupin and Con mines for major ion geochemistry and stable isotope analysis. Samples from the Lupin mine were collected by researchers from the Geological Survey of Finland as well as the personnel from the University of Waterloo. Analysis of major and minor ion chemistry for these samples was completed in the Geolaboratory at the Geological Survey of Finland while tritium as well as oxygen and hydrogen isotope analyses were completed at the University of Waterloo. The University of Waterloo also measured gas content measurement and collected gas samples from the same boreholes sampled for noble gases. A detailed description of results and methods are reported in Frape et al. (2004).

Major ion geochemistry and stable isotope analysis for water samples collected from the Con Mine were completed at the University of Ottawa by the researcher. Samples were collected from boreholes using 1 L Nalgene HP or amber glass bottles. High salinity samples were diluted between 2 to 4000 times for major ion analysis to ensure results would fall within the detection limits of the analyzer. Dilutions were based on predicted results assembled from a historical record of results obtained from the same boreholes as those sampled in the current research (Frape et al., 1984; McDonald, 1986; Douglas, 2000; and Battye, 2002). Analysis involved the use of SCP Science standards with every sixth sample being a duplicate.

Chloride was measured by means of a potentiometirc titration using a Beckman chloride electrode. The remaining major ion analysis was completed with the assistance of Monika Wilk on a simultaneous radial Vista-Pro ICP-OES that was optimized for power viewing height and nebulizer flow. Samples analysed on the Visto-Pro ICP-OES were filtered through a 0.45 μm HT Tuffryn membrane and then acidified to a pH of 1 by adding 0.2 ml of concentrated nitric acid.

Prior to stable isotope analysis for ^{18}O and ^{2}H grains of charcoal were added to remove unwanted organics while fragments of copper were added to remove sulphur. Oxygen-18 content in water was measured by CO_2 equilibrium, and δ^2H by equilibrium with H_2. Platinum Hoco sticks were used as catalysts to decrease equilibration and exchange time for ^{2}H analysis. Stable isotope analysis was completed at the G.G. Hatch Isotope Laboratories at the University of Ottawa.

3.2 Noble Gas Collection and Analysis

Water samples along with dissolved gas samples were taken from the Lupin and Con mines for noble gas analysis. Specific collection and analysis methods for both water and dissolved gas samples are described in the following sections. Time constraints imposed by mine operations prohibited collection of both water and dissolved gas samples at all boreholes.

3.2.1 Copper tube sampling

Water samples were collected in 3/8 " (outer diameter) un-annealed copper tubing and sealed on both ends with pinch tools. The pinch off tools used bolt directly over the ends of the copper tubes to create a cold weld seal. To ensure comparable volumes each water

sample was clamped in a small cradle system which creates a constant 30.35 cm long sample yielding approximately 13.94 cc of water (Figure 3.1).

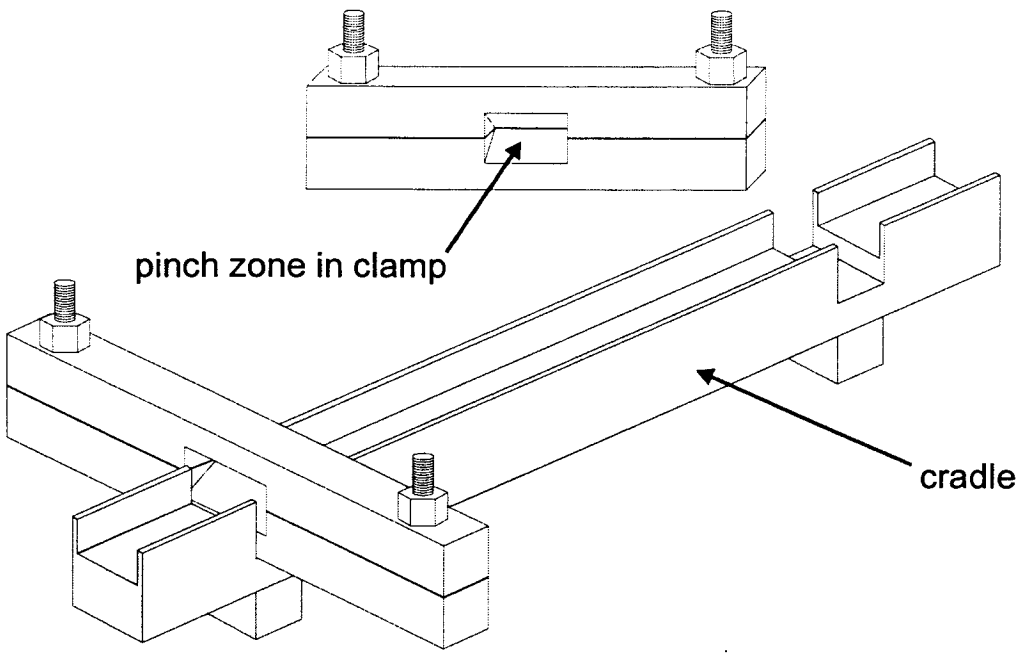

Figure 3.1 Pinch tool and cradle system used to create a cold weld seal for copper tube water samples.

To obtain the water samples a series of pipe connections were attached to a margo plug in the drift wall as shown in Figure 3.2. Copper tubes were attached in series and connected to the margo plug via a valve used to control flow from the borehole. A second valve was placed on the distal end of the series of copper tubes to control outflow from the copper tubes. Pressure gauges were located upstream of flow control valves to monitor pressure within the borehole and copper tubes both before as well as after flushing and sampling.

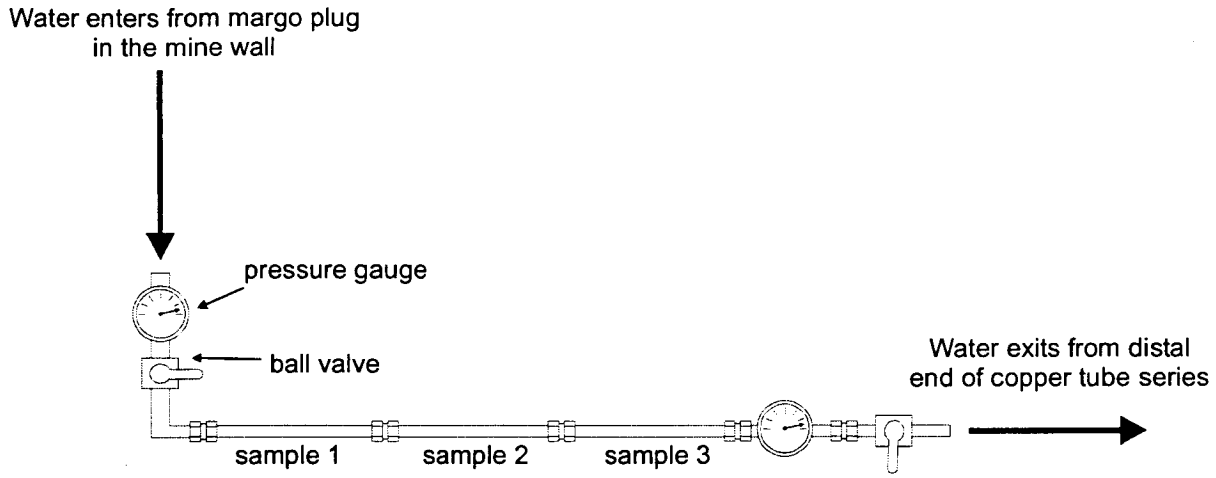

Figure 3.2 Plan view of the setup for retrieval of copper tube water samples from the mine wall.

After the series of copper tubes was attached to the margo plug the boreholes were flushed between 1 – 2 hours. Flushing time was based on the status of the borehole before sampling for the reason that, in many instances at the Lupin mine, the boreholes were previously flushed by other researchers from the PERMAFROST project.

Boreholes were flushed for several reasons:

- to remove air and other impurities or solid particles from the copper tube series which may have entered during transport,
- to remove a significant column of water or gas from the borehole to ensure a pristine sample,
- to fill bottles and a flow cell for in-situ field measurements.

Once flushing was completed water flow was reduced and pressure recovery within the borehole was monitored. Once pressure had stabilized or reached pre-flushing values the second control valve was opened slightly to release any gas which may have accumulated during pressure recovery. Next, tubes were gently tapped to remove any additional trapped

air bubbles and samples were clamped using the cradle apparatus. Finally, copper tube water samples were removed from the margo plug and the gas diffusion samplers were installed.

3.2.2 Gas Sampling with Diffusion Samplers

The second apparatus, the diffusion sampler, involves a recently developed method designed to sample only the dissolved gases from the water. Dissolved gas sampling for noble gases has traditionally used the copper tube method described above whereby a sample of groundwater is taken from which dissolved gases are later extracted. The Lupin PERMAFROST project was the first deployment of a diffusion sampler of this kind, which had been modified for the elevated hydraulic pressures present deep within these mines.

3.2.3 Diffusion Sampler Theory

The diffusion sampler is part of a new effort to develop a method to passively sample dissolved gases in-situ through re-equilibration (Sheldon, 2002). A sampler constructed of tubing and a tire stem schraeder valve had been used to sample helium and neon concentrations in groundwater (Sanford et al. 1996). Ping-pong balls have also been used as samplers to examine dissolved gases in lake water and sediments (Dyck and Da Silva, 1981; Gascoyne and Sheppard, 1993; Stephenson et al. 1994). However, these methods proved unable to prevent leakage or re-equilibrium following re-deployment.

The basis of the diffusion sampler is that dissolved gas will diffuse through a semi-permeable membrane (ping-pong ball wall, latex or silica tubing) until the partial pressure of gases within the water is equal to the partial pressure within the sealed membrane.

The time necessary for this will depend on both the physical properties of the sampler itself as well as the diffusive properties of the dissolved gases. The internal volume of the

sampler, the area of membrane exposed and membrane thickness are the major physical parameters to be considered. Individual gas diffusion coefficients through the membrane and the gas phase concentration, both within the sampler and dissolved within the water are the diffusive properties to be considered. The following equation was developed by Sanford et al. (1996) to evaluate equilibration time necessary based on the above factors.

Equation 3.1

$$C_r = H_{cc}\, C_w \left(1 - \exp\left[-DAt / V_i L \right]\right)$$

Where: C_r = gas phase concentration within the sampler ($M\ L^{-3}$)
H_{cc} = dimensionless Henry's constant
C_w = dissolved concentration ($M\ L^{-3}$)
D = effective gas diffusion coefficient in membrane (L^2/T^{-1})
A = area of membrane exposed to water (L^2)
t = time
V_i = internal volume of sampler (L^3)
L = membrane thickness (L)

The value received from Equation 3.1 can only be considered an estimate of the time necessary to obtain equilibrium between dissolved gas concentration and gas concentration in the sample as the result was not verified by field tests. In addition, values for the effective diffusion coefficients for all dissolved gases have not been determined (eg. krypton). A more direct approach described in Sheldon (2002) measures equilibration times for different systems. Sheldon has listed an equilibration time of 7 hours for a single sided sampler similar to the setup used in this project which used a double-sided / two-ended sampler instead. Accordingly, our equilibration time should be approximately 14 hours. However, owing to an increase in internal volume by a factor of 2 and a relatively small increase in the exposed membrane area, the minimum sample equilibration time for this project was set to 24 hours.

The diffusion sampler method is still being tested and will have a number of advantages over traditional water samples if found viable. Primarily it allows for a much "cleaner" sample which in turn permits a shorter laboratory analysis time and substantially shorter sample turnover rate. Smaller and lighter sample size is the major logistical advantage.

3.2.4 Design and Operation

The prototype design was based on the diffusion sampler described in Sheldon (2002) but was modified to operate at the high formation water pressures encountered within the deep groundwaters of the Canadian Shield. The sampler consists of the main body or water chamber and the 1/4"(outer diameter) un-annealed copper tubes that attach to it as shown in Figure 3.3.

The main body of the diffusion sampler is a stainless steel cylinder that is solid across the bottom with an open top giving access to a chamber in the centre of the cylinder. The central chamber is sealed with an o-ring and Plexiglas lid, which creates a water-tight seal by attachment with a stainless steel ring and retaining bar to prevent deformation at high water pressure.

There are eight ¼" holes through the main body; on the outside, ¼" threaded ports have been welded around these holes while inside, these holes continue as cylinders into the chamber. These small cylinders then act as nipples to which silica tubing is attached. The silica tubing is filled with silica glass beads to prevent crushing by water pressure. Both ends of three separate pieces of silica tubing are attached to opposite ports and clamped to create a seal over the nipple. The two ports that remain unattached by silica tubing are used, via attachment of valves, to control water flow in and out of the central chamber.

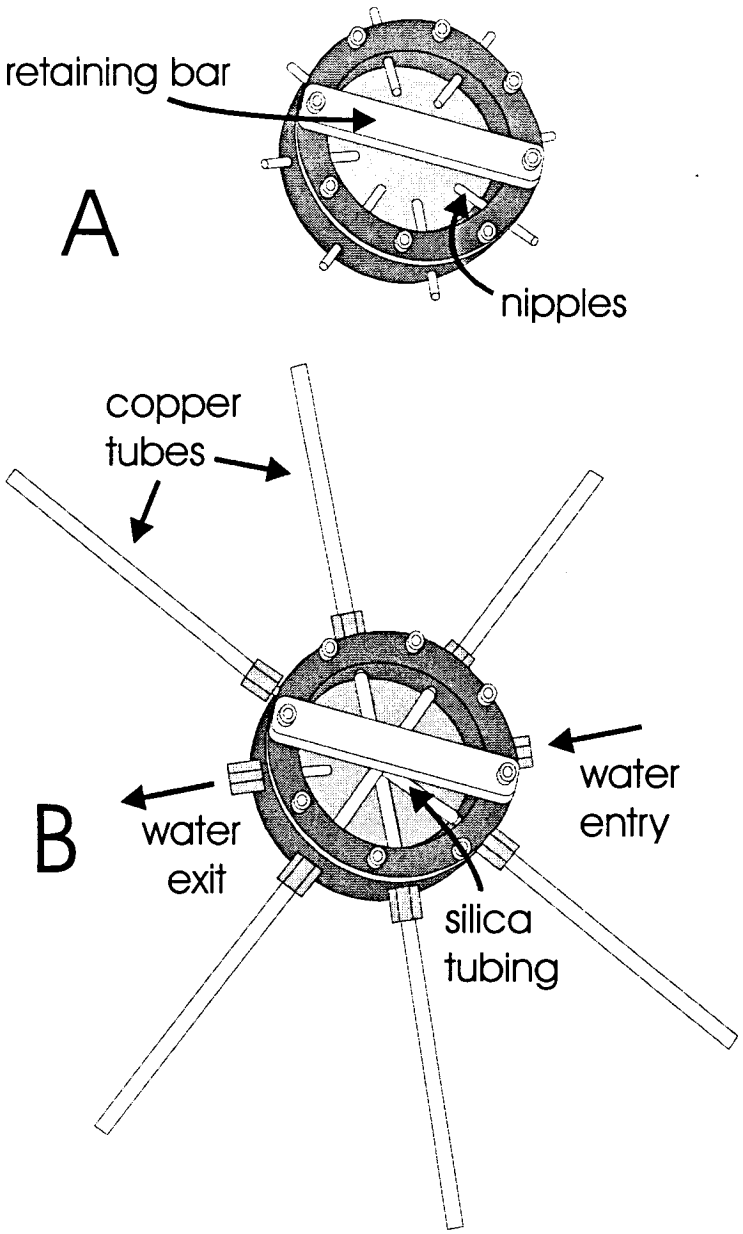

Figure 3.3 Modified diffusion sampler A) with copper tubes and silica tubing off B) silica tubing and copper tubes attached.

Six ¼" copper tubes, ~ 13-14 cm long that are attached to the threaded ports outside the sampler are pinched and soldered on the distal end to maintain an air tight cold seal. Glass wool is placed between the copper tubes and the silica tubing to prevent the glass beads from entering the copper tubes.

The sampler is attached to the margo plug in the mine wall via one of the two remaining free ports. Once attached to the margo plug sampling operates much the same as with copper tube water sampling; the sampler is flushed and flow reduced. The diffusion sampler is left with reduced flow for a much longer period of time, typically at least 24 hours. This allows gases within the sampler to diffuse out and gases within the water to diffuse in. When the apparatus is ready, pinch off tools are again used to create a cold weld seal, the samples are removed from the sampler and ready for transport.

No such cradle existed for the ¼" diffusion samples as with the water samples at the time of sampling and as a result the volume varies from sample to sample. A separate volume calculation is therefore completed for each individual air sample based on the individual lengths of analysed sections.

3.3 Inert Gas Analysis – Isotope Dilution

For an accurate determination of the concentration of noble gases within both water and gas diffusion samples a method of isotope dilution described in Youngman, (1989) is used. This involves using a precisely measured air volume whose noble gas isotopic composition and concentration is known. This air standard is used to determine the isotopic composition of noble gases in a known volume of tracer spike. The spike is enriched in minor isotopes of each of the noble gases in air (i.e. ^{3}He, ^{22}Ne, ^{36}Ar, ^{78}Kr and ^{136}Xe). Using the known ratios of each noble gas in air allows for the calculation of the concentration of noble gases within the fixed volume spike.

Knowing the isotopic composition of the tracer spike provides the means to calculate the noble gas concentration in the water or gas diffusion samples. Using the ratio of known

tracer values to a known volume of sample the volume of noble gases in the sample can be calculated. The following calculations are based on Youngman (1989) and use argon as an example where each noble gas is substituted:

a) a simplified version of Youngman's equation:

Equation 3.2

$$R = \frac{^{36}V_t}{^{40}V_{at}}$$

Where: R = ratio

V_{at} (Ar) = volume of atmospheric (sample) Ar at STP

V_t (Ar) = volume of tracer Ar at STP

b) Youngman's equation including trace amounts of both minor and major isotopes found in both the atmosphere and tracer.

Equation 3.3

$$R = \frac{^{36}Ar}{^{40}Ar} = \frac{\left(^{36}X_{at} \times V_{at}(Ar)\right) + \left(^{36}X_t \times V_t(Ar)\right)}{\left(^{40}X_{at} \times V_{at}(Ar)\right) + \left(^{40}X_t \times V_t(Ar)\right)}$$

In the case of argon:

$^{oo}X_{at}$ = mole fraction of the isotope ^{oo}Ar in atmospheric Ar

$^{oo}X_t$ = mole fraction of the isotope ^{oo}Ar in tracer Ar

V_{at} (Ar) = volume of atmospheric (sample) Ar at STP

V_t (Ar) = volume of tracer Ar at STP

c) Rearrangement of Equation 3.3 solving for V_{at} gives:

Equation 3.4

$$V_{at}(Ar) = \frac{V_t(Ar) \times \left({}^{36}X_t - ({}^{40}X_t \times R)\right)}{\left(({}^{40}X_{at} \times R) - {}^{36}X_{at}\right)}$$

The ability to achieve good accuracy on small samples is the main benefit of using ratios instead of absolute values. The spike volume is systematically checked on a regular basis by running air standards between samples to monitor any slight changes that may be occurring in spike volume over time.

3.3.1 Sample Extraction and Isolation in Water and Gas Samples

Essentially, sample extraction and analysis is completed on an ultra-high vacuum stainless steel gas line that separates the noble gases from other gases, and then separates the noble gases into three portions. These portions include: (i) neon and helium, (ii) krypton and xenon, and (iii) argon and helium. A more detailed description of this method can be found in Battye (2002) while modifications to Battye's procedure for this research can be found in Appendix A. What follows is a summary that utilizes the reference letters from Figure 3.4, a schematic diagram of the noble gas vacuum line, to explain the extraction process.

The noble gas analytical procedure begins with a heating and cleaning of the vacuum line. Cleaning acts to minimize background interference and assists in maintaining a high vacuum within the line. Following cleansing the line generally evacuates to a value near 2.0 x 10^{-7} Torr. Next a sample is attached at the sample inlet (**E**) and the line is re-evacuated to a pressure of approximately 10^{-5} Torr.

To start the procedure, the sample is released from **E**. If the sample is water, it passes through a methanol–dry ice trap whose temperature is approximately -80°C. Any liquid water is frozen as ice, which keeps the vacuum line dry. If the sample is gas, the copper tube is immersed in a methanol-dry ice trap to prevent water contamination of the vacuum line in case the diffusion sampler seal was compromised during sampling. Next a fixed quantity of tracer is released from the tracer spike tank at **N** and enters the main line through a series of valves where it mixes with the sample.

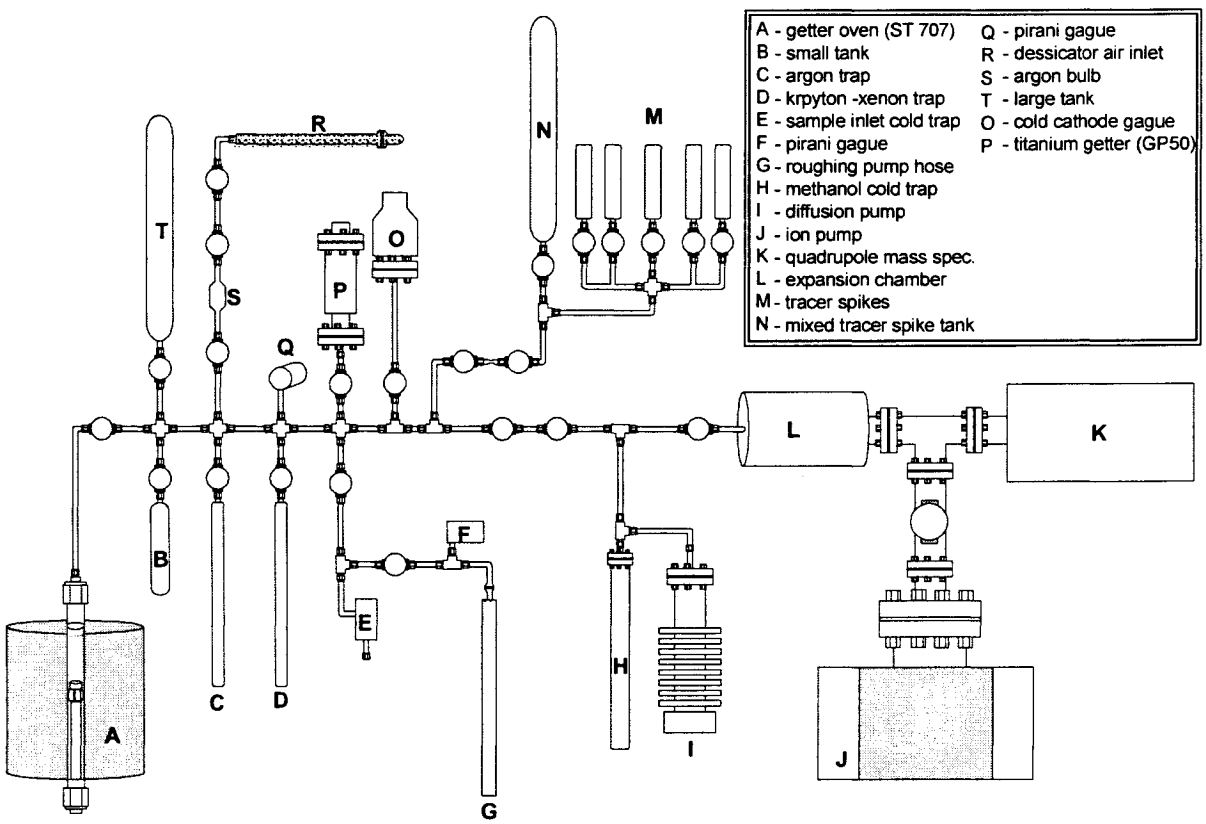

Figure 3.4 Schematic of the high vacuum noble gas extraction and isolation line.

Now that both the sample and the tracer are present in the main line the first gas separation is achieved through gettering. Gettering involves removal of unwanted gases including N_2, O_2, CO_2 and CH_4 through absorption by reaction with zirconium-vanadium-iron pellets at **A**.

When gettering is complete the second gas separation technique adsorbs argon and krypton-xenon on specific activated carbon traps at sub-zero temperatures for later release and analysis. Before absorption onto carbon an initial analysis of argon and helium is run through the gas expansion chamber (**L**) and the quadrupole mass spectrometer (**K**) for later comparison. When ratio measurement is complete the quadrupole and expansion chamber are evacuated by the StarCell Ion Pump (**J**).

Krypton and xenon are removed first by freezing onto an activated carbon trap at roughly - 80°C (**D**). A bulb of argon and helium is then taken at **S** for later analysis. After the argon bulb is taken the remaining argon is removed by freezing on a separate carbon trap (**C**) at approximately -196°C. Once this remaining argon has been trapped neon and helium are theoretically the only gases remaining. Neon is then analyzed using a reduced electron activation energy to avoid measurement of doubly charged argon which may still remain in small quantities.

Following neon analysis the main line is evacuated using the diffusion pump (**I**). Krypton and xenon are then released by heating of the carbon traps to between 350 – 400 °C, after which analysis of these two gases occurs simultaneously. The line is again evacuated and finally argon and helium are released from the argon bulb and analyzed.

3.4 Sampling Sites

Sample sites at both the Lupin and Con mines were located at existing diamond drilled boreholes. The following section describes the location and type of samples taken from each mine level and borehole.

3.4.1 Lupin Mine

Within the Lupin Mine sampling for noble gases was completed on existing boreholes included within the PERMAFROST project. Two mine levels, the 890 m (2920 ft) and 1130 m (3707ft) levels were sampled during May 2003 and May 2004. The first sampling round was completed by the author while the second round was completed by representatives of the PERMAFROST project from Ontario Power Generation (OPG) and the University of Waterloo.

890 m (2920 ft) Level

The only borehole sampled on this level was B-188 which is located in the middle of the mine workings near the end of the most easterly drift (Figure 3.5). The borehole, drilled horizontal and toward the southeast, is 523 m in length and intersects fracture zone V1. Although the borehole is horizontal flushing of the borehole prior to sampling should remove any air pockets present.

Copper tube water samples collected in May 2003 had a final shut-in pressure of roughly 290 psi after the borehole had recovered from a pump test. This ensured the borehole was well flushed. Six gas diffusion samples were also collected during the May 2004 sampling round.

1130 m (3707 ft) Level

Figure 3.5 indicates the location and direction of the five boreholes sampled on the 1130 m level. All five boreholes were drilled horizontal and towards the SE. Boreholes 192, 217 & 191 are located in a new exploration drift opened in April 2002 allowing sampling

farther from the main body of the mine then any other location. The other two boreholes, 197 and 219, are in close proximity to this new exploration drift.

The length of boreholes sampled on the 1130 m level varies between approximately 336 m for B-219 to nearly 575 m for B-197. Four of the five boreholes sampled (B-191, 192, 197, and 217) intersect fracture zone V1 while B-219 intersects fractured bedrock close to V1. Shut in pressures ranged from 715 psi for B-197 to 190 psi for B-219. Shut-in of boreholes with these pressures was hypothesized to help avoid degassing of water prior to sampling.

The only gas diffusion samples taken during the first sampling round in May 2003 were from borehole 197 where six samples were retrieved. Three copper tube water samples were taken from all the other boreholes, as well as from borehole 197 during this sampling round. During the May 2004 sampling round six gas diffusion samples were taken from boreholes 188, 192 and 273.

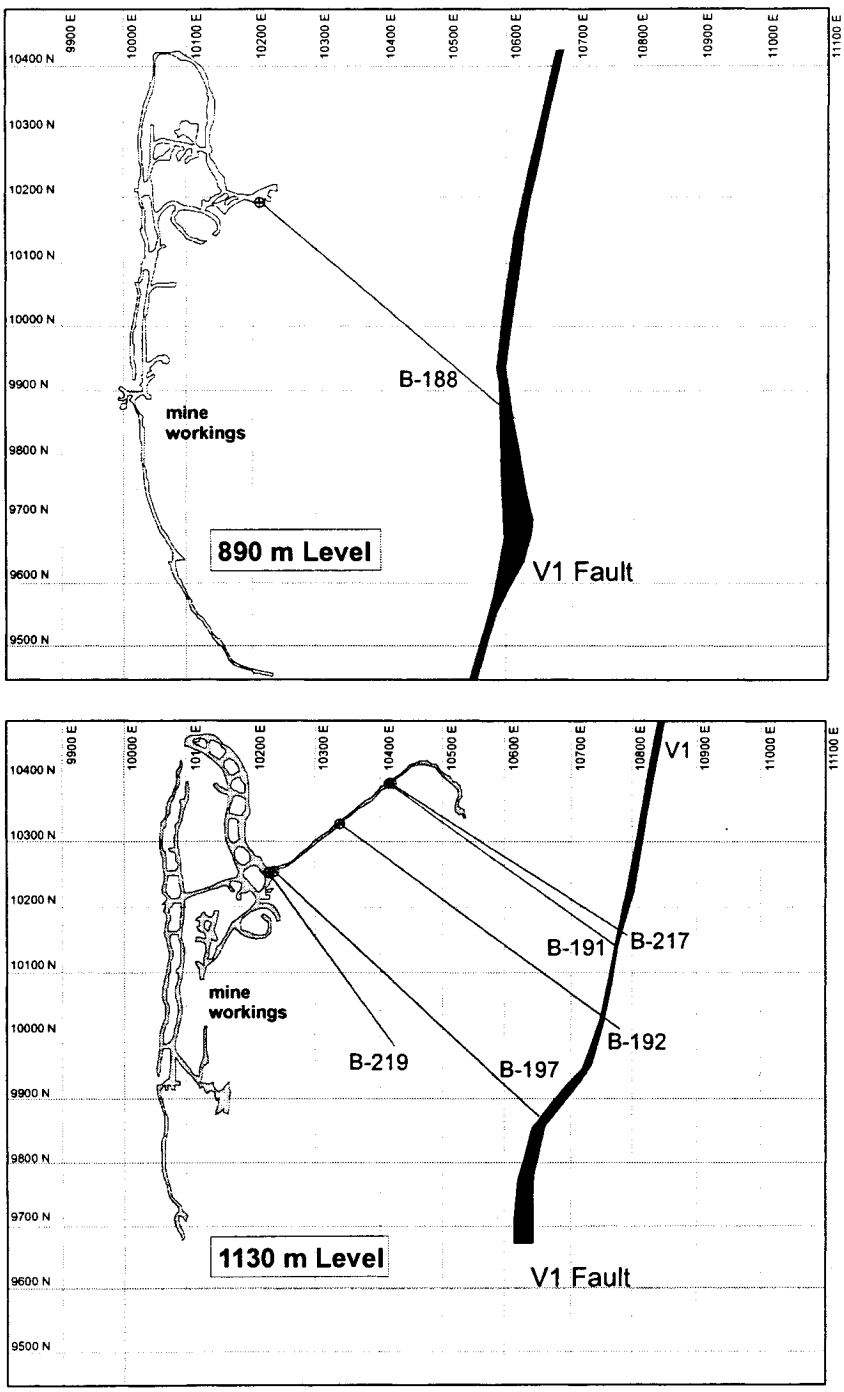

Figure 3.5 Plan view of the mine workings on the 890 and 1130 m levels, Lupin mine (modified from Ruskeeniemi et al., 2002).

3.4.2 Con Mine

Within the Con Mine, water was sampled by the author for noble gas concentration as well as water geochemistry and stable isotopes between September 30 – October 3, 2003. Four mine levels; 1070 m (3500 ft), 1370 m (4500 ft), 1490 m (4900 ft) and 1615 m (5300 ft), were sampled for water geochemistry and stable isotopes (Figure 3.6). Alternatively three levels, 1070 m (3500 ft), 1490 m (4900 ft) and 1615 m (5300 ft), were sampled for noble gases. Sampling at the Con Mine took place at a number of existing boreholes previously analyzed by others (Frape et al. 1984; McDonald, 1986; Intera Consulting Ltd. et al, 1997; Battye, 2002).

1070 m (3500 ft) Level

The only borehole sampled on the 1067 m level, B-8906, is located near the end of the southern drift as shown in Figure 3.7. Orientation of the borehole is northwest and intersects the Angel Fault at approximately 9 m and is 13 m in total length. Sampling for water geochemistry and stable isotopes was followed by deployment of a diffusion sampler from which six gas diffusion samples were retrieved. Unfortunately due to time constraints and mine scheduling no copper tube water samples were taken from this level.

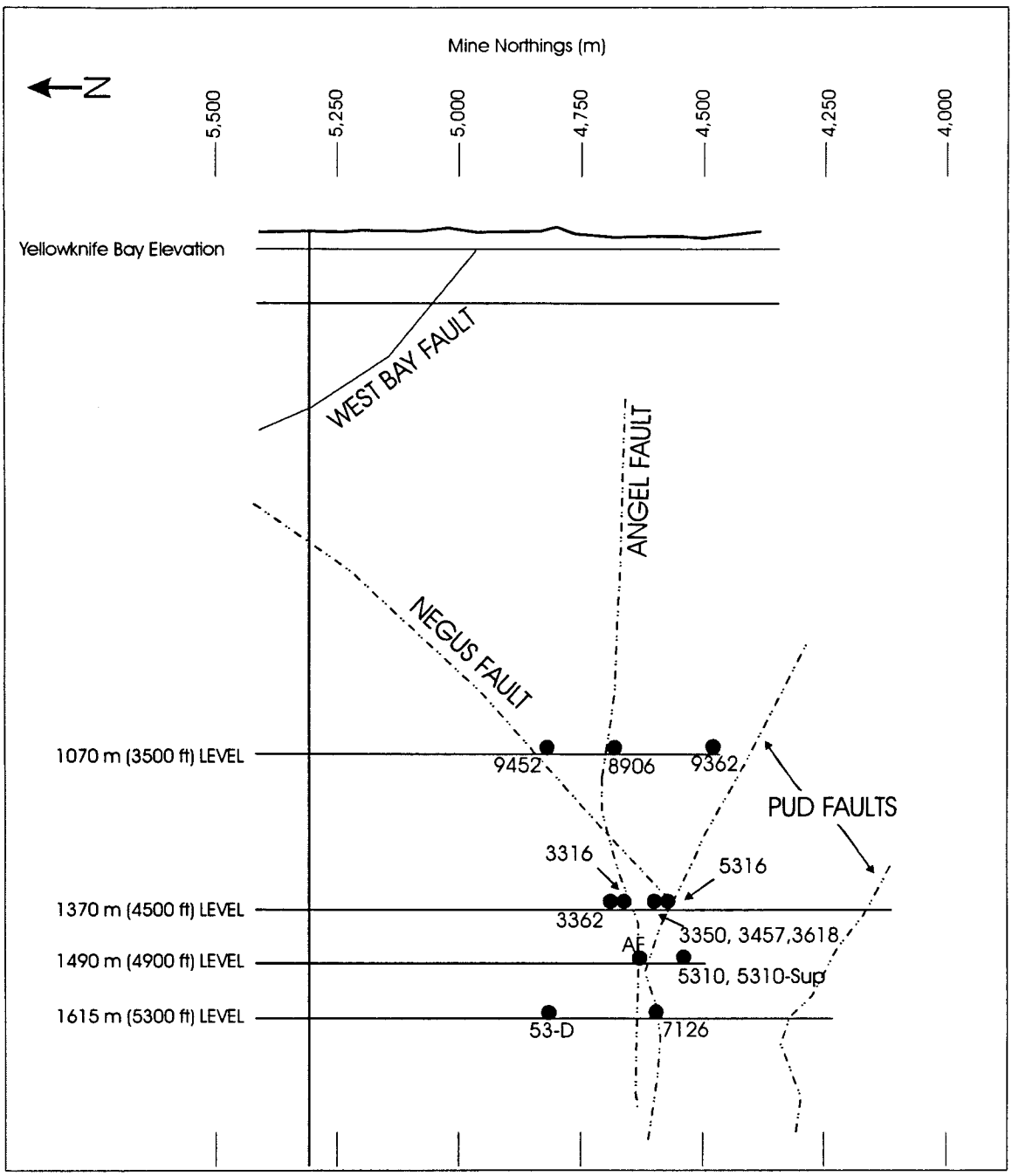

Figure 3.6 Cross-section of the Con Mine (modified from Intera Consulting Ltd. et al., 1997).

1370m (4500 ft) Level

Sampling on the 1370 m level was concentrated to the middle section of the drifts south of the Robertson shaft in an area where the Angel, Pud and Negus faults intersect as

seen in Figure 3.7. Three of the six boreholes sampled on this level intersect multiple faults through their lengths. Table 3.1 lists these intersections along with orientation and total length for each borehole based on information reported in Intera Consulting Ltd., (1997). Sampling on the 1370 m level was restricted to water geochemistry and stable isotope sampling; no water or gas diffusion samples were collected from this level.

Table 3.1 Orientation, length and fault intersections of boreholes sampled on the 1370 m (4500 ft) level.

Borehole	Orientation	Total Length (m)	Fault intersections
B-3362	east	179	negus, angel, pud
B-3316	south	92	angel and pud
B-3450	east	107	negus
B-3457	southeast	270	negus
B-3618	southeast	360	negus
B-5316	east	193	pud, negus

1490m (4900 ft) Level

The location of the only borehole sampled on the 1490 m level (B-5310) is shown on Figure 3.6. Although there is no plan view available for this location, the borehole is oriented in an easterly direction with a total length of 189 m. The borehole intersects the Pud and Negus faults. In addition to this borehole, the Angel fault was also sampled via collection of water draining from the ceiling on this level and is shown on Figure 3.6 as **AF**. Water samples were collected for geochemistry and stable isotope analysis at both locations. In addition, six copper tube water samples as well as six gas diffusion samples were collected from B-5310 for noble gas analysis.

1615 m (5300 ft) Level

Figure 3.7 shows the sampling location B-7126 on the 1615 m level, the deepest level sampled at the Con Mine. Another borehole, with an unknown ID number other than the

geochemical label ID (53-D) listed by Intera Consulting Ltd. et al. (1997), was sampled for geochemistry and stable isotopes. This small diameter borehole appears to be drilled along the same azimuth as B-5586 and probably intersects the same features, that is, various Pud fault splays. An offset of the Angel fault by the Pud fault has been suggested on this level and B-7126, drilled to the east for 13 m, intersects one of these offsets. In addition to water sampling for geochemistry and stable isotopes, six copper tube water samples as well as twelve gas diffusion samples were collected from B-7126.

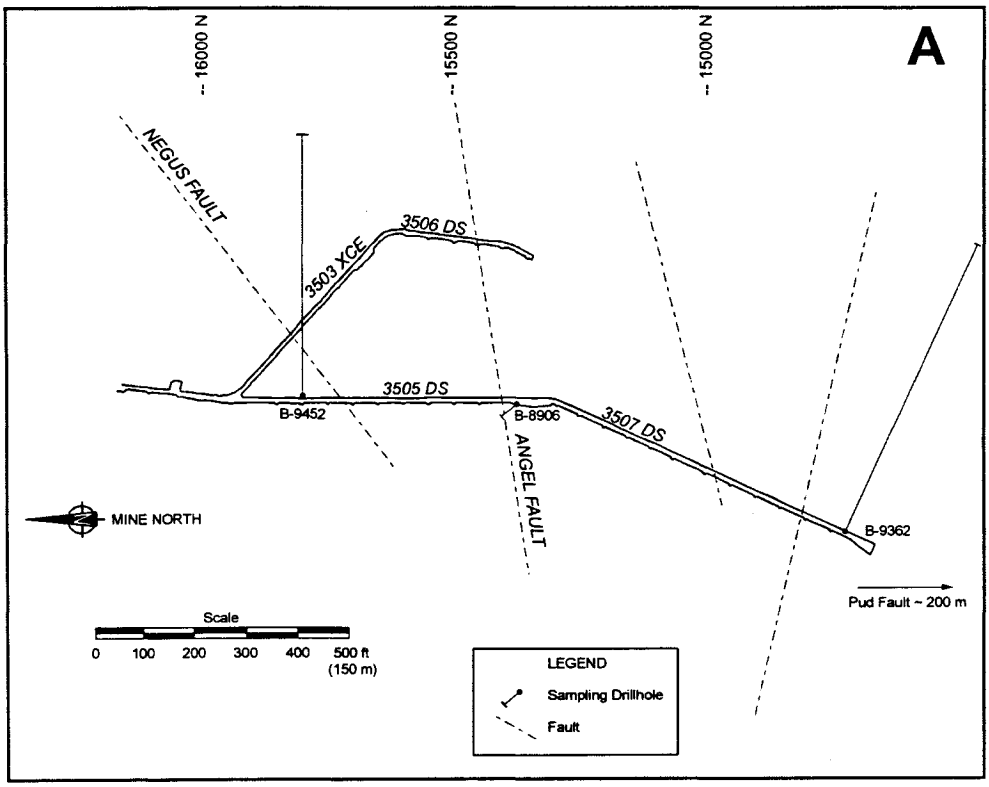

Figure 3.7 **cont. on next page**

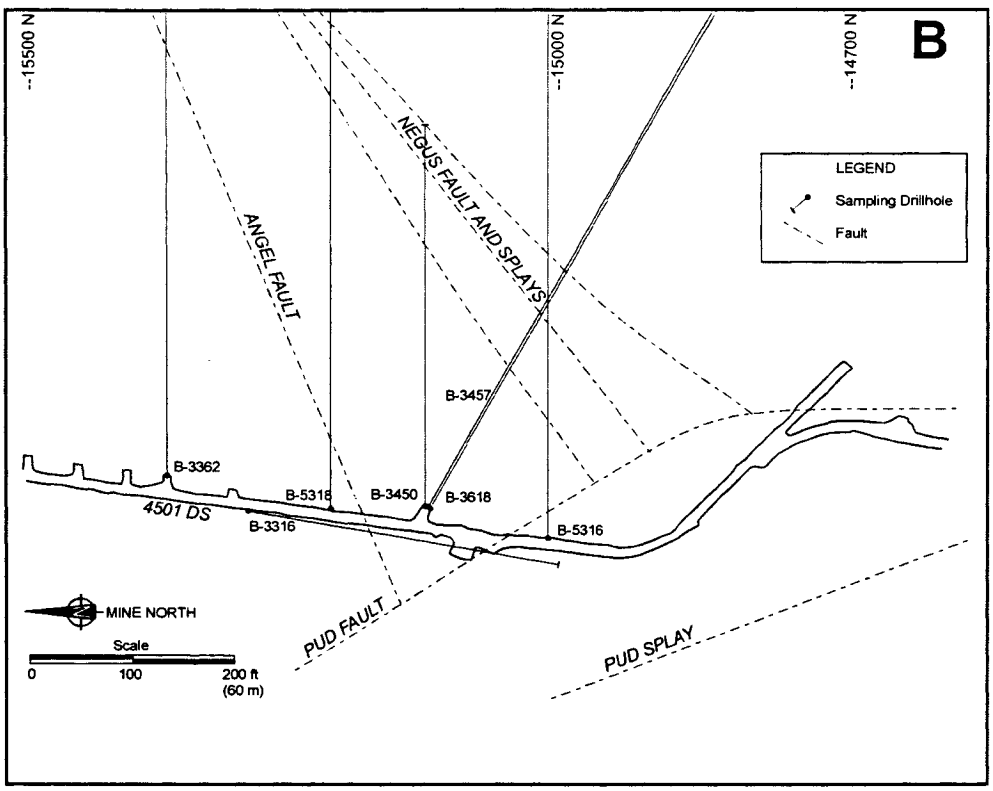

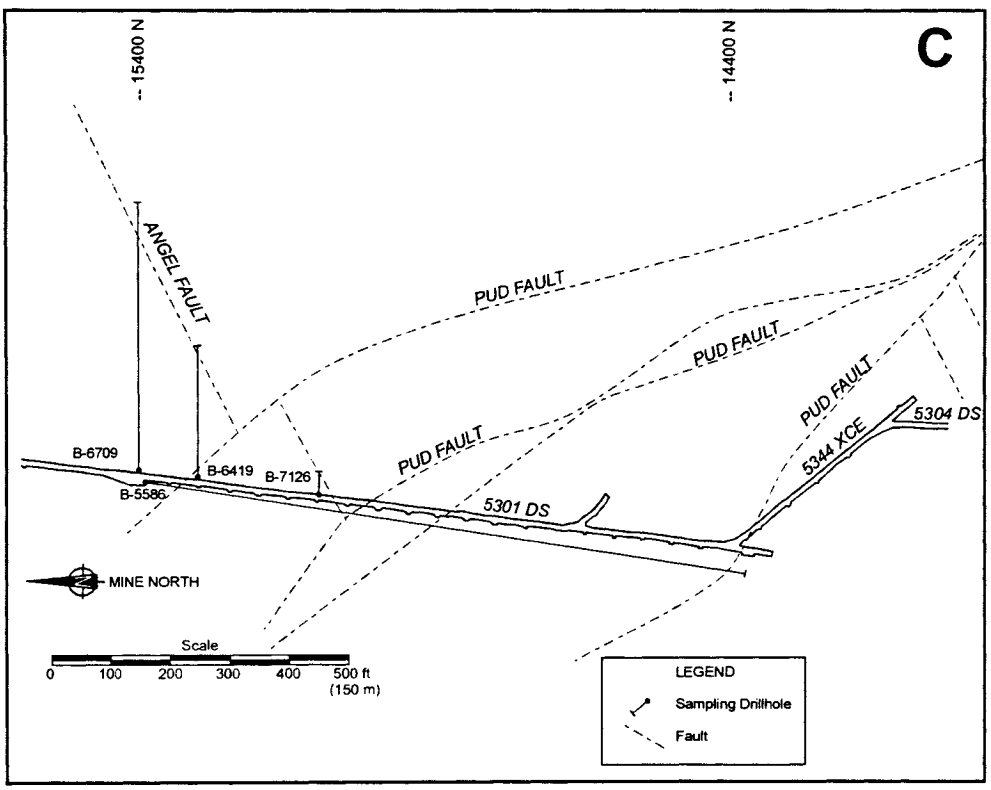

Figure 3.7 Plan view of mine workings on the 1067, 1370, and 1615 m levels, Con mine (modified from Intera Consulting Ltd. et al., 1997).

4 Results and Discussion

Results of field sampling and laboratory analysis along with a discussion of their significance are presented in the following chapter. Major ion and stable isotope geochemistry for the Con mine are presented along with a general overview of measured noble gas concentrations at both mine locations. Detailed analysis of noble gas results are presented in Chapters 5 and 6 for the Con and Lupin mines, respectively.

The hydrogeochemical and stable isotope data for the Lupin mine has been reviewed in section 2.1.4 as presented by representatives from the Geological Survey of Finland and the University of Waterloo in Ruskeeniemi et al. (2002) and Frape et al. (2004).

4.1 Major Ion and Stable Isotope Geochemistry – Con Mine

The data in the following sections summarizes the geochemical character of the deep groundwater collected from four levels within the Con Mine (1070 m, 1370 m, 1490 m, and 1615 m). Based on duplicate samples average percent errors for major ion and stable isotope analysis were generally lower than 3% and 1% respectively. Stable isotope data have been corrected for salinity effects as outlined in Sofer and Gat (1972).

4.1.1 Major Ion Geochemistry – Con Mine

Table 4.1 presents major ion and stable isotope geochemistry for boreholes sampled within this study and compares them with historic values reported for the same boreholes. Unfortunately, analysis of HCO_3 was not possible, however at concentrations historically

reported less than 50mg/L, its contribution to salinity is minimal. Similar to previous results reported in Frape et al., 1984; McDonald, 1986; Intera Consulting Ltd. et al., 1997; and Battye, 2002, groundwaters at the Con Mine during the October 2003 sampling had a Ca-Na-Cl geochemical facies and a general increase in the dominance of these ions with increasing depth.

The dominant ions continue to be Ca, Na, and Cl with maximum values of approximately 67, 27 and 183 g/L, respectively, observed from B-7126, 1615 m level. Minimum values for these ions were 0.22, 0.25, and 1.2 g/ L as observed in B-8906, 1070 m level. Observed changes in mixing ratios were generally found to coincide with observed changes in major ion concentrations.

Table 4.1 Major Ion and Stable Isotope Geochemistry of Con Mine Waters (1980-2003). Sources include; Frape et al., 1984; Mcdonald, 1986; Intera Consulting Ltd. et al., 1997; Battye, 2002.

	Sample	Concentration (mg/L)								
Borehole	Date	Ca	Na	Mg	K	Cl	SO4	TDS	$\delta^{18}O$ (‰)	$\delta^{2}H$ (‰)
1070m level										
8906	May-95	210	200	32	3	428	129	1002	-19.26	-159.8
8906	Jun-96	226	245	33	9	610	154	1277	-19.72	-159.4
8906	Sep-00	241	236	31	3	533	170	1214	-19.38	-154.4
8906	Oct-03	226	246	32	4	562	116	1186	-19.19	-158.3
9362	May-95	1640	1870	37	9	3853	602	8011	-20.79	-159.1
9362	Jun-96	1671	2007	33	14	6389	581	10694	-20.73	-160.8
9362	Sep-00	1780	2040	34	8	5815	580	10257	-20.85	-161.6
9362	Oct-03	1678	2033	48	13	6929	590	11290	-20.78	-162.5
9452	Nov-95	2167	1852	141	17	7680	726	12583	-19.72	-155.8
9452	Jun-96	925	872	73	12	3181	603	5667	-19.52	-158.6
9452	Sep-00	1210	1110	83	7	3685	638	6733	-19.77	-157.3
9452	Oct-03	1228	1148	96	9	4624	678	7784	-19.79	-156.3
1370m level										
3316	Jun-96	48515	21669	257	170	141287	489	212387	-16.93	-100.4
3316	Sep-00	36800	21200	211	165	119500	15	177891	-17.02	-100.0
3316	Oct-03	45431	20100	186	240	131165	467	197589	-16.83	-90.5
3362	Jul-80	54400	35800	1340	483	135000	1	227024	-14.3	-82.0
3362	Apr-81	23400	13600	468	109	60200	715	98492	-19	-133.0
3362	May-95	25750	12740	210	93	59979	424	99196	-18.36	-130.3
3362	Jun-96	38171	17284	231	133	90166	369	146354	-17.61	-115.4
3362	Sep-00	23900	14700	190	111	73750	28	112679	-18.69	-129.1
3362	Oct-03	36651	16425	154	133	107330	435	161127	-17.50	-107.8
3450	Jul-80	15700	9420	250	110	31900	198	57578	-19.7	-145.0
3450	Apr-85	14330	6970	162	62	38590	214	60328	-19.34	-135.3
3450	May-95	13710	7590	150	50	34326	452	56278	-19.51	-144.8
3450	Jun-96	14540	7202	145	55	41271	738	63952	-19.22	-143.6
3450	Sep-00	18900	12400	190	83	52700	41	84314	-19.26	-136.0
3450	Oct-03	13211	6658	132	63	37410	552	58025	-19.19	-143.6

Table 4.1 Continued..

Borehole	Sample Date	Concentration (mg/L) Ca	Na	Mg	K	Cl	SO4	TDS	$\delta^{18}O$ (‰)	$\delta^{2}H$ (‰)
1370m level cont.										
3457	Jul-80	12900	10900	268	111	37100	746	62025	-22.84	-163.0
3457	Apr-81	10500	8050	209	53	29400	715	48927	-22.27	-162.0
3457	Apr-85	4217	2970	73	22	18000	723	26005	-20.81	-159.2
3457	May-95	4060	2850	87	17	11283	562	18859	-20.29	-156.5
3457	Jun-96	2524	2480	43	17	7845	609	13517	-20.60	-162.0
3457	Sep-00	2800	2500	50	13	8190	603	14156	-20.10	-157.8
3457	Oct-03	4789	3603	107	29	15204	537	24270	-20.22	-157.7
3618	May-95	10340	6440	130	38	26772	502	44222	-19.99	-148.4
3618	Jun-96	11495	6919	132	47	40035	693	59321	-20.09	-151.4
3618	Sep-00	13800	7910	126	55	32100	99	54090	-20.19	-147.5
3618	Oct-03	6149	4138	65	29	18572	579	29533	-20.22	-157.8
5316	May-95	17990	10330	300	73	48630	441	77764	-19.21	-137.4
5316	Jun-96	4796	3683	77	25	15137	584	24301	-20.46	-157.5
5316	Sep-00	4450	3320	78	21	12250	587	20706	-20.47	-160.5
5316	Oct-03	4030	3093	48	21	12385	561	20138	-20.35	-160.5
1490m level										
5310	May-95	20530	12690	200	75	59245	660	93400	-20.12	-139.6
5310	Jun-96	27057	14801	248	100	77986	642	120834	-19.56	-133.6
5310	Sep-00	21800	11100	294	83	69900	36	103213	-19.72	-134.4
5310	Oct-03	18736	11388	200	84	52448	792	83648	-19.75	-138.8
Angel Fault	Oct-03	47060	20825	171	230	130398	508	199191	-16.68	-86.3
1615m level										
5300 (53D)	Jun-96	57562	24920	271	197	152589	271	235810	-15.70	-84.4
	Oct-03	57290	24825	237	276	152258	314	235200	-15.70	-70.0
7126	May-95	60310	26000	200	250	156100	225	243085	-14.61	-68.0
7126	Jun-96	62811	25664	188	230	185555	247	274694	-14.45	-73.2
7126	Sep-00	96100	36900	486	391	168500	2	302379	-14.76	-73.3
7126	Oct-03	66795	27413	186	341	182867	277	277878	-15.34	-56.2

The significant increase in Ca, and Na values reported in 2000 for B-7126 were not repeated in 2003 . These increases do not coincide with the slight decrease in Cl concentration. Results from the 2003 sampling were more similar to results obtained in 1995 and 1996 (Figure 4.1).

TDS values continue to increase with depth and range between 1.2 and 278 g/L in B-8906 (1070 m) and B-7126 (1615 m), respectively. Strong linear relationships also persist between TDS values and the major ions Cl, Ca, Na, and K.

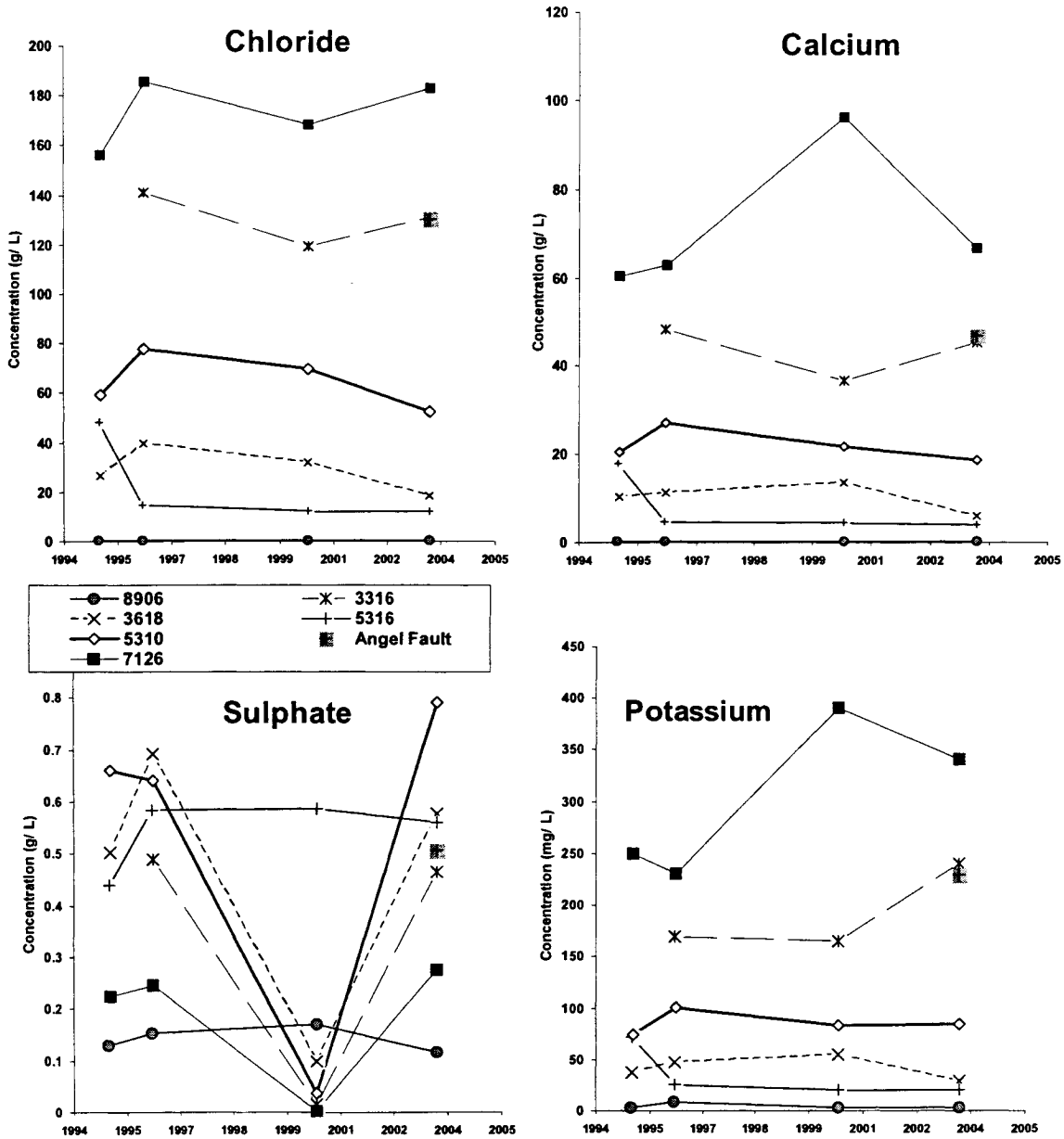

Figure 4.1 Changes in concentrations of chloride, calcium, sulphate, and potassium for selected boreholes from each level sampled between 1995-2003.

Sulphate concentrations measured in this research are consistent with sampling from 1995 and earlier. Measurements from the 2000 sampling are clearly in error. Sulphate concentrations have remained relatively stable at the 1070 m level with the biggest change being a rise of 75 mg/L in B-9451 since 1996. On the other hand, with the exception of B-

3362, all boreholes on the 1370 m level display a drop in sulphate concentration since 1996. Two of three boreholes from this level (B-3362 and B-3457), reveal a continuous decreasing trend in sulphate concentration since 1980. Finally, sulphate concentrations on the 1490 m and 1615 m levels have increased compared with values reported from June 1996 sampling.

4.1.2 Stable Isotopes – Con Mine

The mixing model described by Douglas (2000) delineates three end-member components in Con Mine deep groundwaters; modern, glacial and brine components. Accordingly the stable isotopic signature of groundwaters from various mine levels represents a mixture of these three end-members. Figure 4.2, modified from Douglas et al. (2000), presents data collected in this research with earlier data from 1980 – 2002. The local meteoric water line (LMWL) with equation $\delta^2H = 6.75\ \delta^{18}O - 20.1$ ‰ was calculated from monthly precipitation between 1989 and 1993 (Moorman et al., 1996).

Values measured from the 1070 and 1490 m levels are similar to previously reported results, with shallow water plotting on the LMWL and water from the deeper levels plotting along a mixing line with equation $\delta^2H = 12.14\ \delta^{18}O + 104.1$ ‰. The deepest groundwater from the 1615 m level was depleted in ^{18}O relative to previous results. Water sampled from the Angel Fault system on the 1490 m level falls relatively close to the trendline for deep groundwaters.

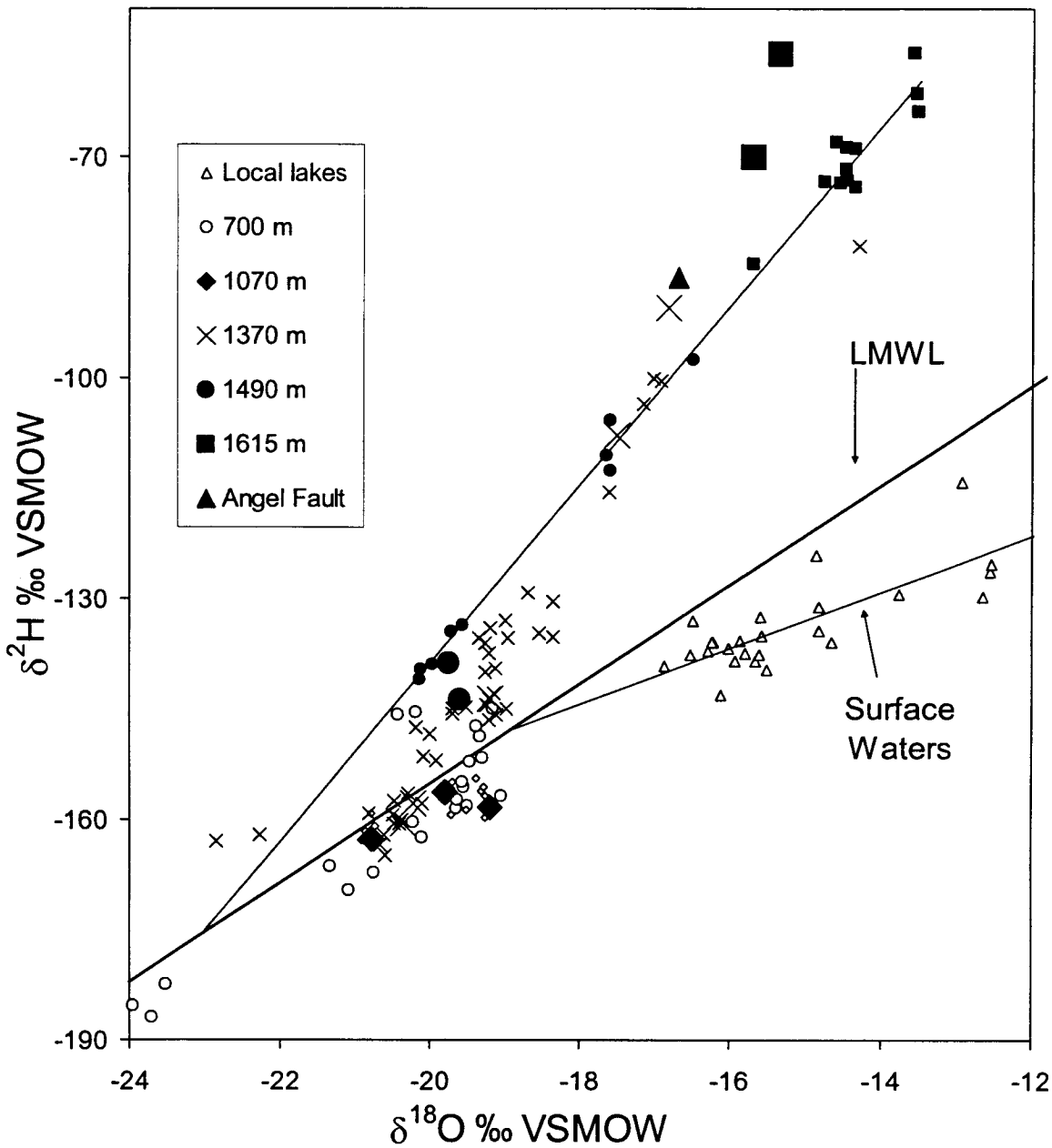

Figure 4.2 Stable isotopic composition of deep groundwaters of the Con Mine in comparison with data from earlier sampling. Values reported from this research are shown as larger size markers. The value recorded for the water retrieved from the Angel Fault is shown as a black triangle. Other sources for the data displayed here include Frape et al., 1984; Intera Consulting Ltd. et al, 1997; Battye, 2002

4.1.3 Mixing Ratios – Con Mine

Changes in major ion, stable isotope and noble gas chemistry within the Con Mine groundwaters are largely dependant on changes in the fraction of the brine, glacial and recent groundwater components, and therefore the mixing ratios.

Table 4.2 reports the three-component mixing ratios that were calculated for this research using the molar Cl^- and $\delta^{18}O$ values as described in Douglas et al. (2000). For comparison, mixing ratios are also reported from Douglas et al. (2000), Battye (2002) and calculated from data in Frape et al (1984).

Table 4.2 Fractions of the recent, glacial and brine components in groundwater collected from boreholes on the 1070, 1370, 1490 and 1615 m levels of the Con Mine. Results are grouped by level. Comparison data from Douglas et al., 2000; Battye, 2002; and Frape et al., 1984.

	Sample			mixing fractions		
Borehole	Date	18O	Cl-	recent	brine	glacial
1070m level						
8906	Oct-03	-19.19	562	0.965	0.002	0.0335
8906	Sep-00	-19.38	533	0.945	0.001	0.0538
8906	Jun-96	-19.72	610	0.909	0.001	0.0903
8906	Nov-95	-19.70	391	0.913	0.000	0.0873
8906	Jul-95	-19.32	323	0.954	0.000	0.0461
8906	May-95	-19.26	428	0.959	0.001	0.0401
9362	Oct-03	-20.78	6929	0.744	0.025	0.2311
9362	Sep-00	-20.85	5815	0.746	0.020	0.2340
9362	Jun-96	-20.73	6389	0.754	0.023	0.2235
9362	May-95	-20.79	3853	0.768	0.012	0.2197
9452	Oct-03	-19.79	4624	0.867	0.018	0.1150
9452	Sep-00	-19.77	3685	0.877	0.014	0.1089
9452	Jun-96	-19.52	3181	0.908	0.012	0.0795
9452	Nov-95	-19.72	7680	0.849	0.031	0.1201

Table 4.2 cont. on next page

Borehole	Sample Date	18O	Cl-	mixing fractions recent	brine	glacial
1370m level						
3316	Oct-03	-16.83	131165	0.114	0.563	0.3229
3316	Sep-00	-17.02	119500	0.192	0.513	0.2953
3316	Jun-96	-16.93	141287	0.018	0.606	0.3761
3362	Oct-03	-17.50	107330	0.243	0.460	0.2967
3362	Sep-00	-18.69	73750	0.401	0.314	0.2845
3362	Jun-96	-17.61	90166	0.377	0.387	0.2364
3362	May-95	-18.36	59979	0.552	0.257	0.1915
3362	Apr-81	-19	60200	0.483	0.256	0.2614
3450	Oct-03	-19.19	37410	0.655	0.159	0.1866
3450	Sep-00	-19.26	52700	0.518	0.223	0.2581
3450	Jun-96	-19.22	41271	0.619	0.175	0.2060
3450	May-95	-19.51	34326	0.647	0.145	0.2081
3450	Jul-80	-19.7	31900	0.647	0.134	0.2189
3457	Oct-03	-20.22	15204	0.733	0.062	0.2053
3457	Sep-00	-20.10	8190	0.805	0.032	0.1632
3457	Jun-96	-20.60	7845	0.755	0.029	0.2156
3457	May-95	-20.29	11283	0.759	0.045	0.1966
3457	Apr-81	-19	60200	0.483	0.256	0.2614
3618	Oct-03	-20.22	18572	0.705	0.076	0.2193
3618	Sep-00	-20.19	32100	0.594	0.134	0.2724
3618	Jun-96	-20.09	40035	0.538	0.168	0.2948
3618	May-95	-19.99	26772	0.660	0.111	0.2291
5316	Oct-03	-20.35	12385	0.743	0.049	0.2078
5316	Sep-00	-20.47	12250	0.732	0.048	0.2199
5316	Jun-96	-20.46	15137	0.708	0.061	0.2312
5316	May-95	-19.21	48630	0.558	0.206	0.2354
1490m level						
5310	May-95	-20.12	59245	0.373	0.249	0.377
5310	Jul-95	-20.13	53060	0.424	0.223	0.353
5310	Nov-95	-19.97	67994	0.315	0.287	0.398
5310	Jun-96	-19.56	77986	0.273	0.330	0.396
5310	Sep-00	-19.72	69900	0.325	0.296	0.379
5310	Oct-03	-19.75	52448	0.469	0.221	0.310
Angel Fault	Oct-03	-16.68	130398	0.135	0.560	0.304
1615m level						
53-D	Oct-03	-15.70	152258	0.055	0.656	0.290
53-D	Jun-96	-15.70	152589	0.052	0.657	0.291
7126	Feb-95	-14.47	147000	0.229	0.636	0.135
7126	May-95	-14.61	156100	0.137	0.675	0.188
7126	Nov-95	-14.36	183368	-0.066	0.791	0.275
7126	Jun-96	-14.45	185555	-0.094	0.800	0.294
7126	Sep-00	-14.76	168500	0.017	0.727	0.256
7126	Oct-03	-15.34	182867	-0.165	0.787	0.378

Mixing ratios on the 1070 m level have essentially remained unchanged since sampling in 1995 and 1996. The slightly increasing trend in the recent component in B-8906 since sampling in 1996 was observed again in 2003.

With the exception of B-3362, boreholes on the 1370 m level have had either relatively constant ratios since sampling in June 1996 (B-3450, 3457, 5316) or increases in the recent fraction between 4 – 20 % (B-3316, B-3618). The observed increases have been paired with decreases in both the brine and glacial component. In contrast, B-3362 shows a decreasing trend of recent component and increasing trend of brine and glacial components.

Comparison with June 1996 data reveals that borehole 5310, the only borehole sampled on the 1490 m level, has increased nearly 20 % in the recent component. Corresponding decreases of roughly 10% were observed in both the brine and glacial components. With a brine fraction of 56 % the water sampled directly from the Angel fault on this level is decidedly brine dominated, although the brine fraction from borehole 5310 on the same level was only 22%. The ratios for the Angel fault sample are nearly identical to those observed in B-3316 for the same sampling event. Data from the 1615 m level reveal little change with only a very slight increase in the glacial component, corresponding with a decrease in the brine and modern fractions.

Decreases in concentrations of chloride, calcium and sodium, reflected in slight changes in mixing ratios at the 1370 and 1490 m levels, indicate that there has been an increase in the continued penetration of recent meteoric water to greater depths within the Con Mine than previously reported. An increase in sulphate concentration on the 1490 level supports this idea. However, these changes have not been dramatically observed in the 1615

m level, the deepest sampled, and it is believed that the groundwater collected from B-7126 has remained relatively unchanged since 1980.

4.2 Noble Gas Analytical Considerations

Noble gas data for both the Con and Lupin mine sample sets are based on results obtained from the experimental procedures described in section 3.2. Concentrations from gas diffusion and water samples were measured using the isotope dilution method.

Analytical problems and laboratory errors were encountered during the analysis of a small percentage of both water and gas diffusion samples. In some instances these problems may have only been gas specific resulting from, for example, low signal strength on the quadrupole mass spectrometer. In such a case the concentration for that particular gas has not been reported here.

Many gas diffusion samples contained high gas pressures within the ¼" copper tubes, most of which was either methane or other gases of no interest to this research. These high pressures lead to difficulties in noble gas measurement due to either a decrease in the signal strength or flooding of the signal for those noble gases with naturally low dissolved concentrations (i.e. Ne, Kr, and Xe). To resolve the problem samples were often split into sections of two or three using pinch off tools, and run separately (Figure 4.3).

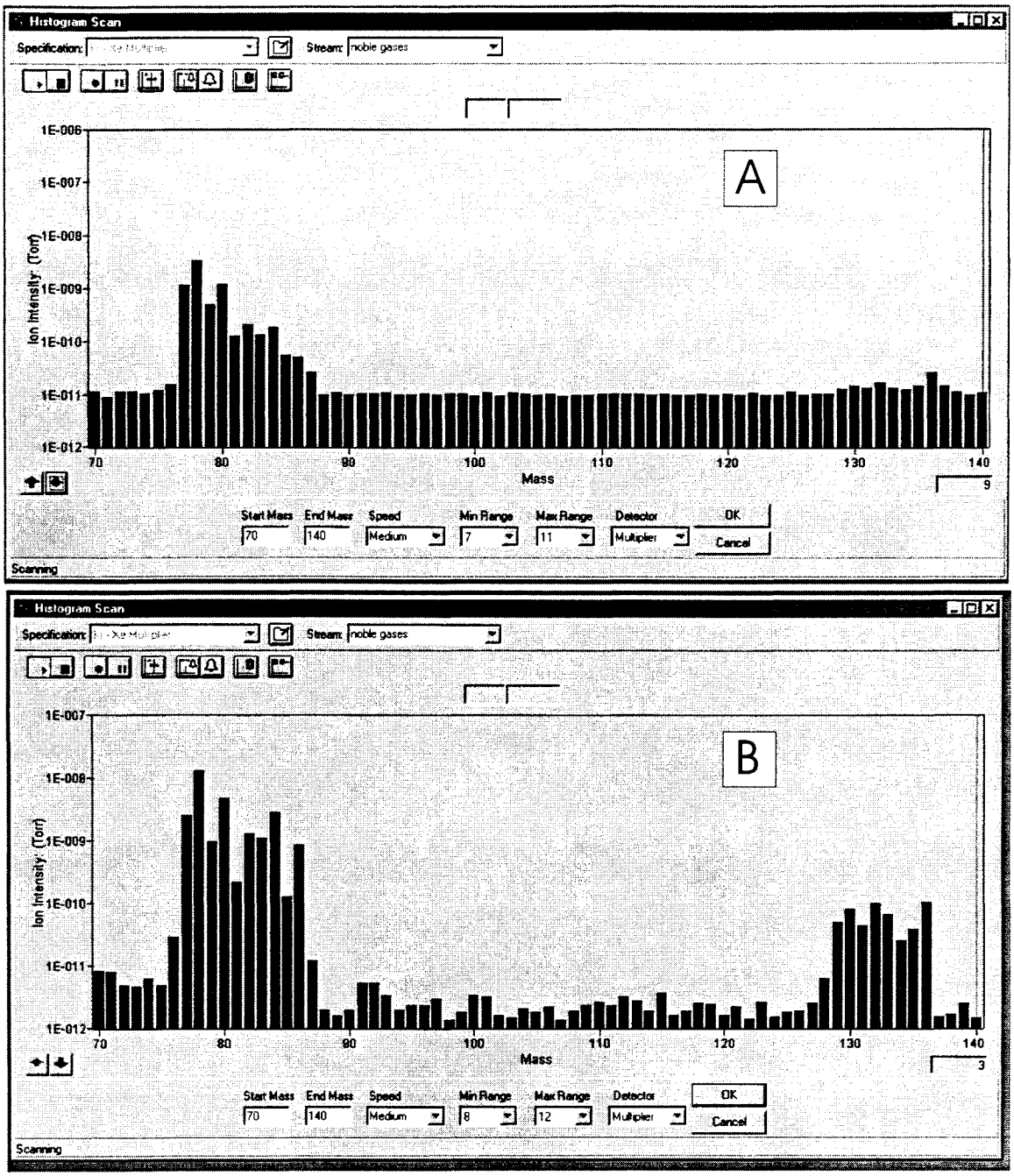

Figure 4.3 The flooding of the xenon signal by high background gas pressures is shown in (A); reduction of this effect was achieved by decreasing sample size (B).

Using air standards as an aid in determining tracer volume is a fundamental component of the isotope dilution method. During analysis of samples, air standards were run on a regular basis to monitor changes in tracer volume as well as provide a more precise and

accurate measure of tracer volume. Over the course of the 71 sample runs (this number includes split sections as a separate analysis), 35 air standards were completed.

Air standards were also used as an indicator of the reproducibility of the analysis method. Because of changes to tracer volume over time reproducibility is based on air standards completed near the same point in time. Based on the last five air standards the standard deviation of noble gas concentrations, expressed as a percentage of the average, was found to be approximately 25, 3, 17, 9 and 25 % for helium, neon, argon, krypton and xenon, respectively.

4.3 Noble Gas Data - Water Samples

Noble gas concentration data for water samples collected at the Con and Lupin mines are presented in Table 4.3. These values are uncorrected for excess air concentration or brine fraction and are expressed as cc STP/ cc H_2O.

For each borehole at least three water samples were collected to ensure reproducibility of results. The highly saline and pressurized nature of some samples caused some storage and laboratory problems. As a result, triplicate analysis was not completed for all boreholes. For those water samples with duplicate and triplicate analysis standard deviation, expressed as a percentage of the average was generally below 20%.

Of the thirty copper tube water samples taken for this research, twenty-four were tested for noble gas concentrations. Of those tested, 18 samples (75%) returned what is believed to be reliable noble gas concentration data. For comparison, data is also listed from Battye (2002) for the Con mine.

Table 4.3 Noble gas concentrations in water samples from the Con and Lupin mines.

		Concentration (cc gas STP/ cc H20 STP)				
Borehole	Sample	He	Ne	Ar	Kr	Xe
		Con Mine Waters				
1070m level						
8906	Battye (2002)*	1.83E-04	4.75E-07	5.82E-04	1.21E-07	3.00E-08
1490m level						
5310	Battye (2002)*	2.91E-03	3.58E-07	2.13E-03	1.78E-07	3.09E-08
5310	water 1	3.22E-03	4.85E-07	1.28E-03	9.61E-08	1.25E-08
5310	water 2	2.68E-03	4.91E-07	1.30E-03	7.59E-08	1.05E-08
5310	**Average (2003)**	**2.95E-03**	**4.88E-07**	**1.29E-03**	**8.60E-08**	**1.15E-08**
1615m level						
7126	Battye (2002)*		8.90E-07	7.08E-03	1.42E-07	3.65E-08
7126	water 1	1.33E-03	1.46E-07	2.72E-03	5.21E-08	6.83E-09
7126	water 2	1.32E-03	1.18E-07	2.50E-03	5.54E-08	5.80E-09
7126	water 3	1.45E-03	1.10E-07	1.77E-03	5.28E-08	7.36E-09
7126	**Average (2003)**	**1.37E-03**	**1.25E-07**	**2.33E-03**	**5.34E-08**	**6.66E-09**
		Lupin Mine Waters				
890m level						
188	water 3	1.57E-03	4.54E-07	1.14E-03	1.46E-07	2.36E-08
1130m level						
191	water 1	8.76E-03	1.12E-06	2.56E-03	1.19E-07	2.34E-08
191	water 2	6.78E-03	4.86E-07	2.95E-03	1.09E-07	2.20E-08
191	water 3	9.56E-03	1.61E-06	4.25E-03	1.20E-07	2.00E-08
191	**Average**	**8.36E-03**	**1.07E-06**	**3.25E-03**	**1.16E-07**	**2.18E-08**
192	water 1	2.46E-03	7.80E-07	5.56E-03	4.04E-08	7.58E-09
197	water 1		3.63E-06	2.23E-03	2.87E-07	1.81E-08
197	water 2	2.84E-04	4.49E-06	2.82E-03	3.53E-07	2.49E-08
197	water 3	4.69E-03	5.41E-07	1.49E-03	1.37E-07	2.26E-08
197	**Average**	**2.49E-03**	**2.89E-06**	**2.18E-03**	**2.59E-07**	**2.18E-08**
217	water 1	2.12E-03	6.21E-07	3.15E-03	7.03E-08	1.76E-08
217	water 2	2.85E-03	5.22E-07	2.78E-03	1.14E-07	2.08E-08
217	water 3	3.43E-03	5.89E-07	1.56E-03	1.15E-07	1.82E-08
217	**Average**	**2.80E-03**	**5.77E-07**	**2.50E-03**	**9.97E-08**	**1.88E-08**
219	water 2	2.21E-03	3.07E-07	1.66E-03	6.39E-08	1.24E-08
219	water 3	7.21E-04	1.21E-07	1.30E-03	5.20E-08	1.05E-08
219	**Average**	**1.46E-03**	**2.14E-07**	**1.48E-03**	**5.79E-08**	**1.14E-08**

4.4 Noble Gas Data – Gas Diffusion Samples

Noble gas concentration data for gas diffusion samples collected from the Con and Lupin mines are listed in Table 4.4 and Table 4.5. Table 4.4 expresses concentration as cc gas per cc volume in copper tube while

Table 4.5 expresses concentration as cc gas per cc H20 making them comparable to the water results.

Of the forty-eight gas diffusion samples taken for this research, forty-one were tested for noble gas concentrations. Due to problems in sample collection and analysis only seventeen of those tested returned a result. Samples listed with an additional letter designation (eg. gas 2a) are split samples from the same copper tube. Splitting was necessary in some instances because of high gas pressures contained within the copper tubes. However, splitting should not affect gas ratios as the volume changes for each individual gas sample and split were measured and results corrected accordingly.

The values reported in Table 4.5 have been corrected to cc gas STP/ cc H_2O STP using the Bunsen Coefficient (Bo). This coefficient is essentially the Henry's coefficient, which describes gas solubility in water, multiplied by the gas constant and temperature (in degrees Kelvin). The correction using Bo is based on converting the measured noble gas volumes in the gas diffusion samplers, to the volume of noble gas that would be dissolved in the groundwater at STP equilibrium conditions. Values for Bo are given in units of gas volume per water volume per pressure (i.e. cc/L/atmosphere), where the noble gas concentration is cc gas at standard temperature and pressure conditions (STP) (Smith and Kennedy, 1983).

Table 4.4 Noble gas concentration in gas diffusion samples from the Con and Lupin mines (gas concentrations as cm^3 gas STP per cm^3 volume in copper tube).

		Concentration (cc gas STP/ cc H20 STP)				
Borehole	Sample	He	Ne	Ar	Kr	Xe
		Con Mine Diffusion Samples				
1070m level						
8906	gas 1A	1.05E-04	2.10E-05	6.79E-03	9.32E-07	8.60E-08
8906	gas 2A	2.33E-03	1.71E-05	3.15E-03	8.83E-07	5.00E-08
8906	gas 2B	2.33E-03	1.78E-05	6.54E-03	8.33E-07	5.58E-09
8906	gas 3B	3.21E-04	8.76E-05	2.82E-02	2.52E-06	4.87E-07
8906	**Average**	**1.27E-03**	**3.59E-05**	**1.12E-02**	**1.29E-06**	**1.57E-07**
1490m level						
5310	gas 1B	9.53E-03	1.53E-05	1.92E-03	4.17E-07	5.19E-08
5310	gas 2A	8.27E-02	1.77E-05	9.12E-03	9.70E-07	1.76E-07
5310	gas 2C	7.49E-02	1.42E-05	4.63E-03	8.72E-07	1.41E-07
5310	gas 3A	1.74E-02	9.22E-06	3.67E-03	5.74E-07	9.80E-08
5310	gas 3C	2.29E-02	1.11E-05	3.87E-03	6.30E-07	7.60E-08
5310	gas 4B	6.48E-04	1.71E-05	2.57E-03	9.89E-07	4.44E-08
5310	**Average**	**3.47E-02**	**1.41E-05**	**4.30E-03**	**7.42E-07**	**9.79E-08**
1615m level						
7126	gas 2A	2.08E-02	1.19E-05	7.77E-03	2.73E-07	
7126	gas 4A	9.08E-04		2.09E-03	5.85E-08	5.68E-08
7126	gas 4B	9.28E-03	9.75E-06	4.10E-03	5.97E-08	6.35E-07
7126	gas 7A	1.25E-02	6.83E-06	4.58E-03	4.26E-07	2.66E-07
7126	**Average**	**1.09E-02**	**9.51E-06**	**4.64E-03**	**2.04E-07**	**3.19E-07**
		Lupin Diffusion Samples				
890m level						
188	gas 1B	6.12E-04	1.30E-05	1.30E-03	9.12E-07	9.39E-08
188	gas 2	1.38E-03	1.83E-05	2.36E-03	1.18E-06	1.36E-07
188	gas 4	3.75E-03	1.38E-05	2.52E-03	1.06E-06	1.43E-07
188	**Average**	**1.91E-03**	**1.50E-05**	**2.06E-03**	**1.05E-06**	**1.24E-07**
1130m level						
192	gas 2B	1.26E-02	1.16E-05	2.25E-03	3.94E-07	3.11E-08
192	gas 3B	2.58E-03	2.78E-05	1.63E-03	1.02E-06	5.00E-08
192	**Average**	**7.58E-03**	**1.97E-05**	**1.94E-03**	**7.07E-07**	**4.05E-08**
197	gas 2	3.63E-01	7.18E-05	5.59E-02	2.22E-06	2.17E-07
197	gas 4A	6.65E-01	6.96E-04	2.87E-01	2.15E-06	2.76E-07
197	gas 4B	2.76E-03	4.02E-05	4.36E-02	1.86E-06	1.73E-07
197	**Average**	**3.43E-01**	**2.69E-04**	**1.29E-01**	**2.08E-06**	**2.22E-07**

Initial gas measurements from the gas diffusion samples have the units, gas volume per volume of sample (ie. cc/cc). Therefore, the partial pressure of the noble gas in the copper tube, as measured in atmospheres, is needed. This measurement is easily derived from rearrangement of the ideal gas law to:

$$P = \frac{nRT}{V}$$

Where: P = pressure in atmospheres
n = moles of the gas, derived from the measured STP volume (n = cc/1000/22.4) 22.4L is the volume of 1 mole of an ideal gas at 1 atm. and 273.15 K
R = the gas constant, equal to 0.08205 $atm \cdot L \cdot mol^{-1} \cdot K^{-1}$
T = temperature in Kelvin
V = the volume in litres

Accordingly, expressing our data as a partial pressure involves converting our cc of gas to moles by dividing by RT for STP (0.08205 · 273) and multiplying by RT for in-situ diffusion sampler conditions (0.08205 · 293). The resulting partial pressure for the given noble gas can then be used with the appropriate Bunsen coefficient (Bo) to determine the dissolved concentration. The effect of this calculation is a correction for the measured amount of noble gas at STP to the measured in-situ temperature. In-situ temperatures for the waters at the Con mine are 20°C at borehole 8906 and 25°C at boreholes 5310 and 7126. In-situ temperatures for waters at the Lupin mine are ~ 10°C for borehole 188 and °15 C for boreholes 191, 192, 197, 217, and 219 (Frape et al., 2004).

Table 4.5 Noble gas concentrations for gas diffusion samples expressed as cc gas per cc H2O.

		Concentration (cc gas STP/ cc H20 STP)					Analysis
Borehole	Sample	He	Ne	Ar	Kr	Xe	Pressure
		Con Mine Diffusion Samples					
1070m level							
8906	gas 1A	9.19E-07	2.20E-07	2.30E-04	5.81E-08	9.61E-09	0.6
8906	gas 2A	2.04E-05	1.80E-07	1.07E-04	5.50E-08	5.58E-09	0.7
8906	gas 2B	2.04E-05	1.86E-07	2.22E-04	5.20E-08	5.15E-09	0.7
8906	gas 3B	2.82E-06	9.18E-07	9.55E-04	1.57E-07	5.44E-08	4.0
8906	**Average**	**1.11E-05**	**3.76E-07**	**3.78E-04**	**8.05E-08**	**1.87E-08**	
1490m level							
5310	gas 1B	5.37E-05	9.58E-08	3.50E-05	1.43E-08	2.98E-09	1.7
5310	gas 2A	4.67E-04	1.11E-07	1.66E-04	3.32E-08	1.01E-08	41.7
5310	gas 2C	4.23E-04	8.91E-08	8.41E-05	2.98E-08	8.09E-09	16.7
5310	gas 3A	9.82E-05	5.79E-08	6.67E-05	1.96E-08	5.62E-09	0.9
5310	gas 3C	1.29E-04	7.00E-08	7.03E-05	2.15E-08	4.36E-09	1.2
5310	gas 4B	3.66E-06	1.07E-07	4.67E-05	3.38E-08	2.55E-09	0.9
5310	**Average**	**1.96E-04**	**8.86E-08**	**7.81E-05**	**2.54E-08**	**5.62E-09**	
1615m level							
7126	gas 2A	3.93E-05	2.22E-08	3.65E-05	2.72E-09		2.1
7126	gas 4A	1.71E-06		9.82E-06	5.82E-10	8.59E-10	0.1
7126	gas 4B	1.75E-05	1.82E-08	1.93E-05	5.95E-10	9.60E-09	1.1
7126	gas 7A	2.36E-05	1.27E-08	2.16E-05	4.24E-09	4.02E-09	1.5
7126	**Average**	**2.05E-05**	**1.77E-08**	**2.18E-05**	**2.03E-09**	**4.83E-09**	
		Lupin Diffusion Samples					
890m level							
188	gas 1B	5.02E-06	1.33E-07	4.89E-05	6.70E-08	1.31E-08	1.7
188	gas 2	7.03E-06	1.17E-07	5.55E-05	5.38E-08	1.18E-08	6.9
188	gas 4	2.06E-05	8.85E-08	6.36E-05	5.24E-08	1.33E-08	17.5
188	**Average**	**1.09E-05**	**1.13E-07**	**5.60E-05**	**5.77E-08**	**1.27E-08**	
1130m level							
192	gas 2B	1.29E-04	1.42E-07	9.10E-05	3.09E-08	4.36E-09	12.5
192	gas 3B	1.93E-05	2.47E-07	4.79E-05	5.82E-08	5.10E-09	2.4
192	**Average**	**7.42E-05**	**1.94E-07**	**6.94E-05**	**4.45E-08**	**4.73E-09**	
197	gas 2	3.08E-03	7.42E-07	1.97E-03	1.49E-07	2.66E-08	48.2
197	gas 4A	6.81E-03	8.67E-06	1.22E-02	1.74E-07	4.10E-08	106.3
197	gas 4B	2.35E-05	4.15E-07	1.54E-03	1.25E-07	2.13E-08	93.9
197	**Average**	**3.31E-03**	**3.28E-06**	**5.25E-03**	**1.49E-07**	**2.96E-08**	

4.5 Gas Diffusion Sampling in Deep Groundwaters

One of the activities in this research was the testing of diffusion samplers to improve the analytical component of noble gas measurements. Diffusion samplers allow collection of dissolved gases by diffusion through a silicon rubber membrane into copper tubes, thus eliminating the water separation step during analysis. While preliminary tests in the lab were positive it is believed that the high pressures of methane, helium and other gases in the mine groundwaters were found to cause gas leakage during storage in the copper tubes. The following summarizes the results in comparison with the water sample results.

Comparison of noble gas concentration data for water samples and gas diffusion samples from the Con indicates an obvious underpressuring of the noble gases in the gas diffusion sampler (Figure 4.4). This potential loss of gas is largely corroborated by the correlation of noble gas concentrations with total gas pressure (Table 4.5) measured during analysis of gas diffusion samples (Figure 4.5).

A comparison between the second series of diffusion samples taken from the Lupin Mine and the water samples taken a year earlier is not warranted due to the elapsed time between their collection. However, one series of gas diffusion samples collected from B-197 show similar depletion compared to water samples collected during the same sampling event (Figure 4.5).

It was noted that the largest concentration of noble gases from a gas diffusion sample did in fact appear very similar to the average concentrations found in water samples at the Con mine. This data supports the conclusion that the sampler did indeed equilibrate with the dissolved gas portion of shield brine but leaking of samples occurred during transport and storage.

In addition, the strong variation in total sample pressure between individual samples of the same deployment (Table 4.5) suggests a problem with the individual copper tubes rather than a systematic problem in gas behaviour. It is suspected that the copper tubes used have slowly leaked gas between sampling and analysis. This would account for the strong variation in sample gas pressure from tubes of the same deployment.

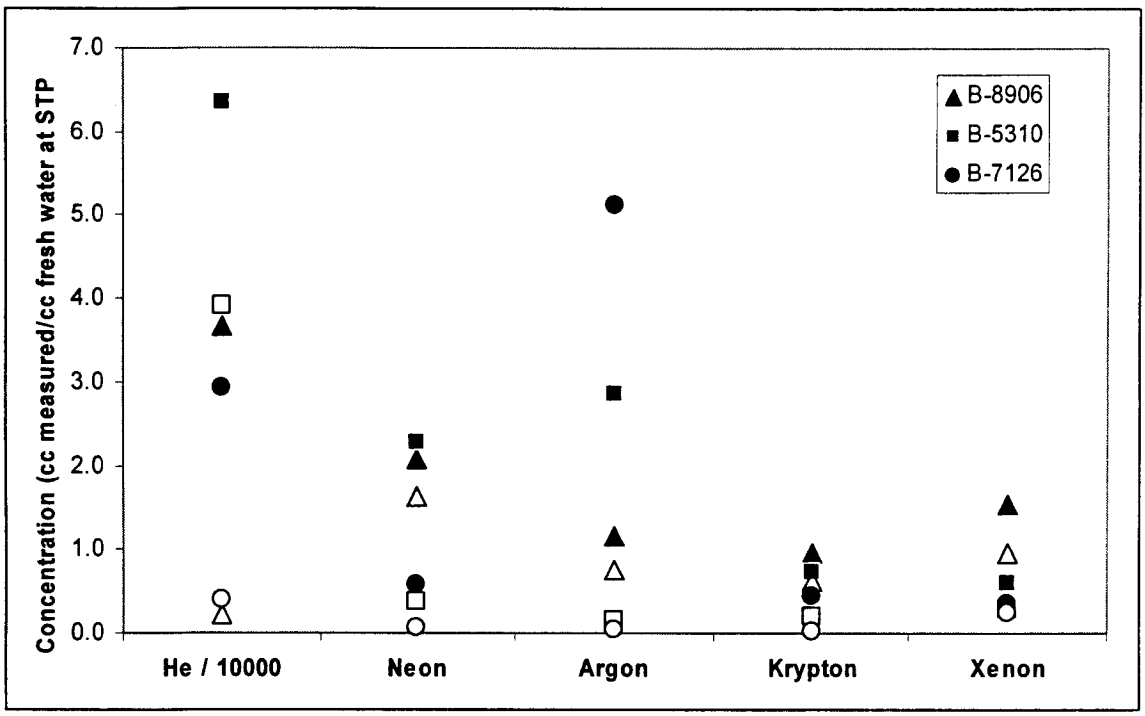

Figure 4.4 Comparison of average noble gas concentration data (normalized to fresh water at 0°C) for water samples and gas diffusion samples for the same boreholes and sampling events from the Con Mine. Solid black markers indicate water samples while hollow markers indicate gas diffusion samples.

The ability of this apparatus to maintain a vacuum seal had been tested at the University of Ottawa prior to sampling. However, the sampling locations described in Sheldon (2002) and Sanford et al. (1996), from which our diffusion sampler was designed, involved dissolved gas pressures close to atmospheric equilibrium. The high gas pressures observed at both the Lupin and Con mine may have proven too great for the cold weld seal of the pinch clamp for the majority of the gas diffusion samples.

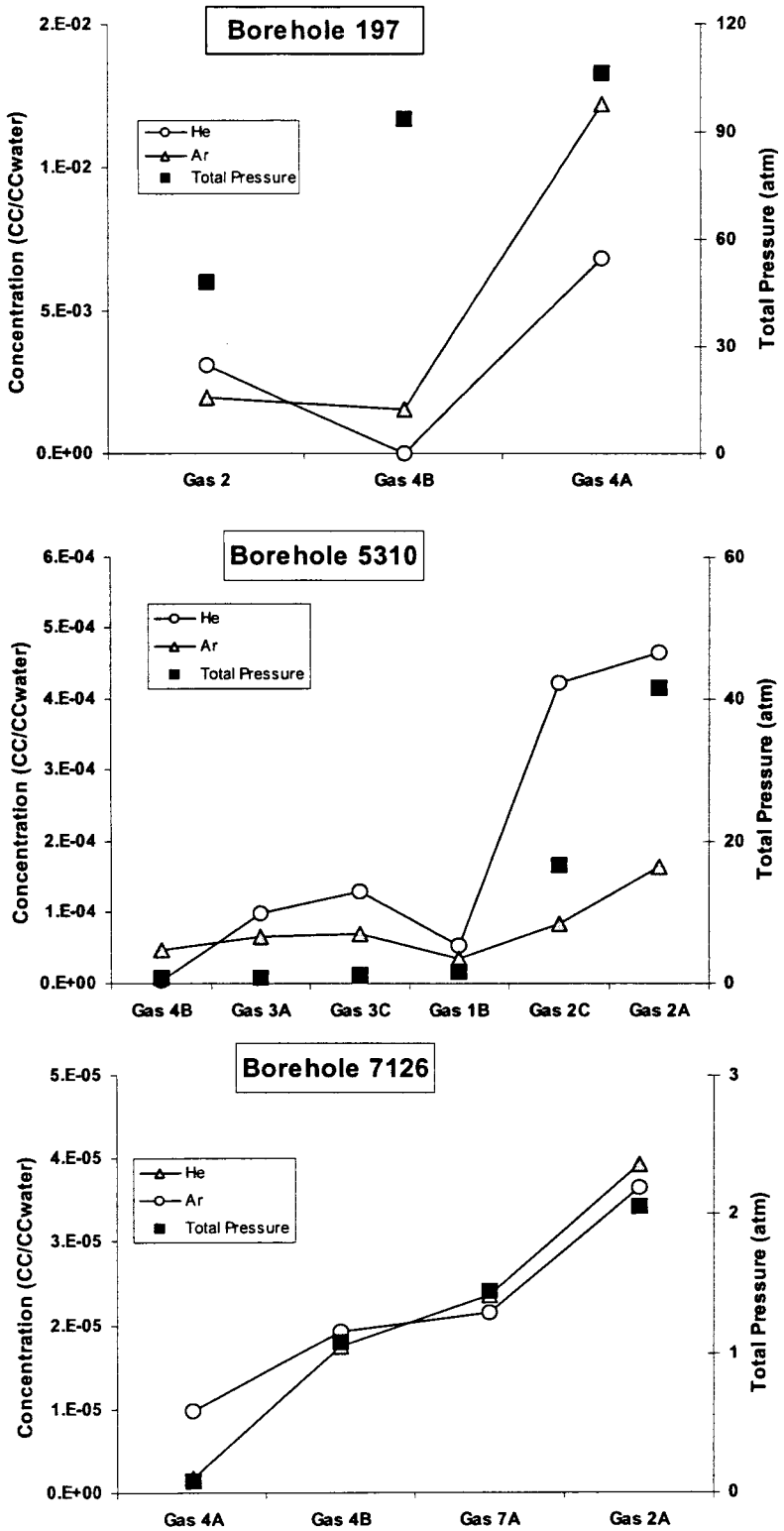

Figure 4.5 Changes in concentration of helium and argon with total gas pressure in gas diffusion samples for select boreholes from the Con and Lupin Mines.

Furthermore, the copper used was not annealed and so the possibility of microfracturing at the pinch-seal site, exacerbated during the un-pinching step of sample analysis, may have caused micro-leaks that allowed loss of gas. Subsequent examination of the tubes with a binocular reflected-light microscope showed evidence of such micro-fracturing. The microfracturing present in un-annealed copper tubes but absent in the annealed copper tubes (Figure 4.6).

Finally, the lead solder used to seal one end of the ¼" copper tubes may have leaked gas slowly over time as long term ability to maintain vacuum was not tested prior to sampling. In addition, an inconsistent solder seal is also a likely candidate for the observed gas loss.

The results of the diffusion gas sampling indicate that a re-assessment and re-design of the diffusion sampler apparatus must be undertaken. It is believed that the technique employed using the main body of the sampler is sound, however an improved technique must be developed for sample retrieval. Use of annealed copper tubing may solve the microfracturing problem but the integrity of a cold weld seal on such thin walled copper tubing may remain an issue at high salinity and formational pressures. Finally, the use of solder on the distal end of the storage tube should be tested for leaks on a long term time scale (several months).

The observed correlation of noble gas concentration with total pressure in the sample was not observed within the water samples. Futhermore, microscopic examination of the pinch-seal sites for copper tube water samples did not reveal the clusters of microfractures present in the gas diffusion samples. Accordingly water samples provide reliable noble gas data.

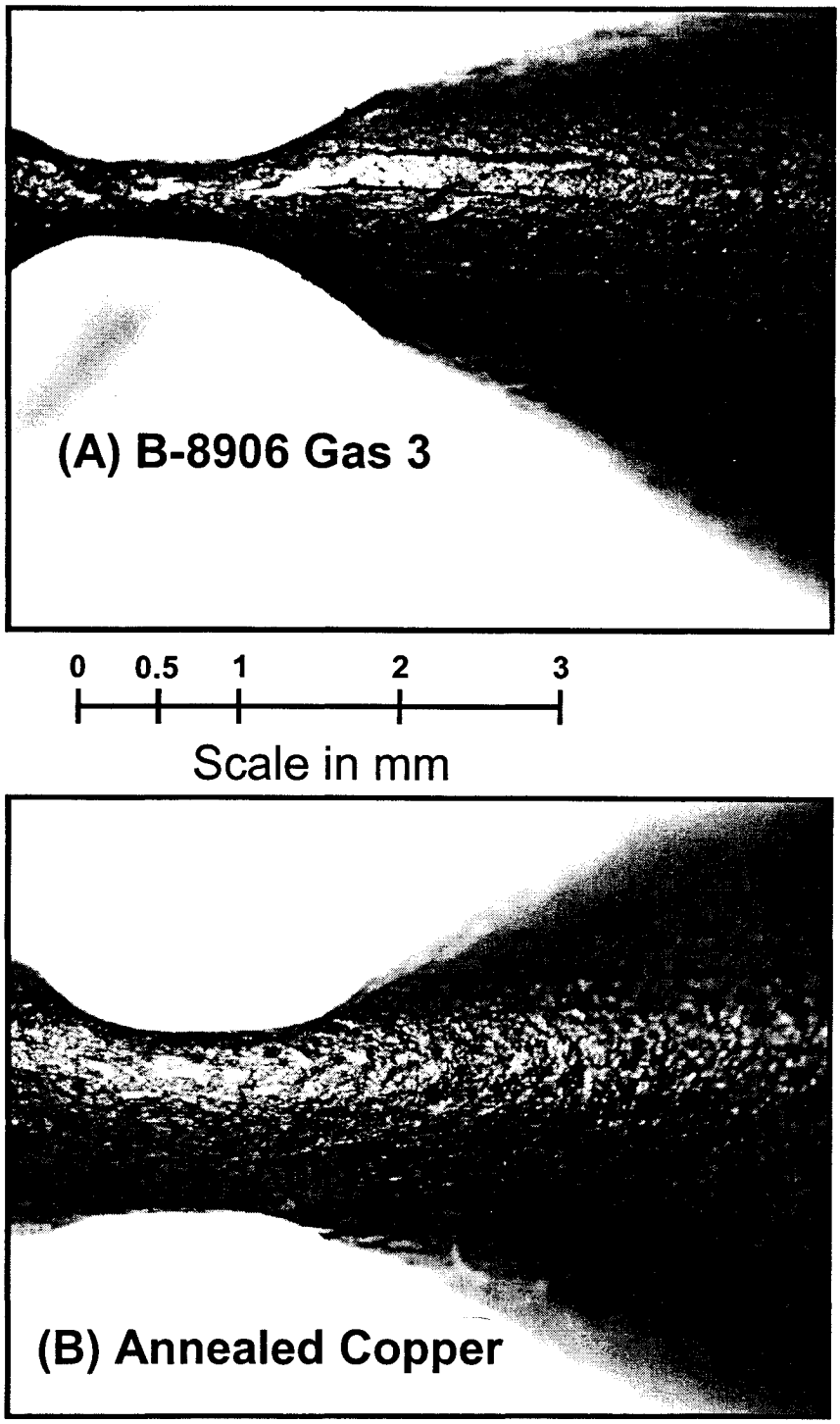

Figure 4.6 Binocular magnification of (A) gas diffusion sample "8906 gas 3" from the 1070 m level of the Con Mine and (B) a laboratory test sample of annealed copper . The obvious microfractures of the unannealed copper shown in (A) are likely responsible for observed gas loss during storage of samples. Differences in the size of the pinch are a result of different photo angle.

5 Noble Gas Data – Con Mine

The following section presents the noble gas data from the Con mine in the context of the study objectives focussing on calculation of paleotemperature of recharge and age estimation. The section is divided into four subsections; comparison of results to Battye (2002); noble gas concentration in brine fractions; calculation of paleotemperature of recharge for the brine fraction and age estimation of the brine fraction.

5.1 Comparison with Battye (2002)

The research presented herein for the Con Mine was completed as a phase II component to a study funded by the Canadian Nuclear Safety Commission. The principal focus of the Phase I research involved the construction of the noble gas analysis line. However, limited analysis of deep groundwaters from the Con Mine was completed. The following compares these results with the current research.

Averages of results from Phase 1 and Phase 2 are presented in Table 4.3 for uncorrected concentrations and in Table 5.1 for correction to 100% brine. Differences in analytical methodologies between the two studies include improved calibration of the mixed spike gas volume and improved separation of gases on the line. For the one comparative sample for helium (B-5310) the results are very good. However, argon is over reported in the Phase 1 samples. Improved argon measurement is a consequence of a spike volume that has

been more accurately calibrated. Overpressuring of helium and argon observed in the Phase 1 analysis (Battye, 2002) was observed again in this research.

Improved measurement of neon (over reported in the Phase 1 sample for the sample with the high brine fraction, B-7126) in Phase 2 is a result of changing the procedure for measuring neon, which is now done on neon released from the argon trap after argon trapping. Measurement of neon in gas that contains excessive argon is hindered by contributions from doubly charged ^{40}Ar. Systematic over reporting of krypton and xenon in the Phase I study is now corrected. A large number of air standards has improved the determination of the spike gas volume.

5.2 Noble Gas Concentration in Brine Fraction

The uncorrected results of noble gas analysis for the copper tube water samples summarized in Table 4.3 have good reproducibility. Calculated results, corrected for excess air and normalized to a 100% brine solution, are summarized in Table 5.1. Normalization to 100% brine corrects for dilution by subtraction of the meteoric, meltwater and excess air components from the total cc/cc_{H2O}, followed by division into the brine fraction. Meteoric water is calculated using the current ambient groundwater recharge temperature of 5°C. The glacial meltwater component is calculated assuming a recharge temperature of 0°C for this water. Excess air is calculated using an iterative calculation that assumes a brine salinity of 270 g/L and a temperature of 0°C. This calculation also assumes a salting coefficient of 7.63 based on a chloride salinity of 183 g/L corrected for dilution to a brine salinity of 270 g/L following the method described in Pearson (1987).

Neon concentrations are all the same value because neon is used to calculate and correct for excess air contributions in the samples. All results are adjusted downward to bring neon concentrations to a value equal to its dissolved concentration in an atmospherically-equilibrated brine at 0°C.

Table 5.1 Noble gas concentrations in Con mine water samples, corrected for excess air and normalized to 100 % brine according to the mixing relationships discussed above.

		Concentration (cc gas STP/ cc H20 STP)					Excess
Borehole	Sample	He	Ne	Ar	Kr	Xe	Air (%)
5310	water 1	1.5E-02	9.6E-09	3.4E-03	-5.6E-08	-1.1E-08	1.72
5310	water 2	1.2E-02	9.6E-09	3.5E-03	-1.5E-07	-2.0E-08	1.75
5310	**Average**	**1.3E-02**	**9.6E-09**	**3.5E-03**	**-1.0E-07**	**-1.6E-08**	**1.74**
5310 - Phase 1		1.0E-02	4.0E-08	3.8E-03	-2.7E-07	8.1E-08	
7126	water 1	2.0E-03	9.6E-09	3.7E-03	1.0E-08	3.3E-10	0.36
7126	water 2	2.0E-03	9.6E-09	3.4E-03	1.8E-08	-1.0E-09	0.21
7126	water 3	2.1E-03	9.6E-09	2.4E-03	1.5E-08	1.4E-09	0.16
7126	**Average**	**2.0E-03**	**9.6E-09**	**3.2E-03**	**1.4E-08**	**8.5E-10**	**0.24**
7126 - Phase 1			3.4E-08	9.3E-03	7.9E-08	3.9E-08	

Helium is the most overpressured gas, with an average brine normalized concentration of 0.002 and 0.013 cc STP / cc H_2O for boreholes 7126 and 5310, respectively. This is over five orders of magnitude higher than atmospherically equilibrated brine at STP (Figure 5.1). Note that helium concentrations in B-5310, although calculated for a lower brine component in the water (22%), are an order of magnitude higher than those observed in B-7126. The high diffusivity of helium may account for higher concentrations in the upper mine level, perhaps mobilized by depressurization related to mining activities. More importantly B-5310 has a much longer borehole length and consequently intersects different fault structures (Negus and Pud Faults) than those intersected by B-7126 (one of Angel fault offsets).

Argon is overpressured, relative to an atmospherically equilibrated brine at STP, by nearly two orders of magnitude with brine corrected concentrations near 0.003 cc STP / cc H_2O in both B-7126 and B-5310. Calculated argon isotope ratios for these two boreholes are as high as 3895 (Table 5.2). These ratios are calculated from the excess argon, attributed to subsurface production of ^{40}Ar. As there are no significant radiogenic sources of ^{36}Ar in the subsurface, this ratio can be considered to be reliable.

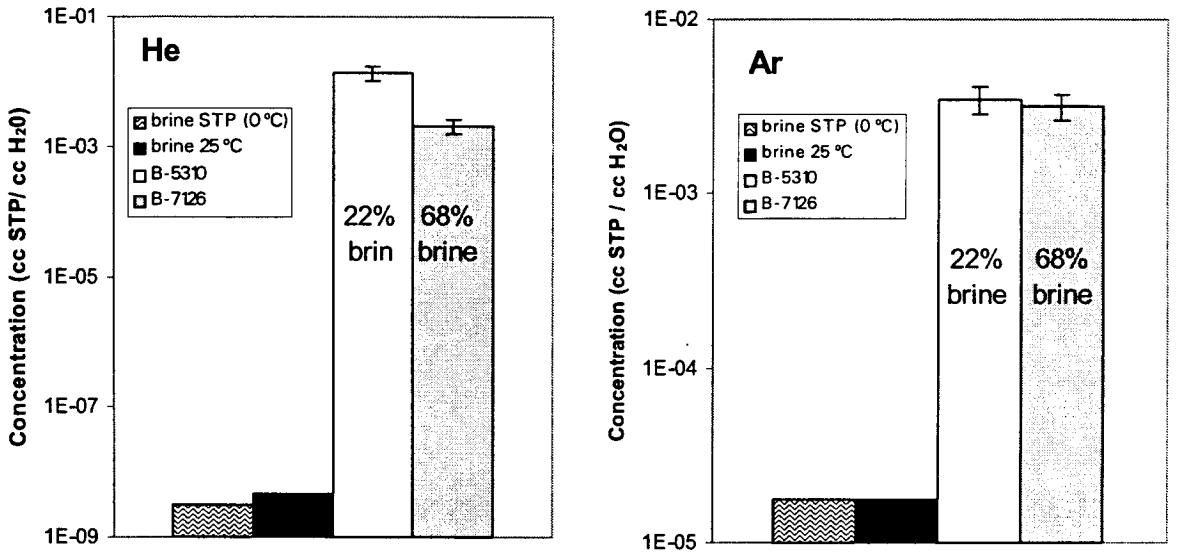

Figure 5.1 Helium and argon brine corrected concentrations in B-7126 and B-5310 compared with concentrations theoretically present in air equilibrated brine at STP (0°C) and 25°C. Error bars are expressed as the % standard deviation based on reproducibility of air standards.

Table 5.2 Argon brine normalized concentrations and isotope ratios from Con Mine groundwaters compared with air.

Borehole	Sample	Ar cc STP /cc H_2O	$40Ar/^{36}Ar$
1470 m level			
5310	water 1	3.4E-03	723
5310	water 2	3.5E-03	733
1615 m level			
7126	water 1	3.7E-03	3895
7126	water 2	3.4E-03	3840
7126	water 3	2.4E-03	2771
Air		9.3E-03	296

Figure 5.2, showing krypton and xenon concentrations normalized to brine, reveals that there is little to no overpressuring of krypton and xenon with respect to an air equilibrated brine at STP for water sampled from B-7126. Within the uncertainties of the calculations described above, these results support an evaporated brine source that had equilibrated with air. If the brine component originated as a fresh water, with a subsequent gain of salinity in the subsurface, higher krypton and xenon concentrations would be anticipated (Figure 5.2).

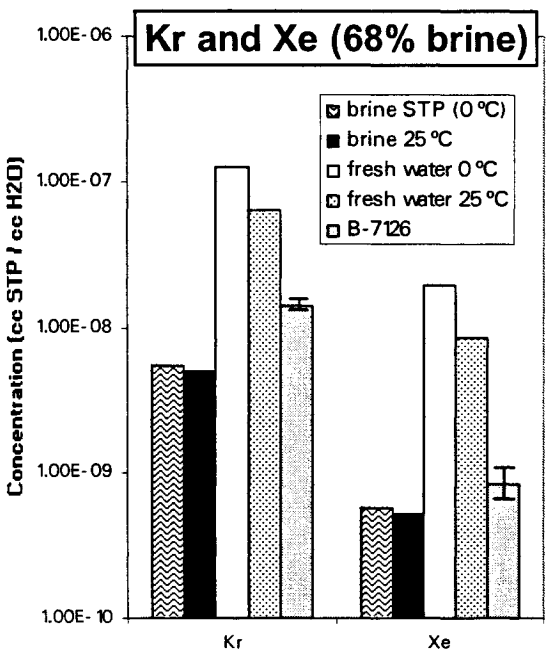

Figure 5.2 Krypton and xenon brine corrected concentrations in B-7126 compared with concentrations theoretically present in air equilibrated brine and freshwater at STP (0°C) and 25°C. Error bars are expressed as the % standard deviation based on reproducibility of air standards.

Water from B-5310 (22% brine) has negative concentrations for krypton and xenon. As these calculated deficiencies are sensitive to the amount of brine represented in the sample, the samples from B-5310 on the 4900 ft level are not considered to be the best representation of krypton and xenon in full brine.

5.3 Paleotemperature Estimates – Con Mine

As described in section 1.2.1, high salinity waters have a reduced noble gas solubility and attenuated temperature relationship. This reduction in sensitivity to changes in temperature demands more precise instrumentation to discriminate between results. Figure 5.3 reveals that the degree of gas separation and analytical precision needed to discriminate between the temperature solubility curves for the brines collected from B-7126 and B-5310 is not yet achievable. As a result, these data are not able to produce recharge temperature estimates.

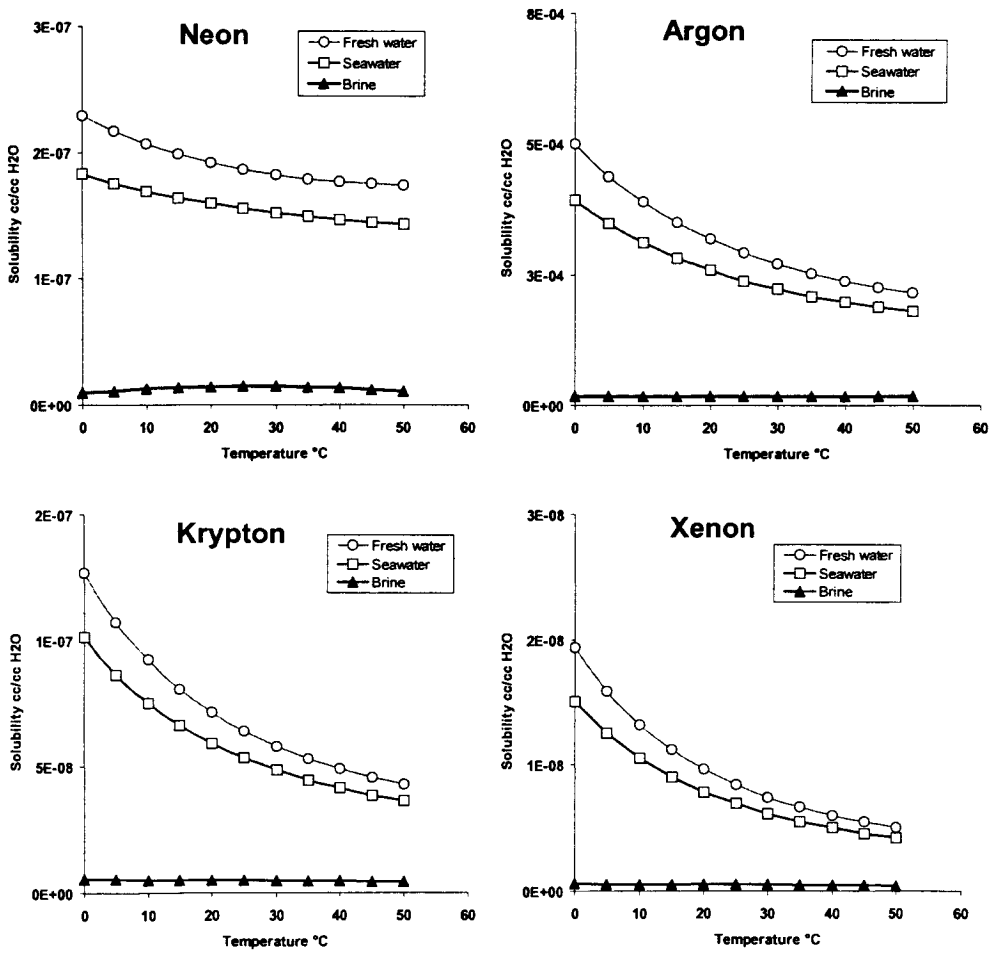

Figure 5.3 Comparison of the relationship between solubility and temperature for fresh water, seawater and Con Mine brine for neon, argon, krypton and xenon.

5.4 Age of Brine estimated from radiogenic production of ^{4}He and ^{40}Ar – Con Mine

The subsurface production and subsequent overpressuring of ^{4}He and ^{40}Ar provides a method for describing the age of the brines collected from the Con Mine. Calculation of subsurface residence time by use of radiogenic isotope production has been demonstrated for both ^{4}He and ^{40}Ar (Andrews and Lee, 1979; Torgersen and Clark, 1985; Osenbrück et al., 1998 and Lippmann et al., 2003). Andrews and Lee (1979) developed a linear relationship (Equation 5.1) between helium accumulation and time based on the properties of the parent rock.

Equation 5.1

$$[He] = \rho\, \phi^{-1}\, t\, (1.19 \cdot 10^{-13}\, [U] + 2.88 \cdot 10^{-14}\, [Th])$$

Where: ρ = the rock density,
ϕ = fractional porosity,
U and Th concentrations in ppm,
and [He] is reported in $cm^3\ g^{-1}$

A similar equation is presented in Lippmann et al. (2003) who references it to Torgersen et al. (1985).

Equation 5.2

$$t = \frac{C(i)}{A_{is}(i) + \left(\frac{J(i)}{n \times h \times \rho_w}\right)}$$

Where: C(i) = the concentration of noble gas i in cm^3 g-1
A_{is}(i) = the in-situ accumulation rate of noble gas i
J(i) = the accumulation of the crustal flux of noble gas i

n = the porosity of the parent rock
h = sampling depth
ρ_w = sample water density

$A_{is}(i)$ is calculated using the following equation:

Equation 5.3

$$A_{is}(i) = \lambda(i) \times \left(\frac{1-n}{n}\right) \times \left(\frac{\rho_s}{\rho_w}\right) \times P(i)$$

Where: $\lambda(i)$ is the release factor
n is the porosity of the parent rock
ρ_s = the rock density
ρ_w = the water density
P(i) = the production rock of noble gas i by the parent rock.
$P_4 = 1.19 \cdot 10^{-13}$ [U(ppm)] + $2.88 \cdot 10^{-14}$ [Th (ppm)] cm^3 STP g^{-1}_{rock} yr^{-1}
$P_{40} = 3.887 \cdot 10^{-14}$ [K(wt %)] cm^3 STP g^{-1}_{rock} yr^{-1}

For our purposes J(i), the accumulation of the crustal flux, has been excluded from Equation 5.2 simplifying it to:

Equation 5.4

$$t = \frac{C(i)}{A_{is}(i)}$$

For the Con mine, a rock density of 3 g cm^{-3} is used with a porosity of 0.01 (Clark et al., 2000). Uranium, thorium and potassium concentrations of 0.57 ppm, 2 ppm and 0.86 wt % were used based on average values measured in the Yellowknife metabasalt by Cousens et al. (2000). Release factors for both helium and argon are conservatively assumed to be 1 as outlined in Lippmann et al. (2003). Water density for the Con Mine water samples has been calculated to be ~ 1.188 g/cm^3.

Helium is assumed to equilibrate between the rock and fluid through dissolution of radiogenic helium, aided by crustal strain and dilation of microfractures (Honda et al., 1982).

Using Equation 5.1 for helium, and Equation 5.4 for both helium and argon return similar ages within the accuracy of the input data. Helium age estimates are for B-5310 only as it has been hypothesized that significant loss of ^{4}He from B-7126 has occurred. Argon concentrations are very similar for B-5310 and B-7126 and both have been used to calculate an age estimate. The average calculated age for the Canadian Shield brine component at the Con mine is now ~ 440 Ma, compared with 230 Ma from the phase 1 study. This age estimate does not fall directly within the Devonian Period. However, within the error limitations of the calculated values, and in light of other evidence provided by Bottomley et al. (1994 & 2002) this age estimate does indicate that these Paleozoic aged brines, are most likely from the Devonian Period.

6 Noble Gas Data – Lupin Mine

A larger data set of noble gas concentrations, derived from copper tube water samples, was compiled for the Lupin mine allowing for comparison of results with other measured parameters of salinity, formational pressure and total dissolved gas pressure (as CH_4). However, a lack of information on mixing relationships between more recent meteoric water and Canadian Shield brine makes mixing fraction separation impossible. Consequently the following presents these data in total gas concentration per cc of water.

6.1 Neon, Krypton and Xenon Concentration

The concentrations of krypton and xenon are the most sensitive to temperature (Figure 1.2) and are of greatest use in establishing recharge temperatures. krypton and xenon, together with neon, are largely unaffected by subsurface sources and in-situ production. In most low-salinity waters, their concentration is essentially established by the dissolution and entrainment of air. The entrainment of air is determined by the degree of neon overpressuring, and a correction for excess air is made from excess neon (Youngman, 1989). This correction has not been made for the data presented in the following analysis unless otherwise stated.

Understanding the behaviour of neon in the subsurface is fundamental to interpreting noble gas concentrations. Figure 6.1 indicates that neon has no correlation with salinity as would be expected if it was added in the subsurface. However, Figure 6.1 also reveals a slight tendency (correlation factor (cf) ~ - 0.62) for neon to decrease with total dissolved gas pressure when only boreholes from the 1130 m level that intersect the V1 fracture zone are

considered. This may indicate that neon has been partitioned in the subsurface by degassing and phase separation. Neon is an atmospherically-derived noble gas and should have no correlation with subsurface geogenic gas concentration. Krypton and xenon may also be affected by these processes, which increases the complexity of a recharge temperature calculation.

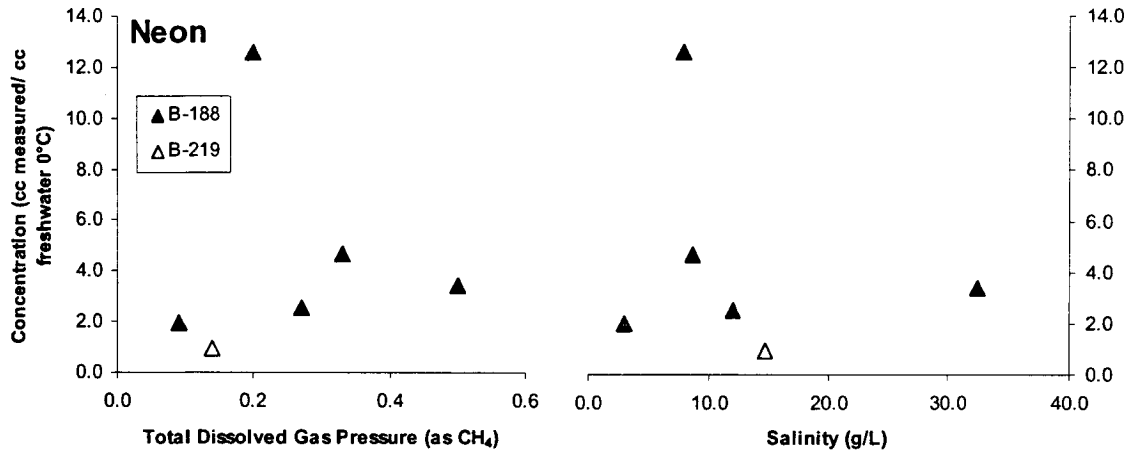

Figure 6.1 Relationship between average (where duplicate or triplicate analysis available) neon concentration (normalized to fresh water at 0°C) and total gas as well as with salinity. Solid triangles represent boreholes from the 1130 that intersect the V1 fracture zone (B-191, 192, 197, and 217). Borehole 219, also from the 1130 m level does not intersect the V1 fracture zone. B-188 is located on the 890 m level and intersects the v1 fracture zone.

Upon initial observation of Figure 6.2 it appears that neither krypton nor xenon concentrations are strongly correlated to total dissolved gas pressure. However, when only boreholes from the 1130 m level which intersect fracture zone V1 (solid black markers) are considered, a strong negative correlation (cf ≈ -0.84 for krypton, -0.89 for xenon) does exist. Both gases decrease with increasing total gas pressure which indicates alteration of gas concentration in the subsurface.

Both krypton and xenon also show a moderate to strong negative correlation with salinity when the only those same boreholes are considered (cf ≈ -0.71 for krypton, -0.99 for

xenon). A loss of krypton and xenon by increased salinity would require exchange with a gas phase in the subsurface, although the range of krypton and xenon measured in these samples is greater than can be accounted for by their range in salinity alone (less than 20% between fresh water and seawater salinity; Smith and Kennedy, 1983). This correlation is more likely to be an artefact of the greater CH_4 content of the more saline water, which affects krypton and xenon during degassing.

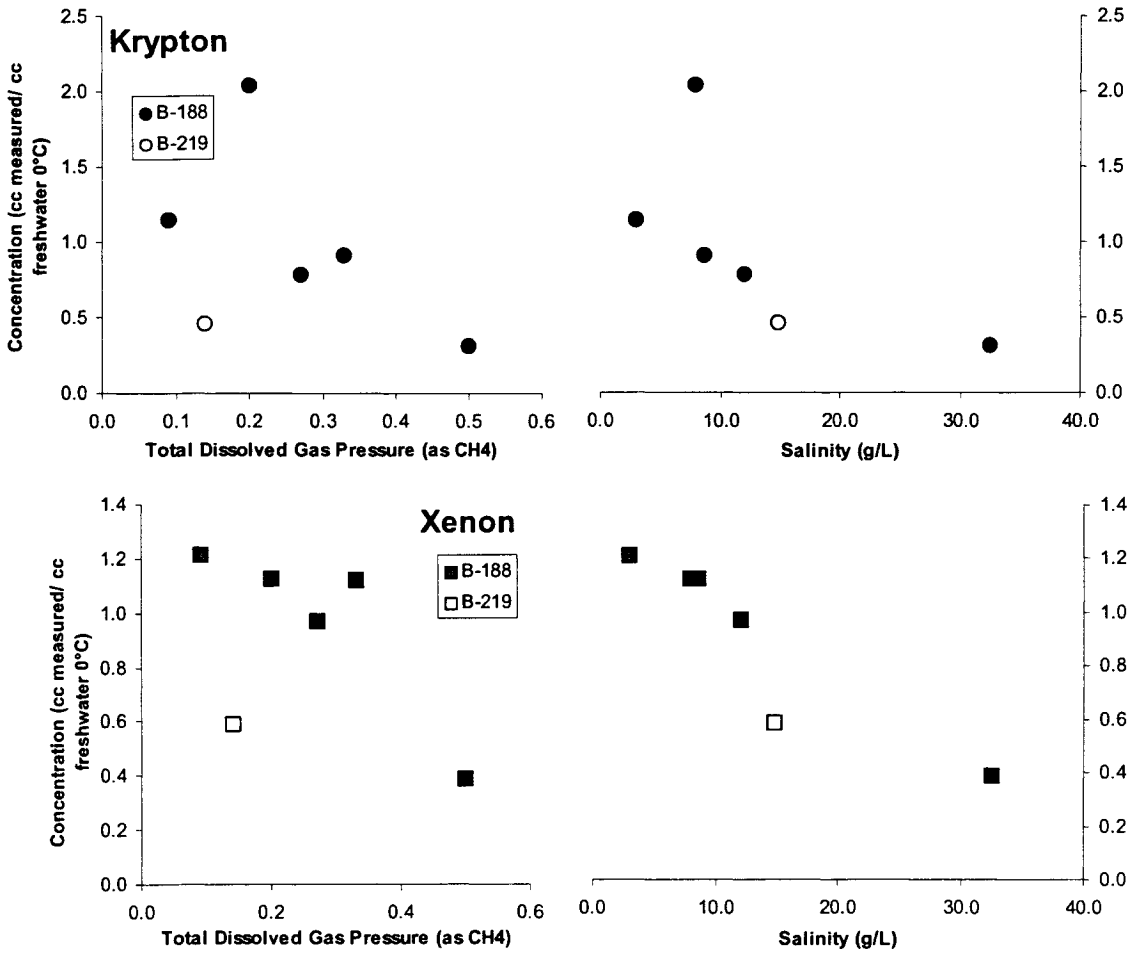

Figure 6.2 Correlation between Krypton and xenon concentrations (normalized to fresh water at 0°C) and total dissolved gas as CH_4 as well as salinity. Solid triangles represent boreholes from the 1130 that intersect the V1 fracture zone (B-191, 192, 197, and 217). Borehole 219, also from the 1130 m level does not intersect the V1 fracture zone. B-188 is located on the 890 m level and intersects the v1 fracture zone.

Figure 6.2 reveals concentrations below fresh water equilibrium for both krypton and xenon in three boreholes (B-192, B-217 and B-219). This may indicate that either there has

been loss of both gases from solution, or that recharge has taken place at temperatures greater than 20°C and without any excess air. The latter is unlikely, considering that this is currently a permafrost region, and that the remaining samples would then have unusually high levels of excess air.

Loss of noble gases from solution is possible considering the high pressures at these depths and the high pressure differentials generated during drilling. Further evidence for degassing is observed in the concentrations for neon. In Figure 6.3, the concentrations of krypton and xenon are compared with neon. Neon is the least sensitive to temperature, and is used to correct for the direct incorporation of noble gases during groundwater infiltration. In this diagram, all three gases are normalized to their concentration in air-equilibrated fresh water at 0°C, the temperature and salinity at which dissolved concentrations are the greatest. The origin of the two lines is at a sample/equilibrium ratio of 1 with no excess air. Sample concentrations higher than this value can be attributed to direct entrainment of air (excess air addition). The trend lines for waters at higher temperatures will have the same origin, but follow slightly steeper slopes to higher relative gas concentrations.

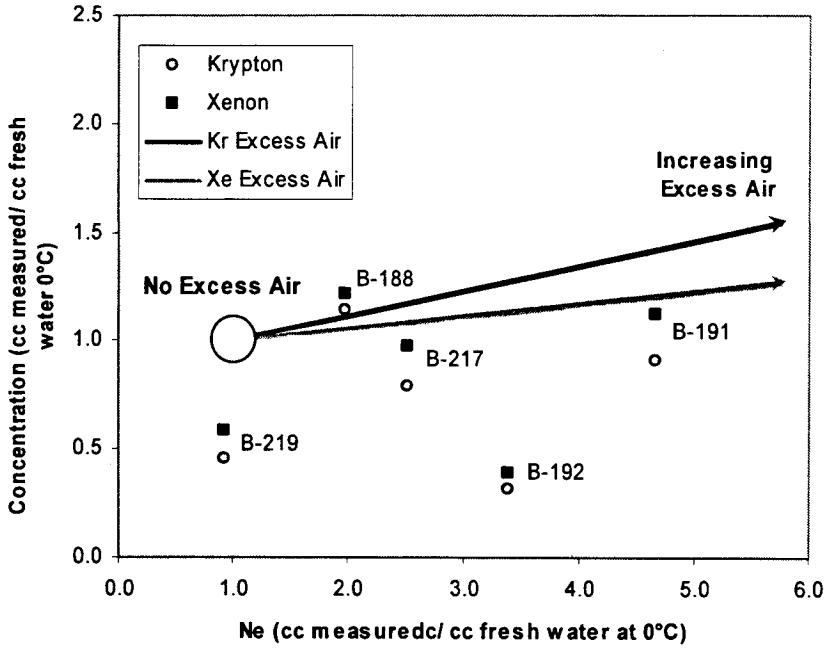

Figure 6.3 Krypton and xenon concentrations vs. neon concentration, normalized to fresh water at 0°C

Results for the Lupin samples are considerably displaced from these lines, and the concentrations of krypton and xenon are not correlated to neon. This suggests that there is an additional process affecting gas concentrations in the subsurface. It seems probable that significant depressurization of the rock and water in fractures encountered by the boreholes cause gas dissolution into the rock mass, or within the borehole. This clearly occurs during sampling, where the groundwater effervesces at the point of discharge at mine air pressure. Accordingly, depressurization within fissures would also result in gas separation.

Gases should re-dissolve when water flow is closed at the mine wall. However, significant alteration of gas concentration may have occurred during depressurization which may be caused by drilling or flushing of boreholes. Extended periods of time may be necessary for re-equilibration of concentrations. Since boreholes were sampled following pump tests and flushing, there is concern that re-equilibration did not occur. As a result the

higher diffusion rate of neon compared with krypton and xenon may have produced the uncoupled behaviour noted in Figure 6.3.

Frape et al., (2004) indicate that a 100 m unsaturated zone appears to exist below the base of permafrost. This zone may provide a second location for degassing and fractionation of noble gases to occur from these deep groundwaters. While this is speculative, the possibility of such dynamics should not be discounted. This could take place during de-saturation and subsequent degassing as groundwaters in this zone migrate downward with the declining water table. In this event, the salinity of the groundwater must also be considered as degassing and re-dissolution of gases would be affected by salinity gained in the subsurface. The reduced solubility of the noble gases under high salinity conditions (Figure 5.3) increases the likelihood of noble gas degassing in the event of depressurization or the presence of an unsaturated zone.

Unfortunately, strong indications of degassing, coupled with a poor correlation between neon and xenon gases precludes recharge temperature calculations at this time. Determination of mixing relationships may help to better separate fractions and calculate brine components as was calculated for the Con mine sampling. Additional samples would also better constrain the variability in the behaviour of these gases.

6.2 Paleotemperature Estimates – Lupin Mine

Noble gas recharge temperature calculation requires neon to correct for excess air, which does not itself provide recharge temperature information. However, in the Lupin

samples, uncertainties remain with respect to the effects of depressurization and subsequent fractionation of neon between gas and water phases. One sample had a saturation value lower than that for water equilibrium while others had an excess of up to 12 times. These inconsistencies suggest a redistribution of neon in these groundwaters, and leave little confidence in using neon for excess air corrections.

The krypton and xenon concentrations were normalized to their respective concentrations in fresh water at 0°C. Calculations were made to normalize them at higher equilibrium temperatures as well. However, it was found that this resulted in much greater overpressuring for these two gases. Calculation of recharge temperatures requires resolution of the potential problem of subsurface gas separation and noble gas partitioning or redistribution.

6.3 Argon and Helium Concentration

Unlike krypton and xenon there is significant overpressuring of helium and argon in the deep groundwaters as shown in Figure 6.4 where both argon and helium are compared with theoretical concentrations present in air-equilibrated freshwater at 0°C and 15°C. If a brine origin was also show on Figure 6.4 it would indicate considerably more overpressuring as solubility in higher salinity was is much lower than freshwater. This confirms a geogenic source for both of these gases as would be expected for their production at depth.

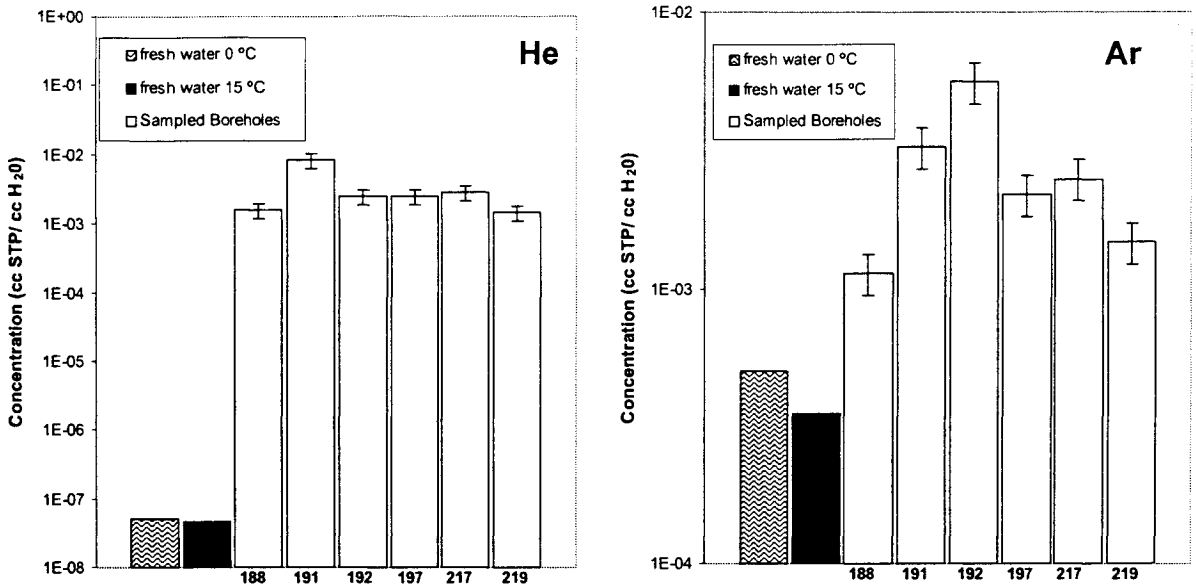

Figure 6.4 Average helium and argon concentrations in boreholes from the Lupin mine (x-axis labels indicate borehole number) compared with concentrations theoretically present in air equilibrated freshwater at STP (0°C) and 15°C. Error bars are expressed as the % standard deviation based on reproducibility of air standards.

Figure 6.5 shows a very good positive correlation (cf ≈ 0.99) between total dissolved gas and argon concentration but no correlation with helium. Furthermore, Figure 6.5 also shows a good positive correlation (cf ≈ 0.85) between argon and groundwater salinity but no relationship with helium. The positive correlation of salinity and total dissolved gas with argon concentration suggests that the increase in CH_4 and salinity are related to increased argon concentration. On the other hand there appears to be little to no effect on helium concentration.

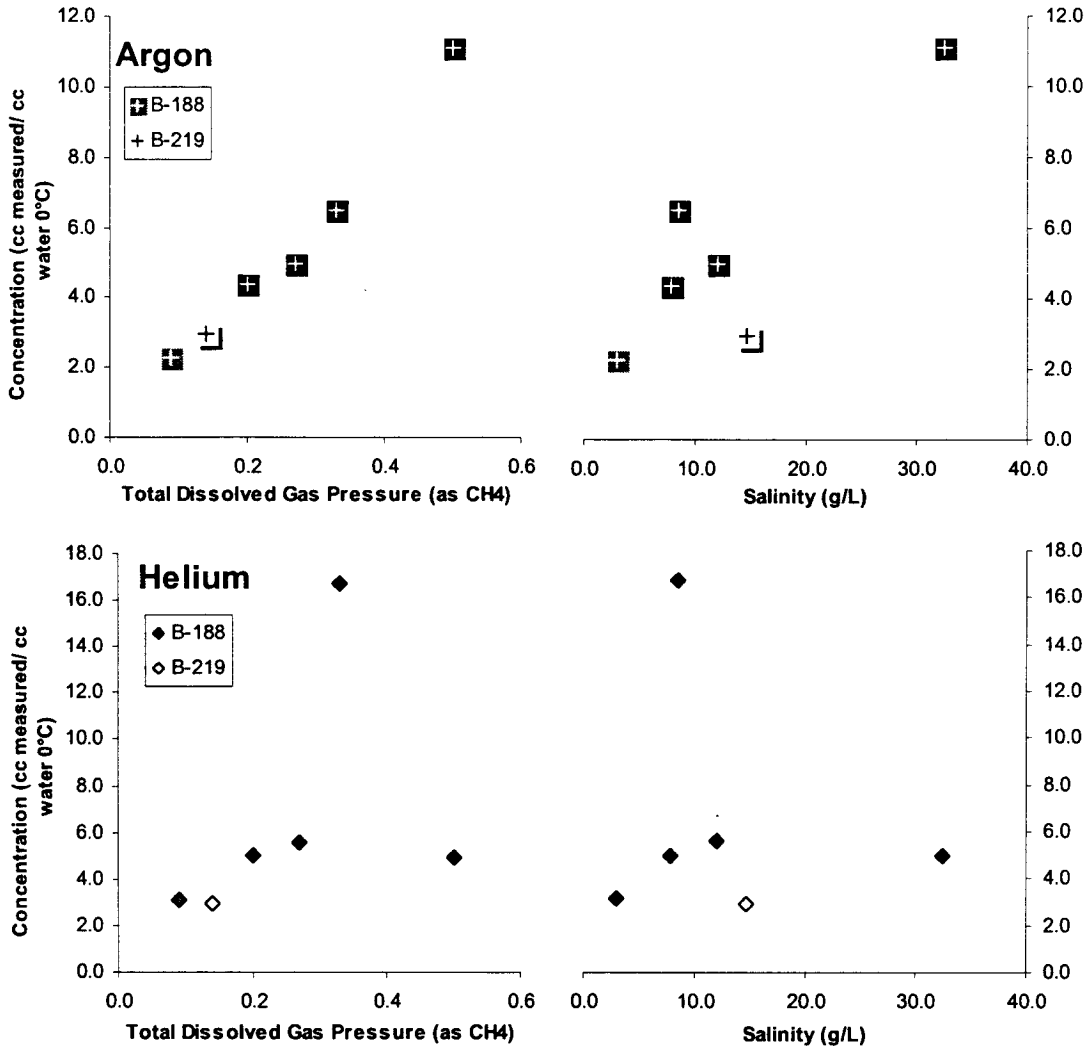

Figure 6.5 Correlation between argon and helium concentrations (normalized to fresh water at 0°C) and total dissolved gas as CH_4. Helium concentrations have also been divided by 1000 for display purposes. Solid triangles represent boreholes from the 1130 that intersect the V1 fracture zone (B-191, 192, 197, and 217). Borehole 219, also from the 1130 m level does not intersect the V1 fracture zone. B-188 is located on the 890 m level and intersects the v1 fracture zone.

Helium has a much higher diffusivity than argon which may explain the absence of a correlation for this noble gas with total dissolved gas and salinity. On the other hand the correlation of argon concentration with these parameters reinforces the idea that these groundwaters are a mixture of more recent meteoric water and high salinity brines (Frape et al., 2004).

6.4 Age of groundwater estimated from radiogenic production of ^{4}He and ^{40}Ar – Lupin Mine

The elevated argon and helium concentrations are likely a result of geogenic production indicating that the brine component of these waters is on the order of millions of years. A better understanding of the groundwater mixing components would be required to constrain the age of the brine component more precisely. However, a rough estimation of residence time can be made using Equation 5.3 and Equation 5.4.

For the Lupin mine, a rock density of 3 g cm^{-3} is used with measured U, and K concentrations of 2 ppm and 1.79 wt% (Ruskeeniemi et al., 2002). Thorium concentration has been estimated at a concentration of 3 ppm from Yamashita et al. (1999). Release factors for both helium and argon are assumed to be 1 as outlined in Lippmann et al. (2003). Water density for the Lupin Mine water samples has been calculated to be ~ 0.999 g/cm^3.

Age estimates from all boreholes for helium and argon calculations average between 20 – 80 Ma for the Lupin waters. Borehole 192 has the highest salinity and returned an age of approximately 130 Ma. This indicates that normalization of these waters to a 100% brine component would likely increase residence time estimates near those recorded for the Con mine brine.

7 Summary

The origin and evolution of saline and brine groundwaters found within the vicinity of mines in the Canadian Shield provide important context relevant to the safe disposal of radioactive waste in a deep geologic repository. The results of investigations of noble gas geochemistry at two Canadian Shield mines, the Lupin in Nunavut, and the Con at Yellowknife, provide valuable insights into the character of these Shield brines.

Major ion and stable isotope geochemistry are used to indicate the degree to which mining has impacted groundwater flow dynamics in the mine. In addition, at the Con mine these data have been used to delineate mixing ratios. At the Con mine these mixing ratios can be applied to further constrain measured noble gas concentrations used to provide information on temperature of recharge for the Shield brines. Although, mixing ratios are not calculated for the Lupin mine, the measured noble gas concentrations provide insight into the groundwater flow dynamics occurring in a mine beneath permafrost. Finally, data from both the Con and Lupin mines provide age estimates based on radiogenic production of helium and argon. What follows is a summary of the major points listed above and their implications in understanding the origin and age of the deep Shield brines.

7.1 Geochemistry of Con Mine Groundwaters

The overall goal of this aspect of the research was to improve our understanding of groundwater recharge and flow deep within the Precambrian rocks of the Canadian Shield in the vicinity of the Con Mine as an analogue for a potential radioactive waster repository. Mixing calculations outlined in Clark et al. (2000) show variations in the modern, glacial and brine components according to sample level depth. General trends include a decrease of

modern component with increasing depth and more sporadic increases in the glacial component as pockets of this water are intersected.

Monitoring of major ion and stable isotope geochemistry of waters sampled since 1980 indicate that mining has moderately increased the depth to which recent meteoric water has penetrated. However, despite 25 years of discharge since mining began at the deepest level sampled (1615m) the Shield brine here has remained relatively unaffected by mixing with recent and glacial components. Average brine component increases from 1.5 to 66.5 % between the 1070 and 1615 m levels, respectively, while the modern component decreases from 86 to 2.7 % between the same two levels.

7.2 Con Mine – Atmospheric Noble Gas Concentrations

Average krypton and xenon concentrations from B-7126 on the 1615 m level shown in Figure 5.2 reveal that there is little to no overpressuring of these gases (krypton 2.6 x , xenon 1.5x) with respect to an air equilibrated brine at STP. In addition, if brines had originated as freshwater, with subsequent gain of salinity in the subsurface, Figure 5.2 indicates substantially higher concentrations for these two gases would be anticipated. Within the uncertainties of the calculations described above, these results support a source as an evaporated brine that had equilibrated with air.

7.3 Con Mine – Helium and Argon Residence Times

The considerable overpressuring of helium and argon (max values; helium ~ $4x10^6$, argon ~ $2x10^2$) within the groundwaters at both the Lupin and Con mines supports the

conclusion that these waters are geologic in age as extensive time is necessary for the observed concentrations to accumulate. For deep groundwaters from the Con mine, age estimates for the brine component were calculated using radiogenically produced helium and argon gas concentrations normalized to a 100% brine solution. These estimates indicate a brine component residence time of roughly 440 $^{+}/_{-}$ 19 Ma. Within the error limitations associated with these age estimate, and in light of other evidence presented in Bottomley et al., (1994 and 2002), on the origin of the deep shield brines, this research further indicates that deep Shield brines are Devonian in age and therefore have a Palaeozoic seawater origin. Such a brine would have evolved by evaporitic enrichment of Palaeozoic seawater before recharge into the Canadian Shield.

7.4 Lupin Mine – Helium and Argon Residence Times

Calculations of residence time for the Lupin Mine do not use normalized noble gas concentrations to a 100% brine solution as the precise mixing ratios are not known for this system. Estimates of residence time for the waters sampled from the V1 fracture zone of Lupin mine indicate a geologic residence time of roughly 20 – 80 million years. However, when boreholes intersecting the V1 fracture zone are considered, a strong positive correlation between argon concentration and salinity, as well as with total dissolved gas (as CH_4) and salinity, are observed. When only the most saline water is considered (B-192) a residence time of 130 Ma is obtained which also supports the idea that the brine component of the Lupin is likely as old as the brines observed from the Con Mine. These correlations point towards an older saline brine end member that has been diluted by a process of mixing with more recent meteoric water.

Another process affecting noble gas concentration at the Lupin mine is gas loss via degassing as a result of depressurization of the rock, mainly observed along the V1 fracture zone. One of the main sources of evidence for degassing along this fracture is the observed concentrations of krypton and xenon below fresh water equilibrium indicating loss of gas from solution. This is corroborated by the absence of a correlation between neon and the two heavier noble gases, krypton and xenon, likely indicating phase-separation and differential diffusion of gases based on mass and size.

7.5 Development of Diffusion Samplers for High Formational Pressure Sampling

In an effort to improve the ease and turnaround time for analysis of noble gases in brines, a diffusion sampler was designed and tested to be used with groundwaters encountered deep within the Canadian Shield. The main advantage of gas samples over water samples is the elimination of a step involving gas separation from water, which in turn permits a shorter laboratory analysis time and substantially shorter sample turnover rate.

Although the design for the main body of the diffusion sampler was successful in handling the high formation pressures encountered, problems arose with sample collection and storage. Laboratory experiments at the University of Ottawa later confirmed that sufficient exchange of gas through the silica membrane does indeed occur (Jones, 2005). However, variations in total pressure in the sample tubes from single deployments, and correlations between total gas pressure and noble gas partial pressure, suggest that gas has leaked through microfractures at the cold weld pinch seal sites as shown in Figure 4.6.

References

Aeschbach-Hertig, W., and M. Stute, J. Clark, R. Reuter, and P. Schlosser. (2002). A Paleotemperature record derived from dissolved noble gases in groundwater of the Aquia Aquifer (Maryland, USA). *Geochimica et Cosmochimica Acta*, **66**, pg. 797-817.

Andrews, J. (1992). Mechanisms for noble gas dissolution by groundwaters. In, Isotopes as Tracers in Environmental Studies. International Atomic Energy Agency, Vienna, pg. 87-109.

Andrews, J., and N. Hussain, M.J. Youngman. (1989). Atmospheric and radiogenic gases in groundwaters from the Stripa granite. *Geochimica et Cosmochimica Acta,* **53**, pg. 1831-1841.

Andrews, J and D. Lee. (1979). Inert Gases in Groundwater from the Bunter Sandstone of England as Indicators of Age and Paleoclimatic Trends. *Journal of Hydrology*, **41**, pg. 233-252.

Bath, A.H., and W.M. Edmunds, J.N. Andrews. (1979). Paleoclimatic trends deduced from the hydrochemistry of a Triassic Sandstone aquifer, United Kingdom. *Isotope Hydrology,* **2**, pg. 545-568.

Battye, N., (2002). Noble gases in Canadian Shield Groundwaters. Unpublished M.Sc thesis, Department of Earth Science, University of Ottawa.

Bein, A., and A. Arad, (1992). Formation of saline groundwaters in the Baltic region through freezing of seawater during glacial periods. *Journal of Hydrology*, **140**, pg. 75-87.

Bottomley, D.J., and R. Renaud, T. Kotzer, I.D. Clark. (2002). Iodine-129 constraints on residence times of deep marine brines in the Canadian Shield. *Geology*, **30**, pg. 587-590.

Bottomley, D.J., and D. Conrad Gregoire, K.G. Raven. (1994). Saline groundwater and brines in the Canadian Shield: Geochemical and isotopic evidence for a residual evaporite brine component. *Geochimica et Cosmochimica Acta*, **58**, pg.1483-1489.

Bottomley, D., and J. Ross, W. Clarke. (1984). Helium and neon isotope geochemistry of some ground waters from the Canadian Precambrian Shield. *Geochimica et Cosmochimica Acta.*, **48**, pg 1973-1985.

Bullis, H.R., and R.A. Hureau, B.D. Penner. (1994). Distribution of Gold and Sulphides at Lupin, Northwest Territories. *Bulletin of the Society of Economic Geologists*, **89**, pg. 1217- 1227.

Clark, J.F., and M. Lee Davisson, G. Hudson, P. Macfarlane. (1998). Noble gases, stable isotopes, and radiocarbon as tracers of flow in the Dakota aquifer, Colorado and Kansas. *Journal of Hydrology.* **211**, pg. 151-167

Clark, I.D., and M. Douglas, K. Raven, D. Bottomley. (2000). Recharge and Preservation of Laurentide Glacial Melt Water in the Canadian Shield. *Ground Water*, **38**, pg. 735-742.

Clayton, R.N., and I. Friedman, D. Graf, T. Mayeda, W. Meents, N. Shimp. (1966). Origin of saline formation waters. *Journal of Geophysical Research.* **71**, 3869-3882.

Cook, P.G., and Herczeg, A.L., (1999) Appendix 4: Liquid and gas-phase diffusion coefficients. In P. Cook and A. Herczeg (Eds.) "Environmental Tracers in Subsurface Hydrology", Kluwer Academic Press, p. 521-522.

Cousens, B. (2000). Geochemistry of the Archean Kam Group, Yellowknife Greenstone Belt, Slave Province, Canada. *Journal of Geology*, **108**, pg. 181-197.

Craig, B.G. (1965). Glacial Lake McConnell, and the surficial geology of parts of Slave River and Redstone River-map areas, District of Mackenzie, Geological Survey of Canada, Bulletin 122, 33p.

Douglas, M., and I.D. Clark, K. Raven, D. Bottomley. (2000). Groundwater mixing dynamics at a Canadian Shield mine. *Journal of Hydrology,* **235**, pg. 88-103.

Douglas, M., and I.D. Clark, K.G. Raven, D. J. Bottomley. (1997). Mixing and temporal variation in the groundwater flow system at the Con Mine, Yellowknife, NWT., Canada; an analogue for a radioactive waste repository. Paper presented at GAC/MAC Meeting, Ottawa, May 19, 1997.

Dyck, W., and F. Da Silva. (1981). The use of ping pong balls and latex tubing for sampling helium content of lake sediments. *Journal of Geochemical Exploration,* **14**, pg. 41-48.

Dyke, A.S. and L.A. Dredge. (1989). Quaternary Geology of the north western Canadian Shield. In, *Quaternary Geology of Canada and Greenland*, ed. R.J. Fulton. Ottawa. Canada: Geological Survey of Canada.

Environment Canada Website. website http://www.msc-smc.ec.gc.ca/climate/climate_normals_1990/show_normals_e.cfm?station_id=758&prov=NW&start_row=1&end_row=13

Florkowski, T., and L. Morawska, K. Rozanski. (1988). Natural Production of Radionuclides in Geologic Formations. *Nuclear Geophysics*, **2**, pg. 1-14.

Frape,S. and R. Stoller, M. Hobbs, T. Ruskeeniemi, L. Ahonen, M. Paannanen. (2004). Hydrogeochemistry of Groundwaters At and Below the Base of Permafrost at Lupin: Report of Phase II. Ontario Power Generation, Report No: 06819-REP-01300-10047-R00.

Frape, S., and P. Fritz, R. McNutt. (1984). Water-rock interaction and chemistry of groundwaters from the Canadian Shield. *Geochimica et Cosmochimica Acta,* **48**, pg. 1617-1627.

Frape, S., and Fritz, P. (1981). The occurrence and chemistry of groundwaters in the Canadian Shield. University of Waterloo, Waterloo Research Institute, Project No. 002-08-18 for Atomic Energy of Canada Ltd., 74 p.

French, H. The Periglacial Environment. Harlow, England: Longman Limited, 1996.

Fritz, P. and Frape, S. (1982). Saline groundwaters in the Canadian Shield - a first overview. *Chemical Geology*, **36**, pg. 179-190.

Gardiner, J.J. (1986). Structural geology of the Lupin mine, Northwest Territories. Unpublished MSC-thesis, Acadia University, Wolfville, Nova Scotia. 206 p.

Gascoyne, M. and M. Sheppard. (1993). Evidence of terrestrial discharge of deep groundwater on the Canadian Shield from helium in soil gases. *Environmental Science and Technology*, **27**, pg. 2420-2426.

Gascoyne, M., and C.C. Davison, J.D. Ross, R. Pearson. (1987). Saline Groudwaters and Brines in Plutons in the Canadian Shield. Geological Association of Canada Special Paper 33: 53-68.

Gierszewski, P., and S. Russell, F. Garisto, M. Jensen, T. Kempe, P. Maak, G. Simmons, A. Vorauer. (2002). Deep Geologic Repository Technology Program – Annual Report 2001. Ontario Power Generation, Report 06819-REP-01200-010080-R00.

Haynes, F.M. (1988). Fluid inclusion evidence of basinal brines in Archean basement, Thunder Bay Pb-Zn-Ba district, Ontario, Canada. Canadian J. Earth Science 25, 1884-1894.

Heaton, T. and J.Vogel. (1981). "Excess Air" in groundwater. *Journal of Hydrology*, **50**, pg. 201-216.

Helmstaedt, H. and W.A. Padgham. (1986). A new look at the stratigraphy of the Yellowknife Supergroup at Yellowknife, N.W.T. – implications for the age of gold-bearing shear zones and Archean basin evolution. *Canadian Journal of Earth Sciences*, **23**, 454-475.

Henderson, J.F. and I.C. Brown. (1966). Geology and Structure of the Yellowknife Greenstone Belt, District of MacKenzie, Geological Survey of Canada, Bulletin 141.

Henderson, J.B. (1970). Stratigraphy of the Archean Yellowknife Supergroup, Yellowknife Bay – Prosperous Lake area, District of Mackenzie. Geological Survey of Canada, Paper 70-26.

Herut, B., and A. Starinsky, A. Katz, and A.Bein. (1990). The role of seawater freezing in the formation of subsurface brines. *Geochimica et Cosmochimica Acta*, **54**, 13-21.

Intera Consultants Ltd., and I.D. Clark, M.C. Douglas. (1997). Hydrological and Hydrogeochemical Study of the Miramar Con Mine – Yellowknife, NWT. Prepared by Intera Consultants Ltd., and I.D. Clark and M.C. Douglas, Ottawa, 128 pg.

Jones, K. (2005). Sampling gases in groundwater with a gas diffusion sampler. Unpublished B.Sc. thesis, Department of Earth Sciences, University of Ottawa, Ottawa, Canada.

Kelly, W.C., Rye, R.O., Livnat, A. (1986). Saline minewaters of the Keweena Peninsula, Northern Michigan: Their natural origin and relation to similar deep waters in the Precambrian rocks of the Canadian Shield. *American Journal of Science*, **286**, pg. 281-308.

Lane, A.C. (1914). Mine water composition, and index to the course of ore bearing currents. *Economic Geology*, **9**, pg. 239-262.

Lindberg, P. (1987). An investigation of the Pud and Negus fault offsets of the Campbell Shear Zone, Con Mine, Yellowknife, Northwest Territories, Report prepared for Nerco Minerals Company.

Lippmann, J., and M. Stute, T. Torgersen, D. P. Moser, J. A. Hall, L. Lin, M. Borcsik, R.E.S. Bellamy, T. C. Onstott. (2003). Dating ultra-deep mine waters with noble gases and ^{36}Cl, Witwatersrand Basin, South Africa. *Geochimica et Cosmochimica Acta*, **67**, pg. 4597-4619.

Leagult, M.I. and B.W. Charbonneau. (1993). Geophysical, geochemical and petrographical study of Contwoyto Batholith, Lupin gold mine area, Northwest Territories, Current Research, Part E; Geological Survey of Canada, Paper 93-1E, pg. 207-218.

Moorman, B.J., and Michel, F.A., Drimmie, R.J. (1996). Isotopic variability in Arctic precipitation as a climatic indicator. *Geoscience Canada*, **23**, pg. 189-194.

MacDonald, I.M. (1986). Water-rock interactions in felsic rocks of the Canadian Shield. M.Sc. project, University of Waterloo, Canada.

MacDonald, D., and N. Duke, R. Hauser. (1993). Geological setting of the NERCO Con Mine and the relationship of gold mineralisation to metamorphism, Yellowknife, NWT. *Exploration Mining Geology,* **2**, pg. 139-154.

Nordstrom, D.K., and Ball, J.W., Donahoe, R.J., Whittemore, D. (1989). Groundwater

chemistry and water-rock interactions at Stripa. *Geochimica et Cosmochimica Acta*, **53**, pg. 1727-1740.

Osenbrück K., and Lippmann J., C. Sonntag. (1998). Dating very old pore waters in impermeable rocks by noble gas isotopes. *Geochimica et Cosmochimica Acta,* **62**, pg. 3041–3045.

Pearson, F.J., Jr, 1987. Models of mineral controls on the composition of saline groundwaters in the Canadian Shield. In: Saline waters and gases in crystalline rocks, Editors: Fritz, P. and Frape, S.K.; *Geological Association of Canada Special Paper 33,* pg. 39-51.

Permafrost, 1995. Map from the National Atlas of Canada, 5th Edition. (1995). National Atlas Information Service, Ottawa, Canada.

Physiographic Regions, 1972. Map from the National Atlas of Canada 4th Edition (1974a). National Atlas Information Service, Ottawa, Canada.

Pinti, D., and E. Van Drom. (1998). Paleotemp: A *Mathematica* Program for evaluating paleotemperatures from the concentration of atmosphere-derived noble gases in ground water. *Computers and Geoscience*, **24**, pg. 31-41.

Poole, J.C, and G. McNeill, S. R. Langman, F. Dennis. (1997). Analysis of noble gas in water using a quadupole mass spectrometer in static mode. Applied Geochemistry, **12**, pg. 704-714.

Ruskeeniemi, T., and M. Paananen, L. Ahonen, J. Kaija, A. Kuivamäki, S. Frape, L. Moren P. Degnan. (2002). Permafrost at Lupin; Report of Phase I. Geological Survey of Finland, Report YST-112.

Sanford, W., and R. Shropshire, D.K. Solomon. (1996). Dissolved gas tracers in groundwater: Simplified injection, sampling, and analysis. *Water Resources Research*, **32**, pg. 1635-1642.

Sheldon, A. (2002). Diffusion of Radiogenic Helium in Shallow Groundwaters: Implications for Crustal Degassing. PhD Thesis. University of Utah, Department of Geology.

Smith, S.P. and B. Kennedy. (1983) The solubility of noble gases in water and in NaCl brine. Geochimica et Cosmochimica Acta, **47**, pg. 503-515.

Sofer, Z. and Gat, J.R. (1972). The isotopic composition of evaporating brines: effect on the isotopic activity ratio in saline solutions. *Earth and Planetary Science Letters*, **26**, pg. 179-186.

Spencer, R.J. (1987). Origin of Ca-Cl brines in Devonian formations, Western Canada Sedimentary Basin. *Applied Geochemistry*, **2**, pg. 373-384.

Stephenson, M., and W. Schwartz, T. Melnyk, M. Motycka. (1994). Measurement of advective water velocity in lake sediment using natural helium gradients. *Journal of Hydrology*, **154**, pg. 63-84.

Stute, M. J.F Clark ,. P. Schlosser, W. Broecker and G. Bonani. (1995). A 30,00 yr continental paleotemperature record derived from noble gases dissolved in groundwater from the San Juan Basin, New Mexico. *Quaternary Research*, **43**, pg. 209-220.

Stute, M., and P. Schlosser (1992). Principles and applications of the noble gas paleothermometer in: AGU Monograph on "Climate change in continental isotopic records", Geophysical Monograph, **78**, pg. 89-102.

Torgersen, T., and W.B. Clarke. (1985). Helium accumulation in groundwater, I - An evaluation of sources and the continental flux of crustal ^{4}He in the Great Artesian Basin, Australia. *Geochimica et Cosmochimica Acta*, **49**, pg. 1211-1218

Tremblay, L.P. (1976). Geology of the northern Contwoyto Lake area, District of Mackenize, Geological Survey of Canada, Memoir 381, 56p.

Vegetation Cover. Map from the National Atlas of Canada, 5th Edition. (1993). National Atlas Information Service, Ottawa, Canada.

Vovk, I.F. (1987). Radiolytic salt enrichment and brines in the crystalline basement of the East European Platform. In: Saline waters and gases in crystalline rocks, Editors: Fritz, P. and Frape, S.K.; *Geological Association of Canada Special Paper 33*, pg. 97-210.

Weyhenmeyer, C, and S Burns, H. Waber, W. Aeschbach-Hertig, R. Kipfer, H. Loosli, A. Matter. (2000). Cool Glacial Temperatures and Changes in Moisture Source Recorded in Oman Groundwaters. *Science*, **287**, pg. 842 - 845.

Yamashita, K., and R. Creaser, J. Stemler, T. Zimaro. (1999). Geochemical and Nd–Pb isotopic systematics of late Archean granitoids, southwestern Slave Province, Canada: constraints for granitoid origin and crustal isotopic structure. *Canadian Journal of Earth Sciences*, **36**, pg. 1131-1147.

Youngman, Michael J. (1989). Dissolved Gases and Radioelements in Groundwaters. The British Library, West Yorkshire, 422p. PHD thesis.

7.5.1.1 Appendix A – Procedure for Extraction and Analysis of Noble Gases

The following addresses additions, changes and or modifications to the extraction and analysis procedure as initially outlined in Appendix B of Battye, 2002. The text makes reference to the figure 3.4, a schematic of the noble gas line with a letter index.

A-2 Status of line at start-up

The line is left overnight with diffusion pumping of the main line, argon bulb, the Titanium getter, argon and xenon traps and ST707 furnace getter. All other components are closed. After a night of pumping the system generally reaches a pressure near $1.0E^{-7}$ Torr.

B-3 Preparation of Samples and Gas Extraction Line

- argon and krypton traps are baked the night before and left to pump clean all night. They are the first thing closed before starting extraction.
- The titanium getter is no longer used for gettering. Instead of turning on this getter the ST707 furnace getter is heated to ~ 400 – 450 °C.
- Preferable the sample is also attached the night before and left to pump using the air pump overnight. Then the next morning the air pump is closed off and V7 open so pumping to the top of the clamp occurs. When the line has pumped below $1.0E^{-5}$ the sample is ready for extraction.
- When gas diffusion samples are extracted the entire copper tube is initially immersed in the dry ice methanol solution to freeze any water that may have potentially condensed or, in the case of a contaminated sample, leaked during sampling.

A-4 Analytical Procedure

- trapping of krypton and xenon now occurs for 15 minutes while argon trapping occurs for 30 minutes.
- analysis for argon and helium ratios occurs both before and after any trapping.
- analysis occurs with both remaining gas after argon, krypton, and xenon trapping as well as with released from the argon trap while still immersed in liquid nitrogen. Gas analyzed from the frozen argon trap generally has less argon interference which is now monitored during neon analysis.

A-5 Isotope ratio measurement

- various aliquots of each gas are run for measurement of ratios to ensure accurate readings. Samples are analyzed for only10 minutes.

A-5 Determination of Sample Volume

All samples were collected using the same cradle giving the same volume each time. Volumes were calculated based on measurements of inner copper tube diameter which avoids the use of inaccurate weighing techniques and density assumptions. For gas diffusion samples volume is also calculated using measurement of inner copper tube

diameter but also using measured length for each individual sample as no cradle currently exits for the copper tube gas diffusion samples.